Volume 68A
Number 3
May-June 1964

Physics and Chemistry

U.S. DEPARTMENT OF COMMERCE

SECTION A

JOURNAL OF RESEARCH

NATIONAL BUREAU OF STANDARDS

Journal of Research

of the

National Bureau of Standards

A. Physics and Chemistry

May–June • 1964

VOLUME • 68A

NUMBER • 3

Editor: C. W. Beckett

Associate Editors: D. D. Wagman
J. M. Richardson

Publication dates:
Feb. 1, Apr. 1, June 1, Aug. 1, Oct. 1, Dec. 1, 1964

JOURNAL OF RESEARCH

The National Bureau of Standards Journal of Research reports research and development in the fields of activity shown at right. Also included from time to time are survey articles on topics closely related to the Bureau's scientific and technical program.

The Journal is published in four separate sections as follows:

A. Physics and Chemistry

Contains papers of interest primarily to scientists working in these fields. Issued six times a year. Annual subscription: domestic, $4.00; foreign, $4.75. Single copy 70 cents.

B. Mathematics and Mathematical Physics

Presents studies and compilations designed mainly for the mathematician and the theoretical physicist. Issued quarterly. Annual subscription: domestic, $2.25; foreign, $2.75. Single copy 75 cents.

C. Engineering and Instrumentation

Reports research and development results of interest chiefly to the engineer and the applied scientist. Issued quarterly. Annual subscription: domestic, $2.25; foreign, $2.75. Single copy 75 cents.

D. Radio Science (formerly Radio Propagation)

Published in cooperation with U.S. National Committee of URSI. Presents papers in radio propagation, communications, and radio science generally. Issued monthly. Annual subscription: domestic, $9.00; foreign, $11.50. Single copy $1.00.

The National Bureau of Standards is a principal focal point in the Federal Government for assuring maximum application of the physical and engineering sciences to the advancement of technology in industry and commerce. Its responsibilities include development and maintenance of the national standards of measurement, and the provision of means for making measurements consistent with those standards; determination of physical constants and properties of materials; development of methods for testing materials, mechanisms, and structures, and making such tests as may be necessary, particularly for government agencies; cooperation in the establishment of standard practices for incorporation in codes and specifications; advisory service to government agencies on scientific and technical problems; invention and development of devices to serve special needs of the Government; assistance to industry, business and consumers in the development and acceptance of commercial standards and simplified trade practice recommendations; administration of programs in cooperation with United States business groups and standards organizations for the development of international standards of practice; and maintenance of a clearinghouse for the collection and dissemination of scientific, technical, and engineering information.

Institute for Basic Standards. Electricity. Metrology. Heat. Radiation Physics. Mechanics. Applied Mathematics. Atomic Physics. Physical Chemistry. Laboratory Astrophysics.* Radio Standards Laboratory: Radio Standards Physics; Radio Standards Engineering.** Office of Standard Reference Data.

Institute for Materials Research. Analytical Chemistry. Polymers. Metallurgy. Inorganic Materials. Reactor Radiations. Cryogenics.** Office of Standard Reference Materials.

Central Radio Propagation Laboratory.** Ionosphere Research and Propagation. Troposphere and Space Communications. Radio Systems. Upper Atmosphere and Space Physics.

Institute for Applied Technology. Textiles and Apparel Technology Center. Building Research. Industrial Equipment. Information Technology. Performance Test Development. Instrumentation. Transport Systems. Office of Technical Services. Office of Weights and Measures. Office of Engineering Standards. Office of Industrial Services.

* NBS Group, Joint Institute for Laboratory Astrophysics at the University of Colorado.
** Located at Boulder, Colo.

U.S. DEPARTMENT OF COMMERCE
Luther H. Hodges, Secretary

NATIONAL BUREAU OF STANDARDS
A. V. Astin, Director

Order all publications from the Superintendent of Documents
U.S. Government Printing Office, Washington, D.C., 20402

Use of funds for printing this publication approved by the Director of the Bureau of the Budget (June 19, 1961).

JOURNAL OF RESEARCH of the National Bureau of Standards—A. Physics and Chemistry
Vol. 68A, No. 3, May–June 1964

Compressibility of Natural Rubber at Pressures Below 500 kg/cm²

Lawrence A. Wood and Gordon M. Martin

(February 3, 1964)

The specific volumes of unvulcanized natural rubber and of a peroxide-cured vulcanizate of natural rubber were measured at pressures of 1–500 kg/cm² at temperatures from 0 to 25 °C. Observations on mercury-filled dilatometers were made through a window in the pressure system. No time effects or hysteresis phenomena were observed. The specific volume V in cm³/g over the range studied can be represented by

$$V = V_{0,25}\{1 + A(t-25)\}\{1 + [a_{25} + k_1(t-25)]\ P + [\beta_{25} + k_2(t-25)]\ P^2\}$$

where P is the pressure in kg/cm², and t the temperature in °C. The constants for the unvulcanized and for the peroxide-cured samples are:

$V_{0,25} = 1.0951$ and 1.1032 cm³/g;
$10^4 A = 6.54$ and 6.36 per degree;
$10^6 a_{25} = -50.5$ and -50.4 (kg/cm²)$^{-1}$;
$10^6 k_1 = -0.227$ and -0.203 per degree;
$10^6 \beta_{25} = 10$ and 11.5 (kg/cm²)$^{-2}$;

and $10^6 k_2 = 0.048$ and 0.073 per degree, respectively. The compressibility of unvulcanized natural rubber at 25° and 1 kg/cm² is thus 50.5×10^{-6} (kg/cm²)$^{-1}$ falling to 40.6×10^{-6} (kg/cm²)$^{-1}$ at a pressure of 500 kg/cm². It is concluded that a low degree of vulcanization produces no significant changes in the constants listed. The values are not far different from those obtained by extrapolating to zero sulfur content the observations of Scott on the rubber-sulfur system. Calculations of values of compressibility (and its reciprocal the bulk modulus), "internal pressure", bulk wave velocity, difference between specific heats, and several other physical properties are in reasonable agreement with those obtained by direct observation by other workers. For the prediction of values at pressures above 500 kg/cm² the use of the Tait equation is recommended.

1. Introduction

The compressibility (or its reciprocal the bulk modulus) is an important physical property of rubber, frequently required in practical applications and in calculations relating to mechanical properties. The quantity is also called the bulk compliance. When this is known, the change of volume on stretching can be calculated from observations of stress and strain, and compared with direct experimental observations [1] [1] or utilized in calculations of the relative contributions of energy and entropy in thermodynamic studies of rubber elasticity [2]. Other relations requiring values of compressibility are discussed in later sections of this paper.

Previous experimental measurements have seldom covered the proper ranges of variables to yield accurate values of the compressibility of unvulcanized or lightly vulcanized rubber near atmospheric pressure. Our paper presents data obtained on unvulcanized natural rubber and on a peroxide-cured natural rubber vulcanizate at pressures between 1 and 500 kg/cm² at temperatures between 0 and 25 °C.

2. Experimental Arrangement

The unvulcanized sample was prepared from natural rubber latex by the purification procedure of McPherson [3]. An analysis showed 98.7 percent rubber hydrocarbon, 0.44 percent protein, and 0.18 percent ash. To this sample 1.00 percent of phenyl-beta-naphthylamine was added as an antioxidant. Another portion of this sample was used in crystallization studies by Roberts and Mandelkern [4], and Martin and Mandelkern [5]. The sample was made into a flat sheet $6 \times 6 \times 0.080$ in. by molding at 100 °C.

The other sample was prepared from a lot of commercially purified rubber obtained from the United States Rubber Co., designated as No. 2103A, Batch 7505. To 100 parts of polymer 3 parts of dicumyl peroxide ("Dicup") were added and the mixture cured 45 min at 140 °C.

The samples, which were relatively transparent, were examined carefully after molding or curing. No visible bubbles or other inhomogeneities were noted.

Specimens of each sample, weighing about 4 g each, were placed in mercury-filled volume dilatometers with 2 mm capillaries. The volume was determined following the practices developed in this laboratory some years ago [6].

The specific volume of a portion of each sample was determined at atmospheric pressure at 25° by hydrostatic weighings in water [7].

The mercury-filled dilatometers were completely immersed in an oil (Plexol) contained in a system [5] designed for the application of pressure at various

[1] Figures in brackets indicate the literature references at the end of this paper.

temperatures. The pressure was built up by the operation of a piston actuated by a manually operated screw. It could be read on a precision Bourdon-type gage. Observations of the level of the mercury in the dilatometer capillary were made through a tempered Pyrex glass window.

The height of the mercury in the capillary was read to the nearest 0.005 cm with a precision cathetometer, as the pressure was raised in increments of 100 kg/cm² from 0 to 500 kg/cm² gage pressure.

The values of compressibility found were so small that the change in volume produced by a change in pressure of 1 kg/cm² was always less than 1 in the last digit reported. Thus no distinction needed to be drawn between gage pressure and absolute pressure, or between observations made at atmospheric pressure as compared with those which might have been conducted at zero pressure.

Once thermal equilibrium was established (within a period of about 15 min), no time effects or hysteresis phenomena were observed over the ranges of pressure and temperature investigated. We consider that our results are the low-frequency limits of the quantities displayed in the viscoelastic spectrum [8].

The total volume change observed was corrected for the volume change of the mercury and the glass, and combined with the specific volume determined at 1 atm at 25° to yield the values of the specific volume given in table 1. These are the complete basic data of this paper.

TABLE 1. *Observations of specific volume*

	Unvulcanized rubber			Peroxide-cured vulcanizate			
P	V_{25}	V_{20}	V_0	V_{25}	V_{20}	V_{10}	V_0
kg/cm²	*cm³/g*	*cm³/g*	*cm³/g*	*cm³/g*	*cm³/g*	*cm³/g*	*cm³/g*
0	1.0951	1.0917	1.0772	1.1032	1.0998	1.0927	1.0857
100	1.0896	1.0864	1.0725	1.0977	1.0944	1.0876	1.0807
200	1.0845	1.0814	1.0679	1.0926	1.0894	1.0828	1.0763
300	1.0795	1.0764	1.0636	1.0877	1.0846	1.0782	1.0719
400	1.0748	1.0718	1.0593	1.0830	1.0801	1.0739	1.0678
500	1.0702		1.0554	1.0786	1.0756	1.0697	1.0637

3. Calculations

It was found possible to represent the specific volume V over the range of observation by an equation of the following form:

$$V=V_{0,25}\{1+A(t-25)\}\{1+[\alpha_{25}+k_1(t-25)]P+[\beta_{25}+k_2(t-25)]P^2\} \quad (1)$$

where P is the pressure, t the temperature in °C, and $V_{0,25}$, A, α_{25}, β_{25}, k_1, and k_2 are constants.

The compressibility B is defined here as

$$-(1/V_0)(\partial V/\partial P)$$

where V_0 is the specific volume at zero pressure at any temperature. For materials conforming to eq (1) one finds:

$$V_0=V_{0,25}\{1+A(t-25)\} \quad (2)$$

and, by differentiation of eq (1),

$$B=-[\alpha_{25}+k_1(t-25)]-2[\beta_{25}+k_2(t-25)]P. \quad (3)$$

From this one obtains

$$\frac{\partial B}{\partial t}=-k_1-2k_2P \quad (4)$$

and

$$\frac{\partial B}{\partial P}=-2[\beta_{25}+k_2(t-25)]. \quad (5)$$

The relations just given are simpler and calculations from them are easier when the compressibility is defined as $-1/V_0(\partial V/\partial P)$, in accordance with the usual practice [9], than when use is made of the "instantaneous" compressibility, defined as $-(1/V)(\partial V/\partial P)$. The latter quantity, of course, is readily obtained from the former by multiplying it by V_0/V. The difference between the two quantities is never greater than a few percent over the present range of investigation.

The constant $V_{0,25}$ was determined, as already mentioned, by a direct measurement of the specific volume at atmospheric pressure and 25 °C by hydrostatic weighings. The constant A was determined by a least squares computation based on eq (2) relating specific volume and temperature for the observations at atmospheric pressure.

The remaining four constants in eq (1) were determined by least-squares computation based on eq (3). Here the mean compressibility over each range of 100 kg/cm² was computed from the finite changes observed, and taken as the compressibility at the midpoint of the range. The bracketed quantities in eq (3) were determined at constant temperatures as the intercept and slope of the predicted linear relation between the compressibility B and the pressure P. The constants α_{25} and k_1 were then determined by least squares as the intercept and slope in the predicted linear relation between the first bracketed quantity and the temperature. The constants β_{25} and k_2 were determined similarly from the second bracketed term. A check on the values was obtained by conducting the computations in reverse order; that is, now the pressure was first considered constant as the temperature was varied and then the temperature taken as constant while the pressure was varied.

The values of the constants obtained in this manner were:

	Unvulcanized sample	*Peroxide-cured sample*
$V_{0,25}$	1.0951	1.1032
$10^4 A$	6.54	6.36
$10^6 \alpha_{25}$	−50.5	−50.4
$10^6 k_1$	−0.227	−0.203
$10^9 \beta_{25}$	10.0	11.5
$10^9 k_2$	0.048	0.073

The pressures are expressed in kg/cm², the temperatures in °C, and the specific volumes in cm³/g.

The specific volumes calculated by eq (1) using these constants reproduce quite well the original

data given in table 1. The differences between calculated and observed values are shown in table 2. The most serious deviations are in the values for the unvulcanized sample at 20°, where the calculated values are systematically too low. The values for the vulcanizate at 20° also tend to be too low, but the difference is not as great.

TABLE 2. *Difference between calculated and observed values of specific volume*

	Unvulcanized rubber			Peroxide-cured vulcanizate			
P kg/cm²	V_{25} cm³/g ×10⁻⁴	V_{20} cm³/g ×10⁻⁴	V_0 cm³/g ×10⁻⁴	V_{25} cm³/g ×10⁻⁴	V_{20} cm³/g ×10⁻⁴	V_{10} cm³/g ×10⁻⁴	V_0 cm³/g ×10⁻⁴
0	0	−2	0	0	−1	0	0
100	1	−2	0	1	0	0	+1
200	0	−2	0	0	−1	0	0
300	0	−1	0	0	−1	0	0
400	−1	−1	+1	0	−2	−1	−1
500	0		0	0	0	−1	0

The lots of raw rubber used in preparing the two samples were of different origin and were purified by different methods. Consequently the specific volumes $V_{0,25}$ of the unvulcanized materials differed. In the first case, $V_{0,25}$ was 1.0951 cm³/g as shown in table 1; in the other, it was observed to be 1.1074 cm³/g. The addition of the dicumyl peroxide to the second sample gave a mixture with a specific volume about 1.1040 cm³/g, and on curing this fell to the value 1.1032 cm³/g shown in table 1.

The compressibility values calculated by eq (3), using the constants obtained above, are given in table 3. The values of $(1/V_{0,25})(\partial V/\partial t)$, obtained by calculations based on a differentiation of eq (1), are given in table 4. The change in this quantity with changes in temperature is seen to be quite small, and will be regarded as negligible in this range.

TABLE 3. *Compressibility* $(-1/V_0)(\partial V/\partial P)$

	Unvulcanized rubber			Peroxide-cured vulcanizate			
kg/cm²	B_{25} cm³/kg ×10⁻⁶	B_{20} cm³/kg ×10⁻⁶	B_0 cm³/kg ×10⁻⁶	B_{25} cm³/kg ×10⁻⁶	B_{20} cm³/kg ×10⁻⁶	B_{10} cm³/kg ×10⁻⁶	B_0 cm³/kg ×10⁻⁶
0	50.5	49.4	44.9	50.4	49.4	47.4	45.3
100	48.5	47.4	43.0	48.1	47.2	45.3	43.4
200	46.5	45.5	41.3	45.8	44.9	43.2	41.4
300	44.5	43.5	39.5	43.5	42.7	41.2	39.5
400	42.5	41.6	37.8	41.2	40.5	39.1	37.6
500	40.6	39.7	36.1	39.0	38.4	37.1	35.8

TABLE 4. *Thermal expansivity* $(1/V_{0,25})(\partial V/\partial T)$

	Unvulcanized rubber			Peroxide-cured vulcanizate			
kg/cm²	Temperature			Temperature			
	25° deg⁻¹ ×10⁻⁴	20° deg⁻¹ ×10⁻⁴	0° deg⁻¹ ×10⁻⁴	25° deg⁻¹ ×10⁻⁴	20° deg⁻¹ ×10⁻⁴	10° deg⁻¹ ×10⁻⁴	0° deg⁻¹ ×10⁻⁴
0	6.54	6.54	6.54	6.36	6.36	6.36	6.36
100	6.29	6.28	6.28	6.13	6.13	6.13	6.13
200	6.04	6.04	6.03	5.92	5.92	5.91	5.91
300	5.81	5.81	5.79	5.73	5.72	5.72	5.71
400	5.59	5.58	5.56	5.55	5.54	5.53	5.53
500	5.37	5.36	5.33	5.39	5.38	5.37	5.36

4. Comparison With Similar Previous Direct Observations

The pressure ranges, temperatures, and samples used in six important previous compressibility studies on rubber are given in table 5. It will be noted that only three authors investigated pressures below 500 kg/cm², only a few used pure-gum vulcanizates, and only one made measurements on unvulcanized rubber. Copeland's experiments were adiabatic rather than isothermal.

TABLE 5. *Summary of six previous investigations*

Authors	Ref	Year	Temp	Pressure range	Samples
			°C		
Adams & Gibson.	[10]	1930	25	1,000–12,000 bars.	1. Vulcanizate Rubber 90- Sulfur 10 2. Vulcanizate Rubber 90- Sulfur 4 Zinc Oxide Accel. 0.25
Scott	[11]	1935	10–85	1–800 bars	Vulcanizates: Rubber 97–69 Sulfur 3–31
Bridgman	[12]	1944		2,000–25,000 bars.	Pure-gum vulcanizate
Naunton, calculated by McPherson 1958.	[13]	1945		48.5–1715 bars	Unvulcanized rubber Pure-gum vulcanizate
Copeland	[14]	1948		1–345 bars	1. Vulcanizate Rubber 100- Sulfur 8 2. Vulcanizate Rubber 100- Sulfur 2.5 Zinc Oxide Accel. 1
Weir	[15]	1953	10–81.5	1,000–10,000 bars.	Vulcanizates: Rubber 90–72 Sulfur 10–28

The only cases yielding values which can reasonably be compared with the present results are the studies of Scott [11] and of Naunton (as calculated by McPherson) [13]. This comparison is made in table 6, where for uniformity all the pressures are to be measured in dynes/cm² instead of kg/cm² (1 kg/cm²=980665 dynes/cm²). This requires a change of exponent and an increase of 2 percent in the previously given coefficients related to the first power of the pressure, and of 4 percent in those related to the second power. These units will be used in the remainder of this paper. The values ascribed to Scott represent extrapolations to 0 and 2 percent sulfur respectively, his observations extending only over the range 3–31 percent sulfur.

TABLE 6. *Comparison of values of constants*

(Pressures measured in dynes/cm²)

Constant	Unvulcanized			Vulcanizates		
	Scott 0% S	Naunton	Present work	Scott 2% S	Naunton "pure-gum"	Present work, peroxide
$V_{0,25}$	1.1015		1.0951	1.0829		1.1032
$10^4\ A$	6.63		6.54	6.61		6.36
$10^{12}\ \alpha_{25}$	−53.7	−53.8	−51.5	−51.0	−50.7	−51.4
$10^{12}\ k_1$	−0.258		−0.231	−0.262		−0.207
$10^{21}\ \beta_{25}$	12.0	13.6	10.4	11.3	11.8	12.0
$10^{21}\ k_2$	0.083		0.050	0.083		0.076

The vulcanizates used in the various studies were all somewhat different. Scott's values refer to the rubber-sulfur system; the composition of Naunton's "pure-gum vulcanizate" was not specified; and the present work was on a peroxide-cured rubber.

The agreement of our values with those published previously is regarded as very good, especially when one considers the differences in the composition of the vulcanizates and the fact that some of the constants are obtained as derivatives of values directly observed.

5. Calculations of Internal Pressure

The "internal pressure" P_i of a liquid [16, 17, 18, 19] is defined in thermodynamics as the change in internal energy U with change in volume.

$$P_i \equiv \left(\frac{\partial U}{\partial V}\right)_T = T\left(\frac{\partial P}{\partial T}\right)_V - P. \tag{6}$$

It will soon be evident from the numerical values below that for an applied pressure P of approximately 1 atm the second term is negligible compared with the first. The temperature in this instance must be expressed in °K. By differentiation of eq (2) one obtains:

$$A = \frac{1}{V_{0,25}} \frac{\partial V_0}{\partial T}. \tag{7}$$

Thus

$$\frac{A}{B} = \frac{V_0}{V_{0,25}} \frac{\partial P}{\partial T} \tag{8}$$

and

$$P_i = \frac{V_{0,25}}{V_0} \frac{A}{B} T. \tag{9}$$

The values calculated by eq (9) from the present data at different temperatures and a pressure of 1 atm are given in the fifth and sixth columns of table 7.

Allen, Gee, and coworkers [17] made a direct measurement of the quantity $T\partial P/\partial T$ for a natural rubber vulcanizate containing 3.5 parts of sulfur and an accelerator. They obtained values of 88.6, 87.4, and 86.1 cal/cm³ at 20, 30, and 40 °C, respectively. The comparison with the corresponding figures in table 7 is exceedingly satisfactory. They report furthermore that the internal pressure of most polymers is approximately 20–40 percent larger than the cohesive energy density determined as the square of δ, the solubility parameter measured in swelling experiments. This relation is apparently valid for rubber also, since values of δ^2 ranging from 64–70 cal/cm³ are normally reported for natural rubber vulcanizates [20, 21].

6. Calculations of Adiabatic Compressibility

The compressibility values were measured in the present work under isothermal conditions. For many applications, particularly where compressional waves are involved, the adiabatic compressibility is of interest. The difference between the isothermal compressibility B and the adiabatic compressibility B_a has often been calculated from the relation [22]

$$B - B_a = A^2VT/C_p \tag{10}$$

where A is the thermal expansion coefficient, V the specific volume, T the temperature in °K, and C_p the specific heat at constant pressure. Taking the values of C_p (shown in table 7) from the work of Bekkedahl and Matheson [23] as the same for both unvulcanized and peroxide-cured rubber, and the other quantities from the present work, one obtains the values shown in the table for A^2VT/C_p and the corresponding adiabatic compressibility B_a.

7. Comparison With Measurements Involving Bulk Wave Velocities

The adiabatic compressibility is the major factor determining the velocity of propagation of com-

TABLE 7. *Values of thermodynamic quantities at 10^6 dynes/cm²*

T		V	B	$(V_{0,25}/V_0)(TA/B)$		C_p [b]	A^2VT/C_p	B_a
Unvulcanized rubber $A=6.54\times10^{-4}$ (deg C)$^{-1}$								
°C	°K	cm³/g	cm²/dyne	dyne/cm²	cal/cm³	j/g °C	cm²/dyne	cm²/dyne
0	273.2	1.0072	45.7×10^{-12}	3980×10^6	95.0	1.785	7.05×10^{-12}	38.6×10^{-12}
10	283.2	1.0844	48.0	3900	93.2	1.816	7.23	40.8
20	293.2	1.0917	50.03	3820	91.4	1.856	7.38	42.9
25	298.2	1.0951	51.5	3790	90.5	1.881	7.43	44.1
30[a]	303.2	1.0987	52.7	3750	89.6	1.906	7.48	45.2
40[a]	313.2	1.1058	55.0	3680	88.1	1.956	7.57	47.4
Peroxide-cured rubber $A=6.36\times10^{-4}$ (deg C)$^{-1}$								
0	273.2	1.0857	46.2	3820	91.3	1.785	6.71	39.5
10	283.2	1.0927	48.3	3780	90.2	1.816	6.89	41.4
20	293.2	1.0998	50.4	3710	88.7	1.856	7.03	43.4
25	298.2	1.1032	51.4	3690	88.2	1.881	7.08	44.3
30[a]	303.2	1.1067	52.4	3670	87.7	1.906	7.12	45.3
40[b]	313.2	1.1137	54.5	3620	86.6	1.956	7.21	47.3

[a] Values given at 30 and 40 °C for V and quantities derived from V are based on an extrapolation of eq (1).
[b] Values observed for unvulcanized rubber by Bekkedahl and Matheson [23].

pressional waves in a sheet of rubber. The effective modulus for this type of wave is $(K_a+4/3\ G)$ where K_a is the adiabatic bulk modulus (the reciprocal of the adiabatic compressibility B_a) and G is the shear modulus. The general equation is then

$$v^2=V(K_a+4/3\ G) \tag{11}$$

where v is the velocity of the compressional wave and V the specific volume of the medium. The present work on the vulcanizate yields $K_a=22{,}600\times10^6$ dynes/cm² at 25 °C and 1 atm. Assuming the reasonable value of 4.3 kg/cm² for G one finds $4/3\ G=5.7$ kg/cm²$=5.6\times10^6$ dynes/cm². Therefore this term can be neglected in the remainder of the present discussion over the range of variables considered here.

The adiabatic bulk modulus K_a, the velocity v of a compressional wave, calculated from eq (11), and the acoustic impedance, defined as v/V, the ratio of velocity to specific volume [24, 25], are each given in table 8 at different temperatures, as calculated from the data in table 7. The significance of the quantity $Vv^{\frac{1}{3}}$ in the last column will be discussed later.

TABLE 8. *Bulk moduli, bulk wave velocities, and derived quantities at 10^5 dynes/cm²*

t	K_a	v	"ρc"$=v/V$	$Vv^{\frac{1}{3}}(=R/M)$
	Unvulcanized rubber			
°C	dynes/cm²	m/sec	g cm⁻³ sec⁻¹	(cm³ g⁻¹) (m sec⁻¹)$^{1/3}$
0	2.59×10⁻¹⁰	1670	1550×10⁻²	12.78
10	2.45	1630	1500	12.76
20	2.33	1600	1460	12.77
25	2.27	1580	1440	12.76
30 [a]	2.21	1560	1420	12.74
40 [a]	2.11	1530	1380	12.74
	Peroxide-cured rubber			
0	2.53	1660	1530	12.85
10	2.42	1630	1490	12.86
20	2.30	1590	1450	12.83
25	2.26	1580	1430	12.85
30 [a]	2.21	1560	1410	12.84
40 [a]	2.11	1530	1380	12.83

[a] Values given at 30 and 40 °C are based on an extrapolation of eq (1).

With dynamic measurements the modulus is expected to be in general a function of the frequency. Ivey, Mrowca, and Guth [26] measured the time shift and amplitude change occurring when a sheet of pure-gum natural rubbber vulcanizate was inserted into the path of a pulsed compressional wave. From the observations they computed bulk wave velocity and bulk modulus.

A decrease in velocity was noted as the frequency was reduced from 10 Mc/s to 1 Mc/s. The magnitude of the decrease was about 5 percent at 0 and 20°, and about 2 percent at 40°. Further decreases were noted between 1 Mc/s and 100 Kc/s amounting about 2 percent at 0° and much less than 1 percent at 20 and 40°. No perceptible decreases were noted between 100 kc/s and 50 kc/s at 0° or any higher temperature. Heydemann [27] likewise could find no variation of bulk modulus with frequency over a range from 0.1 to 10,000 c/s at 20° for natural rubber samples of widely different compositions and moduli. At any given temperature the velocity thus decreases monotonically with decreasing frequency approaching asymptotically a low-frequency limit. We know of no experimental evidence for or reason to expect any further variation at lower frequencies than those mentioned.

It can be concluded from these results that dynamic measurements on pure-gum natural rubber vulcanizates at frequencies of 1 Mc/s and below, when conducted at 0° and above, will yield values of velocity not more than about 2 percent greater, and values of bulk modulus not more than about 4 percent greater, than the respective low-frequency limits. This important conclusion means that in this region in which occur almost all practical applications of rubber, the variation of bulk modulus with frequency can be neglected. The shear modulus, on the other hand, shows appreciable dispersion for several decades below 1 Mc/s at 0°, finally reaching a minimum change of 1–2 percent per decade at the lowest frequencies.

Figure 1 shows the adiabatic bulk modulus K_a as a function of temperature as determined in the present work, in comparison with some values obtained by dynamic measurements reported in the literature.

The values ascribed to the B. F. Goodrich Co. [28] were calculated as v^2/V from the sound velocity v at 5-degree temperature intervals, and a density value given as 0.98 g/cm³ at 25 °C. The rubber was a pure-gum natural rubber vulcanizate designated as Rho-C, Type 35000 (formerly 79SR32), with a Shore hardness of 35.

Values ascribed to Ivey et al. [26] are those read directly from the low-frequency limits of the bulk modulus in their figure 11 at 0 and 20°.

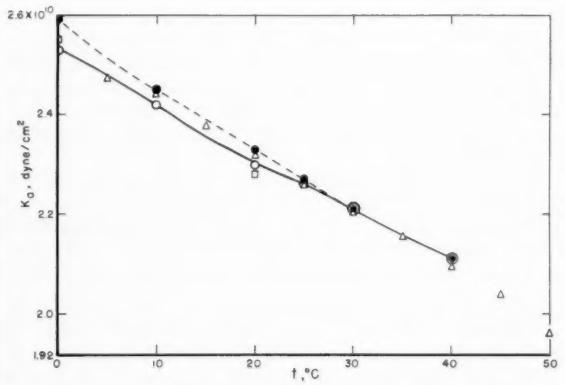

FIGURE 1. *Adiabatic bulk modulus of rubber as a function of temperature.*

● Present work—Unvulcanized
⊙ Present work—Peroxide-cured
⊡ Ivey et al. [26] figure 11—Pure-gum vulcanizate
△ B. F. Goodrich data [28] on Rho C rubber vulcanizate

Other literature values at a single temperature (omitted from figure 1 for simplicity) are:

Temp. °C	K_a dyne/cm²	Authors	Reference
0	2.60×10^{10}	Cunningham and Ivey	29
25	2.25	Nolle and Mowry	30
25	2.3	Nolle	31
30	2.22	Cramer and Silver	32

The agreement with the values shown in figure 1 at the respective temperatures is thoroughly satisfactory.

Cramer and Silver [32] measured the bulk modulus of a pure-gum vulcanizate at 30° by means of a resonant tube method [33] using a frequency of 1530 c/s.

It should be noted that the density of the normal pure-gum vulcanizates containing zinc oxide, sulfur, and an accelerator is approximately 0.98 g/cm³ ($V=1.02$ cm³/g), about 7 percent higher than that of the peroxide-cured vulcanizate used in the present work. According to the results just presented, this difference has no significant effect on the bulk modulus. The bulk wave velocities, however, are found to be about 3–4 percent lower than those given in table 8, in accordance with the predictions of eq (11).

In addition to the results just given, there are also literature values which are not properly comparable or do not agree so well with those we are reporting. For example, Wada and collaborators [34] made measurements on unvulcanized natural rubber latex, diluted with water until the rubber was about 10 percent by volume. They measured the velocity of a pulsed compressional wave in the suspension and compared it with that in the suspending liquid. The frequency used was 1 Mc/s. We see no obvious explanation for the fact that the bulk moduli they reported are about 10 percent lower than those we observed for unvulcanized rubber.

Heydemann [27] has reported values of dynamic compressibility for a number of rubber vulcanizates of unspecified composition. The highest value, which might be presumed to be that characteristic of a pure-gum vulcanizate, was 45.0×10^{-12} cm²/dyne at 20° corresponding to a bulk modulus of 2.22×10^{10} dyne/cm². This is about 4 percent less than the values shown in figure 1. The discrepancy is not surprising in view in the uncertainty regarding the composition.

McKinney, Belcher, and Marvin [35] measured the dynamic compressibility of a vulcanizate containing 12.1 percent sulfur. Their values have not been tabulated, since their vulcanizate can not be regarded as a soft or lightly vulcanized rubber. It was in fact chosen to permit measurements in the vicinity of the glass transition. They found that the value of isothermal compressibility B, at 25° and 1 atm was 41.4×10^{-12} cm²/dyne. Scott [11] reports 37.5×10^{-12} cm²/dyne for a vulcanizate containing 12 percent sulfur.

Some observers have reported their results only in terms of the bulk wave velocity without giving density values. In many instances the densities of the pure-gum vulcanizates would be expected to be near 0.98 g/cm³, and the velocities 3–4 percent lower than those given in table 8, as already mentioned.

Unpublished measurements of Barnes [36] are reported as yielding a compressional wave velocity of about 1600 m/s, at 10,000 to 50,000 c/s, in essential agreement with the values in table 8.

The values of bulk wave velocity for natural rubber observed by Natta and Baccaredda [37] are also in close conformity with the extrapolation of the present values to higher temperatures. Assuming a value of $\partial v/\partial t=3.0$ m/sec^{-1} deg^{-1} on the basis of the data in table 8, one obtains a velocity of about 1440 m/s at 70 °C for both unvulcanized and peroxide-cured rubbers. This is in good agreement with the values 1465 ± 20 m/s at this temperature observed directly by Natta and Baccaredda.

On the other hand, compressional wave velocities about 9 percent lower than those given in table 8 were measured by Levi and Philipp [38] who observed the frequencies at which successive maxima in transmission occurred in sheets about 1 mm thick, immersed in mercury. A dozen or more resonances were observed at frequencies between 1.5 and 8.6 Mc/s. The temperature was not specified. The velocities measured were 1430 and 1479 m/s for two different samples of unvulcanized evaporated latex and 1450 m/s for a pure-gum vulcanizate made from the first latex sample. A commercial soft-rubber vulcanizate gave 1440 m/s. No significant variation with frequency could be observed over the range studied.

The acoustic impedance "ρc" given in the next to the last column of table 8 governs the extent of reflection of compressional waves at the boundary of a medium. Zero reflection is obtained when the acoustic impedances on the two sides of the boundary are equal. This is important in underwater sound devices, where acoustically transparent protective materials are required for sonar domes, transducer covers, hydrophone tubes, and similar applications.

The acoustic impedance of fresh water [39, 40] increases from about 1403×10^{-2} CGS units at 0° to about 1493×10^{-2} at 25°, while that of sea water [41] rises from about 1490 to 1570×10^{-2} over the same range. In the region of greatest practical importance, 10–15 °C, the value for sea water is about 1530×10^{-2}. As can be seen from the table, the acoustic impedance of rubber decreases with increasing temperature. Consequently a matching of ρc for sea water with that for rubber can occur at only a single temperature. From the values for rubber given in table 8 it is concluded that only slight increases in the quantity ρc are required to attain the value of 1530×10^{-2} at 10–15°. Experience verifies this conclusion and at least one commercial vulcanizate has been designed for this purpose [28]. At each temperature the density is higher, the velocity lower, and ρc slightly higher than the values used or given in table 8 for the peroxide-cured rubber.

Cramer and Silver [32] found that when an EPC (Easy Processing Channel) carbon black was used as a filler in natural rubber, there was a considerable

increase in bulk modulus and a considerable increase in density. The velocity, depending as it does on the ratio of these quantities, was found to decrease slightly with filler content. The increase in density overbalanced the slight decrease in velocity so that the product "ρc" increased with increasing filler content. For rubber with a filler content sufficient to raise the density to 1.10 g/cm^3 and the Shore hardness to 52, the Goodrich company [28] has reported similar results, except that they found at most temperatures a very slight increase in velocity as compared with the pure-gum vulcanizate.

8. Calculation of Values of Other Properties

The compressibility B may be combined with Young's modulus E to give the value of Poisson's ratio μ. From classical mechanics the general relation for an infinitesimal deformation is:

$$\mu=\frac{1}{2}-\frac{1}{6}BE. \tag{12}$$

For the peroxide-cured vulcanizate at 25° $B_{25}=50.4\times10^{-12}$ cm^2/dyne (table 3) and a reasonable value of E would be 13 kg/cm^2, yielding 0.49989 for Poisson's ratio for an infinitesimal deformation.

The ratio E/G from classical mechanics is given by

$$E/G=3-\frac{1}{3}BE. \tag{13}$$

With the quantities already mentioned, this ratio is calculated as 2.99977 for the rubber vulcanizate.

The quantities measured in the present work may be utilized to compute the difference between the specific heats at constant pressure C_P and at constant volume C_V. The relation given by thermodynamic considerations [42] is

$$C_P-C_V=A^2VT/B. \tag{14}$$

The values given in table 7 for the unvulcanized rubber at 25 °C and at atmospheric pressure can be inserted into the right-hand member of the equation to yield 0.0648 cal/g °C for the difference in specific heats. This may be compared with a value of 0.066 cal/g °C at 27° given by Rehner [43] as the difference between $C_P=1.891$ j/g °C$=0.452$ cal/g °C measured directly by Bekkedahl and Matheson [23] and $C_V=0.386$ cal/g °C calculated from the structure by a method described by Tarassov [44].

The ratio C_P/C_V can be obtained by combining equations (10) and (14).

$$C_P/C_V=B/B_a. \tag{15}$$

Values for B/B_a computed from the data given in table 7 decrease from 1.184 at 0° to 1.160 at 40° for the unvulcanized material and from 1.170 at 0° to 1.152 at 40° for the peroxide-cured rubber. Independent values for C_P/C_V other than those derived from the values of C_P and C_V given in the preceding paragraph seem to be unavailable. The ratio in that instance is 1.171 at 27°.

The present results may be used to study the validity (for rubber) of the relation

$$MVv^{1/3}=R \tag{16}$$

where M is the molecular weight, V the specific volume, v the bulk wave velocity, and R is a constant, independent of temperature. This equation was proposed by Rao [45] some years ago as an empirical relation valid for organic liquids of low molecular weight.

Table 8 (col 5) shows that this relation holds reasonably well for the two rubbers over the range of temperature investigated, the molecular weight being assumed constant in each instance.

Lagemann and Corry [46] have shown how the value of R in Rao's relation may be predicted (for compounds of low molecular weight) from structural considerations, utilizing the additivity of "bond increments". In each mer unit of rubber (C_5H_8), for example, 8 C—H bonds would contribute 95.2 units each, 4 C—C bonds 4.25 each, and 1 C=C bond 129 units, for a total of 908. The value of R for the average molecule would then be 908 n and the molecular weight M would be 68.119 n, where n is an average degree of polymerization. Consequently the use of Lagemann and Cory's bond increments would predict a value of $908/68.119=13.33$ for R/M, the quantity given in table 8, col 5. The difference is about 4 percent.

Replacing v in Rao's eq (16) by the value given by eq (11) (G being assumed negligible in comparison with K_a), and differentiating with respect to T one obtains [47] at $P=0$:

$$\frac{\frac{1}{B_a}\frac{\partial B_a}{\partial T}}{\frac{1}{V}\frac{\partial V}{\partial T}}=7. \tag{17}$$

The left-hand member of this equation, as calculated from the numerical values at $P=0$ obtained in the present work, decreases from 8.3 at 0° to 7.2 at 40° for the unvulcanized rubber and from 7.4 at 0° to 6.6 at 40° for the peroxide-cured material.

The constants k_1 and A are, respectively, the dominant factors in determining the numerator and denominator of the left-hand member of eq (17). The ratio of their values as measured here, consequently, is approximately that derived using Rao's relation.

9. Values Predicted at Pressures Above 500 kg/cm^2

It is not intended that eq (1) through (5) be used for pressures above 500 kg/cm^2. It is well known from previous work that an expression involving higher powers of P is required instead of eq (1) for an adequate representation of the data.

For this purpose, the applicability of a relation known as the Tait equation has become increasingly apparent in recent years.[2] The validity of this form of relation in representing data on hydrocarbons with molecular weights as high as 350 has been demonstrated by Cutler, McMickle, Webb, and Schiessler [48]. These authors give references to several previous applications of the relation but it seems not to have received the attention it deserves. For example, it is not mentioned in the well-known treatise of Bridgman [9].

The Tait equation can be written:

$$\frac{V_0-V}{V_0}=c\log_{10}(1+P/b) \tag{18}$$

where b and c are constants.

A change to natural logarithms and a series expansion yield:

$$\frac{V_0-V}{V_0}=0.4343\,c\left[(P/b)-\frac{1}{2}(P/b)^2+\frac{1}{3}(P/b)^3-\ldots\right]. \tag{19}$$

From eq (1) if $\alpha=\alpha_{25}+k_1(t-25)$ and $\beta=\beta_{25}+k_2(t-25)$, one obtains

$$\frac{V_0-V}{V_0}=-\alpha P-\beta P^2. \tag{20}$$

It is apparent that eq (20) and its parent eq (1) represent only an approximation obtained by neglecting higher powers of pressure in eq (19). It is found on direct test that by the proper choice of constants b and c the Tait equation will yield as good agreement with observed values of volume as has already been shown in table 2 for the approximation. In other words, within the precision of our measurements the two equations are indistinguishable over the range of pressures below 500 kg/cm^2. At 25° our data for the unvulcanized rubber were well represented by $c=0.240$ and $b=2050$ kg/cm^2 in the Tait equation; for the peroxide-cured rubber the corresponding values were $c=0.193$ and $b=1640$ kg/cm^2.

Equation (20) was used in the present work below 500 kg/cm^2 because it is simpler than eq (18), and the coefficients can be evaluated more readily. In view of the excellent agreement of calculated and observed values shown in table 2, it was not considered necessary to use the complete expansion. In each equation, of course, the variation of the coefficients with temperature can be calculated from observations at different temperatures. Previous work [48] on nonpolymeric compounds has found c to be independent of temperature and to have a value near 0.2.

The success of the Tait equation in representing data for hydrocarbon liquids up to the highest pressures investigated suggested an examination of its applicability to rubber at pressures above 500 kg/cm^2. It was found that the data of Scott [11] (extending to about 800 kg/cm^2), Naunton [13] (extending to about 1750 kg/cm^2), Adams and Gibson [10] (extending to about 12,000 kg/cm^2), and Bridgman [12] (extending to 25,000 kg/cm^2) could all be well represented by expressions in the form of eq (18), with values of b in the range 1500–2200 kg/cm^2 and values of c in the neighborhood of 0.2. None of these authors had utilized the Tait equation.

In view of the results just mentioned, the Tait equation is suitable for representing the volume of rubber at all pressures up to the limit of observation. It is to be strongly preferred for the range above 500 kg/cm^2, where McPherson [13], for example, found it necessary to add a term involving P^3 to eq (1).

The compressibility, obtained by differentiation of eq (18), is

$$B=\frac{0.4343\,c}{P+b}. \tag{21}$$

A series expansion of this expression in powers of P shows that eq (3) also is an approximation valid only for low pressures.

10. Conclusions

The compressibility values and their coefficients describing changes with pressure and temperature are not far different from those estimated by extrapolation from Scott's data on the rubber-sulfur system. There is no significant change of compressibility on vulcanization with dicumyl peroxide, and the changes in the coefficients are slight.

The compressibility at 25° extrapolated to zero pressure (α_{25}) found here is slightly greater than that of cesium, the most compressible crystalline solid for which we have found values in the literature [49]. It is appreciably less than that of most normal organic liquids of low molecular weight. As already mentioned it is nearly the same as that of water, a distinctly abnormal liquid. This fact, while not of any obvious theoretical or structural significance, is of considerable practical importance since it becomes possible to make rubber vulcanizates which will have a minimum reflection or scattering of underwater sound waves, as already mentioned.

The value of α_{25} found here is essentially the same as that found by Jessup [50] to represent the compressibility of high viscosity petroleum oils (gas oils and lubricating oils) of the same specific volume as the rubber. This may be of theoretical significance since the structures involved may well be similar in all respects except molecular weight. Values given in the literature [51] for other organic oils (such as almond, castor, linseed, olive, and rapeseed oils) are nearly the same. Glycerine is apparently the only organic liquid appreciably less compressible than these.

[2] We thank Professor Robert Simha of the University of Southern California for bringing the Tait equation to our attention.

Most of the limited number of available literature values for other elastomers are not far different from those for natural rubber. The values for semi-crystalline polymers and polymers below their glass transition temperatures tend to be somewhat lower.

The thermal expansion coefficient A is also found to have essentially the same value as that given for the high viscosity petroleum oils [50].

From the compressibility values and their coefficients it has been shown that one may calculate values for a considerable number of other properties of rubber, obtaining good agreement with available direct experimental values. These include internal pressures, sound wave velocities, and specific heats.

We are indebted to Rachel J. Fanning for the purification and analysis of the sample of vulcanized rubber, and to Fred A. Quinn, Jr., for preparing the dilatometers used in this work.

11. References

[1] G. Gee, J. Stern, and L. R. G. Treloar, Volume changes in the stretching of vulcanized natural rubber, Trans. Faraday Soc. **46,** 1101 (1950).

[2] P. Thirion and R. Chasset, A study of the relation between tension and temperature at equilibrium. Chapter in book Rheology of Elastomers, ed P. Mason and N. Wookey, p. 17 (Pergamon Press, New York, 1958); Rev. Gen. Caoutchouc **36,** 873 (1959) (In English).

[3] A. T. McPherson, A method for the purification of rubber and properties of purified rubber, BS J. Research **8,** 751 (1932) RP449; Rubber Age **31,** 477 (1932); Rubber Chem. Technol. **5,** 523 (1932).

[4] D. E. Roberts and L. Mandelkern, Thermodynamics of crystallization in high polymers: natural rubber, J. Am. Chem. Soc. **77,** 781 (1955).

[5] G. M. Martin and L. Mandelkern, Effect of hydrostatic pressures on the crystallization kinetics of natural rubber, J. Appl. Phys. **34,** 2312 (1963).

[6] N. Bekkedahl, Volume dilatometry, J. Research NBS **43,** 145 (1949) RP2016.

[7] L. A. Wood, N. Bekkedahl, and F. L. Roth, Measurement of densities of synthetic rubbers, J. Research NBS **29,** 391 (1942) RP1507; Ind. Eng. Chem. **34,** 1291 (1942); Rubber Chem. Technol. **16,** 244 (1943).

[8] J. D. Ferry, Viscoelastic properties of polymers, p. 416, (John Wiley & Sons, Inc., New York, 1961).

[9] P. W. Bridgman, The physics of high pressure, p. 169, (G. Bell & Sons, Ltd., London, 1949).

[10] L. H. Adams and R. E. Gibson, The compressibility of rubber, J. Wash. Acad. Sci. **20,** 213 (1931); Rubber Chem. Technol. **3,** 555 (1930).

[11] A. H. Scott, Specific volume, compressibility, and volume thermal expansivity of rubber-sulfur compounds, J. Research NBS **14,** 99 (1935) RP760.

[12] P. W. Bridgman, The compression of 61 solid substances to 25,000 kg/cm² determined by a new rapid method. Proc. Am. Acad. Arts Sci. **76,** 9 (1944). See p. 238 Smithsonian Physical Tables 9th Edition. Ed by W. E. Forsythe. Smithsonian Inst. Wash., D.C. (1954).

[13] A. T. McPherson and A. Klemin, ed, Engineering uses of rubber, page 74. (Reinhold, New York, 1956.) Calculations are based on experimental data given by W. H. S. Naunton, Rubber in engineering, Ministry of Supply, London, 1945, p. 30.

[14] L. E. Copeland, Thermodynamics of a strained elastomer II. Compressibility, J. Appl. Phys. **19,** 445 (1948).

[15] C. E. Weir, Temperature dependence of compression of natural rubber-sulfur vulcanizates of high sulfur content, J. Research NBS **50,** 153 (1953).

[16] G. Allen, G. Gee, and G. J. Wilson, Intermolecular forces and chain flexibilities in polymers. I. Internal pressures and cohesive energy densities of simple liquids, Polymer **1,** 456 (1960).

[17] G. Allen, G. Gee, D. Mangaraj, S. Sims, and G. J. Wilson, Intermolecular forces and chain flexibilities in polymers II. Internal pressures of polymers, Polymer **1,** 467 (1960).

[18] G. Allen, D. Sims and G. J. Wilson, Intermolecular forces and chain flexibilities in polymers III. Internal pressures of polymers below their glass transition temperatures, Polymer **2,** 375 (1961).

[19] C. Rossi and U. Bianchi, Thermodynamic properties of high polymers: internal pressure, Chim. e Ind. (Milan) **44,** 1362 (1962).

[20] L. A. Wood, Chapter 10 in G. S. Whitby, Synthetic Rubber, p. 349 (John Wiley & Sons, Inc., New York, 1954).

[21] G. M. Bristow and W. F. Watson, Cohesive energy densities of polymers, Trans. Faraday Soc. **54,** 1731, 1742 (1958).

[22] Mark W. Zemansky, Heat and thermodynamics, Fourth Edition, p. 260 (McGraw-Hill, New York, 1957).

[23] N. Bekkedahl and H. Matheson, Heat capacity, entropy, and free energy of rubber hydrocarbon, J. Research NBS **15,** 503 (1935) RP844; Rubber Chem. Technol. **9,** 264 (1936).

[24] Lawrence E. Kinsler and Austin R. Frey, Fundamentals of acoustics, p. 352 (John Wiley & Sons, Inc. New York, 2d edition, 1962).

[25] Vernon M. Albers, Underwater acoustics handbook, p. 9 (Pennsylvania State University Press, University Park, Pa., 1960).

[26] D. G. Ivey, B. A. Mrowca, and E. Guth, Propagation of ultrasonic bulk waves in high polymers, J. Appl. Phys. **20,** 486 (1949); Rubber Chem. Technol. **23,** 172 (1950).

[27] P. Heydemann, The dynamic compressibility of high polymers in the frequency range 0.1 c/s to 60 kc/s, Acustica **9,** 446 (1959) (In English).

[28] B. F. Goodrich Co., Akron, Ohio, Brochure, Products-materials for underwater sound applications, 2d edition, July 1961.

[29] J. R. Cunningham and D. G. Ivey, Dynamic properties of various rubbers at high frequencies, J. Appl. Phys. **27,** 957 (1956).

[30] A. W. Nolle and S. C. Mowry, Measurement of ultrasonic bulk-wave propagation in high polymers, J. Acoustical Soc. Am. **20,** 432 (1948).

[31] A. W. Nolle, Dynamic mechanical properties of rubber-like materials, J. Polymer Sci. **5,** 1 (1950).

[32] W. S. Cramer and I. Silver, Acoustical properties of rubber as a function of chemical composition, NAVORD Report 1778, Feb. 1951, U.S. Naval Ordnance Lab., White Oak, Md.

[33] C. S. Sandler, An acoustic technique for measuring the effective dynamic bulk modulus of elasticity and associated loss factor of rubber and plastics, NAVORD Report 1534, Sept. 1950, U.S. Naval Ordnance Lab., White Oak, Md.

[34] Y. Wada, H. Hirose, H. Umebayashi, and M. Otomo, Volume viscoelasticity of polymers and other highly dissipative materials, J. Phys. Soc. Japan **15,** 2324 (1960) (In English).

[35] J. E. McKinney, H. V. Belcher, and R. S. Marvin, Dynamic compressibility of a rubber-sulfur vulcanizate and its relation to free volume, Trans. Soc. Rheol. **4,** 347 (1960).

[36] N. F. Barnes, General Electric Co., quoted in chapter by R. F. Boyer and R. S. Spencer in book Advances in Colloid Science, ed H. Mark and G. S. Whitby (Interscience, New York, 1946) Vol. II, p. 15.

[37] G. Natta and M. Baccaredda, Velocity of propagation of ultrasonic waves and the form of the molecules of high polymers, Gazzetta Chimica Italiana **79,** 364 (1949) Translated in Rubber Chem. Technol. **23,** 151 (1950).

[38] F. Levi and H. J. Philipp, Sound velocity in rubber, Helv. Phys. Acta **21,** 233 (1948).

[39] M. Greenspan and C. E. Tschiegg, Speed of sound in water by a direct method, J. Research NBS **59,** 249 (1957) RP2795; Results summarized in J. Acoust. Soc. Am. **31,** 75 (1959).
[40] Wayne D. Wilson, Speed of sound in distilled water as a function of temperature and pressure, J. Acoust. Soc. Am. **31,** 1067 (1959).
[41] Wayne D. Wilson, Speed of sound in sea water as a function of temperature, pressure, and salinity, J. Acoust. Soc. Amer. **32,** 641 (1960).
[41a] R. B. Montgomery, Chapter Oceanographic Data, p. 2–118 in American Institute of Physics Handbook, Dwight E. Gray, ed (McGraw-Hill, New York, 1957).
[42] Reference 22, p. 251.
[43] J. Rehner, Jr., Heat conduction and molecular structure in rubberlike polymers, J. Polymer Sci. **2,** 267 (1947).
[44] V. V. Tarassov, A theory of low temperature heat capacity of linear macromolecules, Compt. Rend. (Doklady) Acad. Sci. URSS **46,** 20, 110 (1945) (In English). Cf. J. Am. Chem. Soc. **80,** 5025 (1958).
[45] M. R. Rao, A relation between velocity of sound in liquids and molecular volume, Indian J. Phys. **14,** 109 (1940); Velocity of sound and chemical constitution, J. Chem. Phys. **9,** 682 (1941).
[46] R. T. Lagemann and J. E. Corry, Velocity of sound as a bond property, J. Chem. Phys. **10,** 759 (1942); R. T. Lagemann and W. S. Dunbar, Relationship between the velocity of sound and other physical properties of liquids, J. Phys. Chem. **49,** 428 (1945).
[47] T. Kishimoto and O. Nomoto, On molecular sound velocity of liquids I, J. Phys. Soc. Japan **9,** 59 (1954) (In English).
[48] W. G. Cutler, R. H. McMickle, W. Webb, and R. W. Schiessler, Study of the compressions of several high molecular weight hydrocarbons, J. Chem. Phys. **29,** 727 (1958).
[49] Reference 9, p. 165, 178, 180.
[50] R. S. Jessup, Compressibility and thermal expansion of petroleum oils in the range 0 to 300° C, BS J. Research **5,** 985 (1930) RP244.
[51] W. E. Forsythe, Editor, Smithsonian Physical Tables, 9th Edition, Smithsonian Institution, Washington, 1954, p. 282.

(Paper 68A3–271)

JOURNAL OF RESEARCH of the National Bureau of Standards—A. Physics and Chemistry
Vol. 68A, No. 3, May–June 1964

A Copolymer With Lamellar Morphology[1]

R. K. Eby[2]

(January 23, 1964)

Electron microscopy, together with wide- and small-angle x-ray diffraction studies, indicates that copolymers of tetrafluoroethylene and hexafluoropropylene are lamellar. The lamellar development is extensive; the lamellae can be broad and extend for many microns. The perfluoromethyl groups are incorporated within the lamellae as point defects.

1. Introduction

Recent work on the structure of polymer crystals has suggested the hypothesis that crystalline polymers consist entirely of lamellae into which the molecules are systematically folded [1].[3] In the extreme, this hypothesis implies that each molecule is completely within a crystal with no extensive interaction with any large amorphous regions. This in turn raises the possibility that some random copolymers may also be lamellar, with the comonomer units included in the crystal lattice as point defects. Indeed, there has been evidence for some time that random methyl groups do enter the polyethylene lattice [2, 3]. However, this evidence has not been universally admitted and it has been argued that exclusion of comonomer units from the crystal lattice would necessarily inhibit the development of lamellae in a copolymer [4].

The purpose of this paper is to present evidence that copolymers of tetrafluoroethylene and hexafluoropropylene are lamellar with the perfluoromethyl groups within the lattice as point defects. The same concepts were used by the author in earlier papers to present an analysis of the variation of copolymer transition temperature with comonomer ratio [5] and to describe the internal friction in copolymers of tetrafluoroethylene and hexafluoropropylene [6].

2. Experimental

Small-angle x-ray diffraction measurements were made on samples of copolymers with about 4, 11, and 17 mole percent hexafluoropropylene. Copper $K\alpha$ radiation, slit collimation, a Rigaku-Denki diffractometer, and a proportional counter were used for most of the measurements. The diffraction curves were corrected for air scatter and backgrounds were established graphically. In a few cases a Kratky diffractometer was used with a Geiger counter; the effects of white radiation were eliminated by the use of balanced Co and Ni filters.

Wide-angle x-ray diffraction measurements of the same copolymers were made with a powder camera using chromium $K\alpha$ radiation. The samples were cut with a square cross section of about 0.09 mm.[2] The camera was flushed with helium; temperature was measured with a thermocouple at the helium inlet. The films on which the diffraction patterns were recorded were corrected for shrinkage.

Electron microscopy was used to examine exterior surfaces of the polymers. These surfaces were formed by crystallizing the same copolymers in contact with air. Chromium shadow replicas were prepared and were examined with a Phillips Model 100 electron microscope.

For optical microscopy, thin films were prepared by melting and spreading a small amount of polymer on a microscope slide placed on a hot plate. After the crystallization induced by removing the slide from the hot plate, these films were examined by reflected light and between crossed polaroids by transmitted light.

3. Results and Discussion

Optical micrographs of a typical thin-film preparation of the intermediate copolymer are shown in figure 1. On the left, the exterior surface is shown in reflected light. Small morphological features can be seen but there is no evidence of larger structures such as spherulites. Similarly, when this region is viewed between crossed polaroids by transmitted light (as shown on the right side of fig. 1) birefringence is observed, but again large structures are not distinguished. This type of region, which is similar to some observed optically in polyethylene [7], is shown by electron micrography in figure 2. Structures which appear to be lamellae can be seen over all the surface. These are aggregated into what appear to be nuclei of many spherulites which impinged upon one another and could not grow more than a micron or two in a lateral direction. This effect, which may result from copious nucleation and/or slow growth, is avoided in thinner portions of the copolymer film where, for a fixed concentration, the nuclei are more widely separated.[4] An example of the spherulites produced in this case is shown by reflected light on the left side of figure 3. The spherulites can also be observed by transmitted light with crossed polaroids, as shown in the right-hand side of figure 3. Both methods of observation indicate the presence of radial structures. An electron micrograph of a

[1] Abstract in J. Appl. Phys. **34**, 2523 and 2532 (1963).
[2] Part of the reported research was performed while the author was employed by the Plastics Department, Du Pont Experimental Station, Wilmington, Del.
[3] Figures in brackets indicate the literature references at the end of this paper.
[4] Also, heating the molten copolymers to higher temperatures was found to reduce the concentration of nuclei.

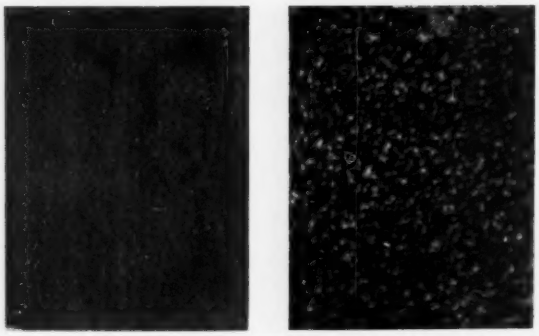

FIGURE 1. *Optical micrographs of a thin film of the intermediate copolymer crystallized from the melt.*

Left: reflected light; right: transmitted light with crossed polaroids.

similar surface is shown in figure 4. Here are seen the more fully developed spherulites characteristic of the thinner film portions. The radial lamellar development is extensive. Individual lamellae are broad and can be followed for many microns. The lamellar nature of the copolmyer is even more evident at higher magnifications as in figure 5 (an enlargement of the upper portion of fig. 4) and in figure 6. In the copolymers with fewer and more perfluoromethyl groups, the structure is similar except that the lamellae are thicker in the former and thinner and much less regularly developed in the latter.

Three questions may be asked about these apparently lamellar structures. Are they artifacts of the surface or are they lamellae and characteristic of the whole material? Are they anomalies associated with very low molecular weight components which might have been in the original polymer or might have been formed as degradation products? Are they composed of uninterrupted homopolymer sequences or are they truly copolymeric in composition?

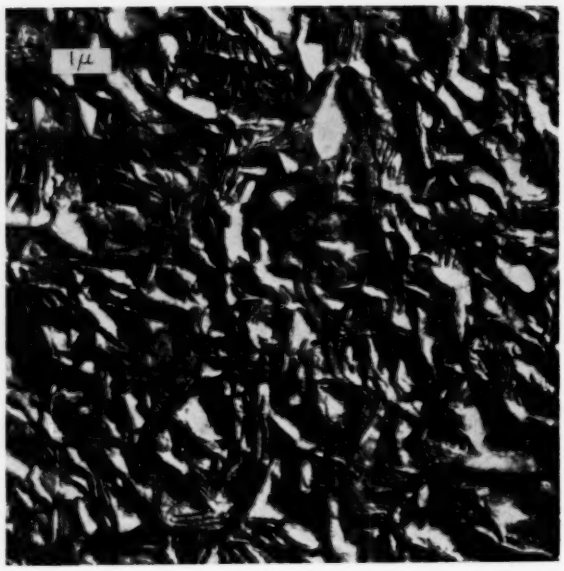

FIGURE 2. *Electron micrograph of a surface similar to that in figure 1.*

Apparently lamellar structures can be seen.

Examination of the diffraction of x rays at small angles showed that samples similar to those used to obtain the micrographs in figure 1 produced dif-

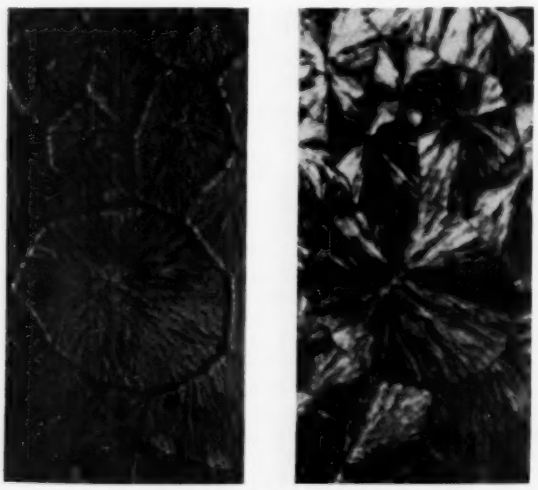

FIGURE 3. *Optical micrographs showing spherulites in a thinner portion of the film in figure 1.*

Left: reflected light; right: transmitted light with crossed polaroids.

FIGURE 4. *Electron micrograph of a surface similar to that in figure 3.*

FIGURE 5. *Enlargement of the upper portion of the electron micrograph in figure 4.*

Lamellar development can be seen. This figure also shows other structural features which are sometimes observed (right center).

FIGURE 6. *Electron micrograph of another region in which lamellar structures are apparent.*

fraction maxima.[5] The Bragg spacings calculated from these diffraction maxima are shown in table 1 where they are compared with the average dimensions of the lamellar structures measured on the electron micrographs. These agree to a degree which is better than should be expected considering the samples and techniques involved. More importantly, however, the data in table 1 show that as the hexafluoropropylene content is increased, the dimensions determined by electron microscopy and by x-ray diffraction decrease in the same fashion.[6] Finally, a piece cut from the center of a bulk sample of copolymer exhibits a diffraction pattern similar to those obtained with the thinner samples. As figure 7 shows, this pattern, which was obtained with a Kratky diffractometer, exhibits only one maximum over a wide angular range. This result is different from that obtained with polyethylene [8] and indicates the absence of a second periodic structure with a period near the lamella thickness. While a few structures in figure 5 resemble the second

TABLE 1. *Comparison of lamella thicknesses determined by electron microscopy and x-ray diffraction*

Electron micrographs	X-ray diffraction
Å	Å
420	450
335	285
260	230

[5] These samples were slightly thicker and had a thermal history similar to that of the samples used in microscopy.

[6] This decrease is similar to that which is observed with increasing methyl concentration in polyethylene [8]. Both these samples and the present ones were crystallized by cooling at some rate rather than isothermally.

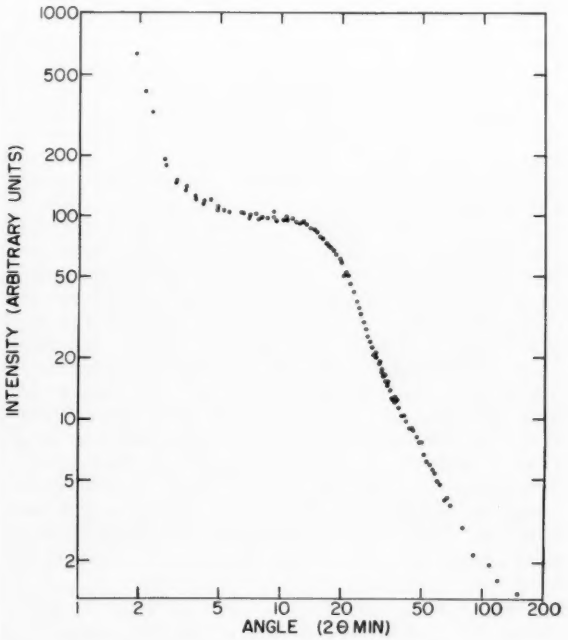

FIGURE 7. *Intensity of diffracted x rays as a function of angle for copper Kα radiation and a piece of the intermediate copolymer cut from a bulk sample.*

Only one diffraction maximum can be definitely identified.

structures observed in polyethylene [9], they appear to be larger and less regular than those in polyethylene and may be a consequence of material depletion at the surface. (Near 55 minutes—95Å–, there may be a small second maximum which would not correspond to the results of electron microscopy. This maximum, which is too small to be definitely identified in figure 7, would be relatively smaller and at a relatively larger angle than the second maximum of polyethylene.) In any event, the results show that the surface structures are indeed lamellae and characteristic of the whole sample.

Observations of the melting temperature of the copolymer films shown in figures 1 and 3 show them to melt at very nearly the same temperature as does the bulk copolymer. Also, the large spherulites can be melted and recrystallized in the more common morphology. These results indicate that the illustrated lamellar regions are not anomalies associated with very low molecular weight components segregated upon preparation of the films.

A statistical analysis based on a consideration of lamellar thickness and the concentration of random perfluoromethyl groups in each of these copolymers indicates that less than one percent of the material can be in homopolymer sequences as long as the lamellar thickness. (Orientation of the molecular axis with respect to the lamellae has not been uniquely determined. The birefringence of the spherulites is consistent with a predominantly tangential orientation of the axis. This observation is consistent with the axis being alined in the direction of lamella thickness. In any event, this alinement permits the largest statistical fraction of sufficiently long homopolymer sequences since the smallest lamella dimension is the thickness.) Even in the unlikely event that *all* these segments could be incorporated into lamellar crystals, they would contribute very little to small-angle diffraction and would not constitute enough material to account for the surface lamellae in two of the cases. In connection with this analysis, it should be noted that the difficulty of polymerizing polyhexafluoropropylene indicates that consecutive hexafluoropropylene units are not likely to occur in the copolymer [10]. Thus it seems that the lamellae contain the perfluoromethyl groups. As shown by figure 6 of reference 6, Stuart-Briegleb molecular models suggest that perfluoromethyl groups can enter the lattice and that the groups would resemble interstitial defects found in atomic solids. This would result in localized disturbance of adjacent molecular rows (shown schematically in figure 1 of reference 5) and should cause an increase in the associated lattice dimension [3]. Wide-angle x-ray diffraction measurements offer evidence for this. The separation of the molecular axes at 23 °C in the intermediate copolymer is 5.76 Å, which is larger than that in polytetrafluoroethylene, 5.66 Å.[7] Thus, it seems reasonable to conclude that the observed variation is a consequence of the presence of point defects in the lattice and supports the results of the above analysis.[8]

4. Conclusion

Evidence is presented that these copolymers are lamellar with the comonomer units included in the lattice as point defects instead of being excluded and forming a separate amorphous phase. The lamella thickness decreases with increasing comonomer content, and lamellar development is extensive; the lamellae can be broad and extend for many microns. It seems probable that this may be the situation in many other copolymers and that the variation of physical properties with comonomer concentration must be thought of in terms of the energetic, configurational, and morphological consequences of the point defects [5, 6].

5. References

[1] P. H. Geil, J. Polymer Sci. **47,** 65 (1960); R. Eppe, E. W. Fischer and H. A. Stuart, J. Polymer Sci. **34,** 721 (1959).

[2] E. R. Walter and F. P. Reding, J. Polymer Sci. **21,** 561 (1956); R. M. Eichorn, J. Polymer Sci. **31,** 197 (1958); C. Sella, Compt. Rend. **248,** 2348 (1959); E. A. Cole and D. R. Holmes, J. Polmer Sci. **46,** 245 (1960); P. H. Geil, J. Polmer Sci. **51,** 510 (1961); P. R. Swan, J. Polymer Sci. **56,** 409 (1962).

[3] J. D. Eshelby, J. Appl. Phys. **25,** 255 (1954); R. W. Balluffi and R. O. Simmons, J. Appl. Phys. **31,** 2284 (1960).

[4] P. J. Flory, J. Am. Chem. Soc. **84,** 2857 (1962).

[5] R. K. Eby, J. Appl. Phys. **34,** 2442 (1963).

[6] R. K. Eby and F. C. Wilson, J. Appl. Phys. **33,** 2951 (1962).

[7] W. Banks, J. N. Hay, A. Sharples, and G. T. Thomson, Nature **194,** 542 (1962).

[8] H. Hendus, Ergeb. Exakt Naturw. **31,** 331 (1959).

[9] F. R. Anderson in Electron Microscopy (Academic Press, New York, 1962), Vol. **I** p. BB–4.

[10] H. S. Eleuterio and E. P. Moore (to be published). See also preprints of 2d International Fluorocarbon Symposium, Estes Park, Colo., June 1962.

[11] R. G. Brown and R. K. Eby, J. Appl. Phys. **35,** 1156 (1964).

(Paper 68A3–272)

[7] It is difficult to make a correction for film shrinkage because the copolymer did not produce many lines at large angles. However, more accurate measurements using a diffractometer and an internal standard also show the separation of the molecular axes in the copolymer to be larger (R. K. Eby and L. H. Bolz, to be published). These measurements also show that the dimension of the copolymer is larger below the first order transitions. This eliminates the possibility that the copolymer dimension is larger at 23 °C merely because it is at a higher temperature with respect to its transition temperature than is polytetrafluoroethylene.

[8] For even thinner lamellae (190 to 440 Å) the unit cell of polyethylene does not exhibit any detectable variation with lamella thickness [11]. This suggests that in this range lamella thickness does not influence unit cell dimension.

JOURNAL OF RESEARCH of the National Bureau of Standards—A. Physics and Chemistry
Vol. 68A, No. 3, May–June 1964

Variation of Glass Temperature With Pressure in Polypropylene

Elio Passaglia and Gordon M. Martin

(February 3, 1964)

By measurement of the specific volume of polypropylene as a function of temperature at various pressures, the variation of glass temperature with pressure, dT_g/dP, was determined. Within experimental error the magnitude of this quantity is the same as the value of $T\bar{v}\Delta\alpha/\Delta C_p$, where $\Delta\alpha$ and ΔC_p are the change in coefficient of expansion and specific heat respectively at the glass temperature. This is an indication that thermodynamics can be applied to the glass transition. The value of dT_g/dP is the same as $\Delta\beta/\Delta\alpha$, where $\Delta\beta$ is the change in compressibility at T_g calculated from the data, but it is shown that this equality must follow as a consequence of the manner in which the experiments were carried out, quite independently of the application of thermodynamics.

1. Introduction

The glass transition as normally observed is almost certainly a consequence of relaxation times associated with molecular motion becoming inordinately long over a small temperature interval as the temperature is lowered to the transition. Nevertheless, the glass transition shows some of the characteristics of an Ehrenfest second-order transition, and indeed a second-order transition associated with the glass transition has been shown to exist on theoretical grounds [1],[1] and this view has some experimental justification [2, 3].

For a second-order transition, two equations, generally called the Ehrenfest equations, hold:

$$\frac{dT}{dP}=\frac{\Delta\beta}{\Delta\alpha} \tag{1}$$

$$\frac{dT}{dP}=\frac{T\bar{v}\Delta\alpha}{\Delta C_p} \tag{2}$$

where T is the transition temperature, P the pressure, $\bar{v}$ the specific volume, and $\Delta\alpha$, $\Delta\beta$, and ΔC_p are the changes at the transition in thermal expansion coefficient, compressibility, and the specific heat, respectively.

In spite of the difficulty of applying thermodynamics to the glass [3], it has been shown that these relations would hold for a glass transition [4], provided this is caused by the abrupt change with temperature of some "ordering parameter" z, and that the glass can be considered as having a definite "frozen in" value of z. In this case, dT/dP should be replaced with $(\partial T/\partial P)z$. However, if more than one ordering parameter exists, or more than one type of order changes suddenly at the glass transition, then it is shown that [4]

$$\frac{T\bar{v}\Delta\alpha}{\Delta C_p}\leq\frac{\Delta\beta}{\Delta\alpha}. \tag{3}$$

It is therefore clear that although eqs (1) and (2) of necessity must be obeyed at a second-order transition, the mere fact that they are obeyed does not insure that the transition in question is a second-order transition.

Data of the type necessary to check the applicability of eqs (1) and (2) to the glass transition are relatively scarce for polymers [5, 6]. In particular, measurements of specific heat are lacking. Recently, however, three independent measurements of the specific heat of atactic polypropylene through the glass transition region have been made [2, 7, 8], so that measurements of glass temperature at various pressures for this material would permit checking the applicability of eqs (1) and (2). It is the purpose of this paper to report the result of such measurements.

2. Experimental Detail

2.1. Apparatus

The apparatus used for measuring volume as a function of temperature at various pressures has been previously described [9]. In this apparatus a glass dilatometer of standard design using mercury as the confining liquid is placed in a chamber in which the pressure may be varied from atmospheric pressure to 1000 kg/cm². The chamber is fitted with windows so that changes of mercury level in the dilatometer tube may be followed with a cathetometer. The whole assembly is placed in a thermostated bath capable of controlling the temperature within ±0.05 °C at any point in the range −30 °C to +150 °C.

2.2. Materials

The polypropylene used for this study was provided by the Avisun Corporation, and was the same material as that previously used for calorimetric studies [2]. It had a viscosity average molecular weight of 15,700. The sample was 2 to 3 percent crystalline; hence it contained some isotactic polymer. Evacuation of a specimen in a vacuum desiccator for a week produced a loss of 0.09 percent in weight, so that contamination by solvents was minimal.

[1] Figures in brackets indicate the literature reference at the end of this paper.

2.3. Procedure

Measurements of volume were taken between +30 °C and −30 °C. In all cases the temperature was raised to +30 °C, pressure applied, and the temperature lowered in 10, 5, or 2½ deg intervals. At each temperature in and below the transition range a minimum of 1 hr, and often several hours, were allowed for equilibrium to be attained. When the lowest temperature was reached, measurements were repeated by raising the temperature. In most of the experiments the data taken with rising temperature below T_g did not exactly check the data taken with decreasing temperature. This is to be expected when the behavior is relaxational in character.

Data were taken at atmospheric pressure and at pressures of 150, 300, 400, 500, and 700 kg/cm².

The pressure equipment did not permit the attainment of a low enough temperature to give an unambiguous value for T_g at atmospheric pressure. For this measurement, the dilatometer, without the pressure chamber, was placed in another refrigerated bath capable of reaching −40 °C, and measurements were taken down to −38 °C. For this experiment at least 24 hr were allowed for equilibrium for all temperatures below −5 °C, and no difference was observed between the data taken with temperature decreasing or increasing. As will be seen, the glass temperature obtained in this way was somewhat lower than would have been predicted from the other experiments.

3. Results

From the results of the volume-temperature measurements, the specific volume of the polymer was calculated in the usual way. For ease in plotting the data the arbitrary straight line

$$\bar{v}=1.150 \times 10^{-4}t+1.1075,$$

where t is the temperature in degrees C, has been subtracted from the observed data and the resulting values are shown in figure 1. It will be apparent that the agreement of the data taken with rising and falling temperature is excellent above the transition temperature.

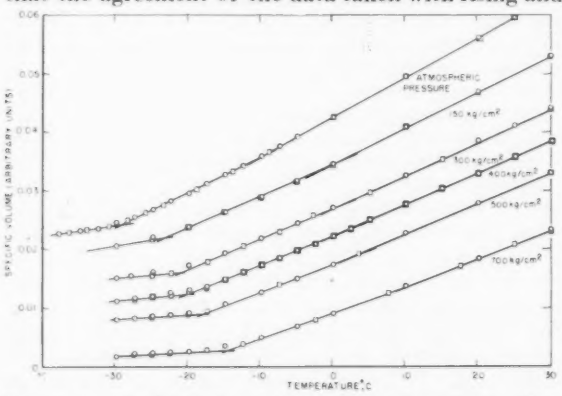

FIGURE 1. *A plot of the specific volume minus the line* $\bar{v}=1.150\times10^{-4}t+1.1075$ *as a function of temperature at various pressures.*

Note the evidence for a second break in the curves some 20 to 25 °C above th main break.

○, cooling.
□, heating.

It will also be apparent that there is a suggestion in each curve of *two* breaks, a small subtle one occurring some 20 deg above the main break. This is much more apparent when plotted on a larger scale. Indeed, it was attempted to fit the curve above the main break by the method of least squares using either two straight lines or a third degree polynomial. Both equations gave the same precision of fit as determined by the residuals, so no judgment about the existence of a second transition could be made on this basis. It cannot be argued that this behavior is due to nonattainment of equilibrium leading to curvature, as always happens near T_g, for the temperature range is too broad, the agreement between the data taken with rising and falling temperatures is excellent, and this type of curvature is limited in the present curves to a region about 5 deg wide near T_g.

Since the present sample does contain some isotactic material and there is evidence that the glass temperature for isotactic polypropylene is higher than that for the atactic [2, 7], it could be assumed that this upper transition is a result of the presence of the isotactic component. This would imply that the atactic polymer is a block copolymer. While such an interpretation of the upper transition is not unreasonable, further discussion would be speculation, and we shall ignore the upper transition, if, indeed, it exists.

The glass temperature was taken as the intersection of the line determined by the lowest temperature data observed with rising temperature, and the line determined by the data for the next 20 or so degrees. If the highest temperature data had been used to determine the $\bar{v}-T$ characteristics of the liquid, all the transition temperatures would be 2 to 3 deg higher, but none of the other conclusions of this paper would be changed.

The glass transition temperatures obtained from these results are shown in table 1. The atmospheric pressure result is somewhat lower than previously reported [2, 7, 8]. Part of the difference may result from the method of analysis, namely, taking the intersection of the lowest straight line with the line defined by the points between −5 and −25 °C, but no doubt part is also due to the very slow rate at which this experiment was conducted.

The table also gives values of $\frac{1}{\bar{v}}\frac{\partial v}{\partial T}$, the coefficient of expansion at T_g for the glass and the liquid, and the difference in this quantity at T_g. To calculate the values of $\partial\bar{v}/\partial T$ above T_g only the highest tem-

TABLE 1. *Glass transition temperatures and coefficients of expansion at* T_g *for the glass and liquid*

P	T_g	α_g	α_l	$\Delta\alpha$
kg/cm²	°C	°C⁻¹	°C⁻¹	°C⁻¹
0	−29.5	2.39×10⁻⁴	6.80×10⁻⁴	4.41×10⁻⁴
150	−24.0	2.64	6.47	3.83
300	−21.7	2.14	6.09	3.95
400	−20.7	2.06	5.89	3.83
500	−19.0	1.29	5.68	3.79
700	−14.7	1.62	5.24	3.62

perature data were used. The value of $\Delta\alpha$ at zero pressure determined by a least squares fit of the data for $\Delta\alpha$ as a function of pressure to a straight line is 4.22×10^{-4} with a computed standard error of 0.12×10^{-4} °C^{-1}.

A plot of T_g against the pressure is shown in figure 2. As was noted above, the value of T_g obtained for the experiment at atmospheric pressure is somewhat lower than would have been expected from our other results. This is no doubt due to the slow rate of this experiment. A least squares fit of these data with a straight line gave a value of 0.020 °C/kg cm^{-2} for dT_g/dP, with a computed standard error of 0.002 °C/kg cm^{-2}. The value is in accord with measurements on other polymers [5, 6].

3.1. Compressibility

A determination of the compressibility difference at T_g requires a determination of the compressibility at various temperatures above and below T_g and extrapolation of the results to T_g. Because of the paucity of data below T_g, only one determination, at −30 °C, was made.

The results for specific volume as a function of pressure at various temperatures are shown in figure 3. The curves require a little comment. The specific volume data could be represented by slightly curved lines curving in the direction to be expected [10]. For the purposes of this paper, the curves were approximated by straight lines, which is an adequate approximation to the volume-pressure relation in this pressure range. The line at −10 °C was obtained by extrapolating the volume-temperature curves from higher temperatures to this temperature. The compressibilities, which were calculated from these lines by dividing the slope by the specific volume at zero pressure at the temperature in question, are shown in figure 4, and listed in table 2. The value of the compressibility of the liquid extrapolated to −30 °C is also given. The value of $\Delta\beta$ at this temperature is 0.87×10^{-5} cm^{-2}/kg, with limits of error estimated subjectively not to exceed $\pm0.04\times10^{-5}$ cm^2/kg.

TABLE 2. *Compressibility at various temperatures for the glass and liquid*

T	β_l	β_g
°C	cm²/kg	cm²/kg
30	4.93×10^{-4}	
20	4.62	
10	4.46	
0	4.23	
−10	4.16	
−30	[1] 3.77	2.90×10^{-5}

[1] Extrapolated value.

3.2. Comparison of Results

Table 3 gives a comparison of the value of dT_g/dP with the values of $\Delta\beta/\Delta\alpha$ and $T\bar{v}\Delta\alpha/\Delta C_p$. The latter was calculated using the specific heat results of Passaglia and Kevorkian [2]; Dainton, Evans, Hoare, and Melia [7]; Wilkinson and Dole [8]. The agreement among the three quantities is seen to be quite satisfactory.

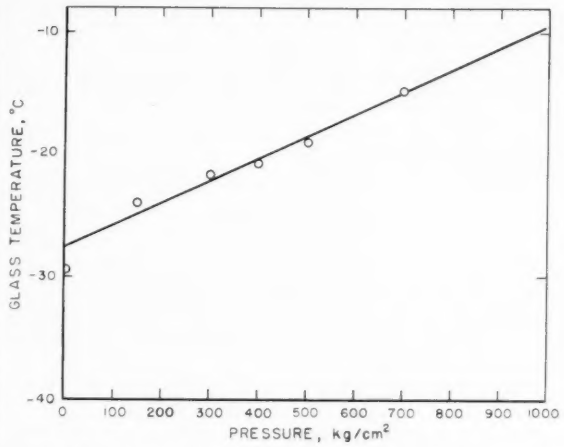

FIGURE 2. *The glass temperature, as determined from figure 1, as a function of gage pressure.*

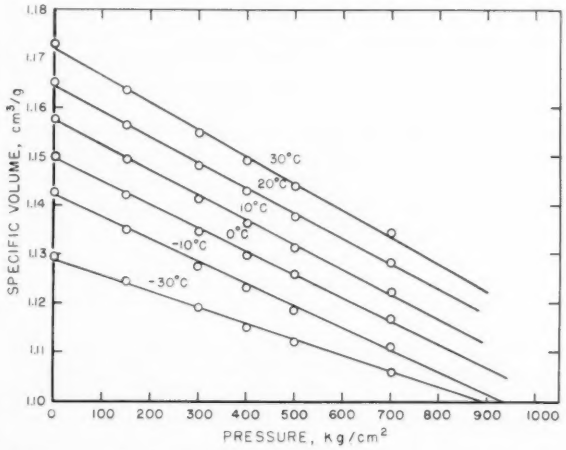

FIGURE 3. *The specific volume at various temperatures as a function of gage pressure.*

The curve at −30 °C is for the material below T_g.

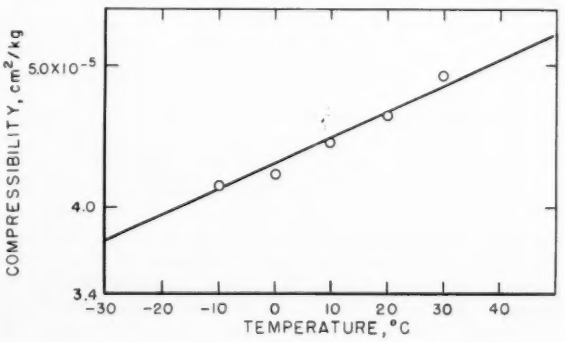

FIGURE 4. *The compressibility,* $\frac{-1}{\bar{v}}\frac{\partial\bar{v}}{\partial P}$, *at zero pressure, as calculated from figure 3, as a function of temperature.*

All the points are for material above T_g.

TABLE 3. *Values of terms in the Ehrenfest equations*

dT_g/dP	$\Delta\beta/\Delta\alpha$	$T\bar{v}\Delta\alpha/\Delta C_p$
°C/kg cm^{-2}	°C/kg cm^{-2}	°C/kg cm^{-2}
0.020 ±0.004*	0.021 ±0.002†	0.024 ±0.001‡

*Twice the computed standard error.
†Subjectively estimated maximum error.
‡Computed from the error in $\Delta\alpha$ alone; T, $\bar{v}$, ΔC_p considered to be error free.

4. Discussion

The agreement between the values of dT_g/dP and $T\bar{v}\Delta\alpha/\Delta C_p$ is in accord with the previous results of O'Reilly [5] on polyvinyl acetate, and we concur with his conclusion that thermodynamics may be applied to the glass transition.

The agreement between $T\bar{v}\Delta\alpha/\Delta C_p$ and $\Delta\beta/\Delta\alpha$ requires more comment. O'Reilly did not observe agreement between these two quantities: they found $\Delta\beta/\Delta\alpha > T\bar{v}\Delta\alpha/\Delta C_p$, which would imply more than one "ordering parameter" at the glass transition. In our own case the agreement between $\Delta\beta/\Delta\alpha$ and $T\bar{v}\Delta\alpha/\Delta C_p$ would imply either a single ordering parameter or indeed a true second-order transition.

However, the agreement between $\Delta\beta/\Delta\alpha$ and dT_g/dP is not a consequence of thermodynamics, but a consequence of the manner in which the experiments were carried out and the results analyzed. For consider the idealized case of figure 1: below the glass-transition temperature, any one of the normalized volume-temperature curves can be represented in the region of interest by

$$\frac{\bar{v}}{\bar{v}_g}=\gamma_g+\alpha_g T \tag{4}$$

where $\bar{v}_g$ is the specific volume at T_g, α_g is the coefficient of expansion, and γ_g is a constant for a particular curve. These quantities are, of course, functions of the pressure. Above T_g the analogous equation is

$$\bar{v}/\bar{v}_g=\gamma_l+\alpha_l T. \tag{5}$$

Clearly T_g is given by the intersection of these two lines, or

$$T_g=\frac{\gamma_l-\gamma_g}{\alpha_g-\alpha_l}=\frac{-\Delta\gamma}{\Delta\alpha}. \tag{6}$$

Consequently, we obtain

$$dT_g/dP=-\frac{1}{\Delta\alpha}\frac{d\Delta\gamma}{dP}+\frac{\Delta\gamma}{\Delta\alpha^2}\frac{d\Delta\alpha}{dP} \tag{7}$$

which relates the change with pressure of T_g with the pressure variations of the constants of the $\bar{v}-T$ curves above and below T_g. Now consider how $\Delta\beta$ is determined from data of this type. By definition, we have,

$$\beta=-\frac{1}{\bar{v}}\frac{\partial\bar{v}}{\partial P}.$$

Hence we have, using eqs (4) and (5)

$$\beta_g=-\frac{\bar{v}_g}{\bar{v}}\left(\frac{d\gamma_g}{dP}+T\frac{d\alpha_g}{dP}\right)-\frac{1}{\bar{v}}(\gamma_g+\alpha_g T)\frac{d\bar{v}_g}{dP}$$

and

$$\beta_l=-\frac{\bar{v}_g}{\bar{v}}\left(\frac{d\gamma_l}{dP}+T\frac{d\alpha_l}{dP}\right)-\frac{1}{\bar{v}}(\gamma_l+\alpha_l T)\frac{d\bar{v}_g}{dP}. \tag{8}$$

At $T=T_g$, noting that $\gamma_l+\alpha_l T_g=\gamma_g+\alpha_g T_g=1$, we have

$$\Delta\beta=\beta_l-\beta_g=\frac{-d\Delta\gamma}{dP}-T_g\frac{d\Delta\alpha}{dP}. \tag{9}$$

Using the value of T_g from eq (6), we obtain finally

$$\frac{\Delta\beta}{\Delta\alpha}=-\frac{1}{\Delta\alpha}\frac{d\Delta\gamma}{dP}+\frac{\Delta\gamma}{\Delta\alpha^2}\frac{d\Delta\alpha}{dP}$$

which is identical to eq (7). Hence as long as experiments are performed in this way and as long as the volume-temperature curves can be approximated by straight lines over the region of interest, $\Delta\beta/\Delta\alpha$ *must* be equal to dT_g/dP.

To say this another way, these measurements of $\bar{v}$ as a function of T and P define a surface in $\bar{v}$, T, P space. So long as we operate only on this surface, then eq (1) follows as a geometric consequence, even though the surface may not represent a thermodynamic equilibrium surface. Only if we were to do another experiment (e.g., measure $\bar{v}$ as a function of P at various temperatures) to map out the same surface could we make any statement about the applicability of thermodynamics.

5. Conclusions

By measurement of specific volume as a function of temperatures at various pressures, dT_g/dP and $\Delta\beta/\Delta\alpha$ were calculated. These quantities agreed within experimental error, and it is shown that they must. The agreement of these quantities with $T\bar{v}\Delta\alpha/\Delta C_p$ indicates that thermodynamics may be applied to the glass transition.

6. References

[1] J. H. Gibbs and E. A. DiMarzio, J. Chem. Phys. **28,** 373 (1958).
[2] E. Passaglia and H. K. Kevorkian, J. Appl. Phys. **34,** 90 (1963).
[3] W. Kauzmann, Chem. Rev. **43,** 219 (1948).
[4] R. O. Davies and G. O. Jones, Proc. Roy. Soc. **A217,** 26 (1953); Adv. in Phys. **2,** 370 (1953).
[5] J. M. O'Reilly, J. Polymer Sci. **57,** 429 (1962).
[6] J. E. McKinney and H. V. Belcher, J. Res. NBS **67A,** No. 1, 43 (1963).
[7] F. S. Dainton, D. M. Evans, F. E. Hoare, and T. P. Melia, Polymer **3,** 286 (1962).
[8] R. W. Wilkinson and M. Dole, J. Polymer Sci. **58,** 1089 (1962).
[9] G. M. Martin and L. Mandelkern, J. Appl. Phys. **34,** 2312 (1963).
[10] L. A. Wood, to be published.

(Paper 68A3–273)

JOURNAL OF RESEARCH of the National Bureau of Standards—A. Physics and Chemistry
Vol. 68A, No. 3, May–June 1964

Perfluorophenyl Ether and Related Polymers[1]

Walter J. Pummer and Leo A. Wall

The syntheses of perfluorophenyl ether and poly(perfluorophenylene ethers) are described. These materials were prepared by the reaction between potassium pentafluorophenoxide and hexafluorobenzene in different solvents with varying conditions of temperature and pressure. In dimethylformamide or tetrahydrofuran, potassium pentafluorophenoxide shows little tendency to react with hexafluorobenzene. In methanol, only exchange products such as pentafluoroanisole were observed. No polymers were obtained in these solvents. In water, the reactivity of pentafluorophenoxide salts was increased greatly, for reaction occurs readily with or without the presence of hexafluorobenzene. The reactions in aqueous systems are complex and give rise to a variety of products. From these reactions the following compounds were isolated and identified: perfluorophenyl ether, bis(pentafluorophenoxy)tetrafluorobenzene, 2,4,5,6-tetrafluororesorcinol, pentafluorophenoxytetrafluorophenol, and various polyperfluorophenylene ethers of varying chain lengths. Identification of the smaller molecules was made by chemical, mass spectrometer, infrared, and nuclear magnetic resonance analyses. Poly(perfluorophenylene ethers) were prepared having molecular weights of 1700, 4300, 6500, and 12,500. A crosslinked polyether of this type was also synthesized, which had rubbery characteristics above 90 °C.

1. Introduction

The synthesis of perfluorophenyl ether has been the object of research by investigators in the aromatic fluorine field for many years. From this compound, thermal stability data could be obtained which may be applicable to polyfluorophenylene ethers. Interest in this compound developed because polyperfluorophenyl [1][2] synthezised in this laboratory had some undesirable physical properties, such as brittleness and insolubility. These properties could possibly be improved by the incorporation of some atom or groups of atoms between the phenyl rings to introduce bond angles other than 180°. Since aryl ethers are among the more stable organic compounds [2, 3], it appeared likely that the poly(perfluorophenylene ethers) (PPPE) may have good thermal stability as well as improved physical characteristics.

Partially fluorinated diphenyl ethers have been prepared by Ullman reactions involving phenolic salts and a halobenzene with copper catalysts at high temperatures in sealed tubes. By this method, 3(trifluoromethyl)phenyl ether [4] and pentafluorophenyl phenyl ether [5] were synthesized. Still other types of fluorophenyl ethers [6, 7] were obtained as byproducts from various nucleophilic reactions.

Some polymers of fluoroaromatic ethers have also been reported. Poly(perfluorophenylene ether) [8] and polyperfluorophenylene thioether [9] were obtained by thermal decomposition of sodium pentafluorophenoxide and potassium pentafluorothiophenol, respectively. Haszeldine [10] has also reported a polyfluoro ether obtained from 2,3,4,5,6-pentafluorobenzyl alcohol.

In an earlier report [5] we disclosed the first synthesis of perfluorophenyl ether. The present article describes some other syntheses of this compound as well as the pertinent details relating to its structure and identification.

2. Pentafluorophenol

Since most of the projected syntheses of perfluorophenyl ether involved the use of pentafluorophenol or its salts, an improved simple process was needed for the synthesis of pentafluorophenol. This intermediate was prepared previously [11–13], however in these methods separation problems were often encountered. The reactions of aqueous ammonia or alkyl amines with hexafluorobenzene gave excellent yields of the various substituted pentafluoroanilines [5]. On this basis, it appeared that an aqueous medium may also be useful for the preparation of pentafluorophenol. An attempt to synthesize pentafluorophenol in aqueous sodium hydroxide from hexafluorobenzene was unsuccessful [13], but aqueous potassium hydroxide [5] and hexafluorobenzene gave consistently good results. The best results [5] were obtained by employing a slight excess over the stoichimetric amount of hexafluorobenzene in relation to the base used, with the reaction conducted in a closed pressure vessel at 175 °C for 5 hr. The potassium pentafluorophenoxide, precipitated upon cooling, is usually pure enough for subsequent reactions. The yields range between 80 and 85 percent.

[1] Based on research supported by the Bureau of Naval Weapons, Department of the Navy. Presented as part of the Symposium on Fluorine Chemistry Division of Industrial and Engineering Chemistry at the 145th Meeting of the American Chemical Society, New York, N.Y., September 1963.

[2] Figures in brackets indicate the literature references at the end of this paper.

Various catalysts such as iron filings, copper powder, or copper oxide cause the reaction to occur as low as 120 °C, but the conversion is lower and longer reaction times are required. In the presence of excess base, high temperature (190 °C), and long reaction times (20 hr), only carbonlike solids were obtained; at 150 °C for 5 hr only slight indication of reaction was observed and 77 percent of the hexafluorobenzene was recovered.

From this latter reaction, however, there was isolated a new tetrafluorodihydroxybenzene. This compound was distillable without decomposition and solidified upon cooling (mp 95 to 96 °C). It was water soluble and gave the characteristic blue ferric chloride test for phenols. Chemical and mass spectrometer (parent peak at 182 mass units) analyses furnished further evidence as to its structure. The near infrared spectra in carbon tetrachloride solution showed the hydroxyl band at 3570 cm^{-1}, which is characteristic of these fluorophenols (see table 1, B). It is of interest to note that this compound does not exhibit the split hydroxyl band in this region, which may have been indicative of the ortho isomer [5]. In the 1100–1350 cm^{-1} region, the C–F absorption occurs at 1105 cm^{-1} and again at 1300 cm^{-1}. Definite assignment of other structural characteristics becomes uncertain in this region because of the C–F absorption even though aromatic fluorine absorption is less in this region than the aliphatic. However, by comparison with some other spectra of fluorine-containing compounds, the band at 1235 cm^{-1} region is peculiar to phenolic-type compounds and may be due to the OH deformation vibration [16]. The para isomer, i.e., 2,3,5,6-tetrafluorohydroquinone, has been synthesized previously [14, 15], but its melting point is much higher (168 to 169 °C). Therefore our compound could only be the ortho or meta isomer. Examination by nuclear magnetic resonance spectra has definitely eliminated the ortho isomer. Therefore, the compound isolated from the above reaction must be tetrafluororesorcinol.

3. Perfluorophenyl Ether

Application of the procedures [5] by which the mixed fluoroaryl ethers were prepared, to the synthesis of perfluorophenyl ether, met with partial success. Unlike potassium phenoxide, which reacts with hexafluorobenzene in *N,N*-dimethylformamide at room temperature, potassium pentafluorophenoxide fails to react under these conditions. By refluxing for 14 hr, a 16 percent yield of perfluorophenyl ether was obtained [5]. These examples also exemplify the differences in reactivity between the phenoxide and pentafluorophenoxide ion, the former being a stronger nucleophile because even at room temperature some of the 1,4-diphenoxy-2,3,5,6-tetrafluorobenzene was isolated. In the above reactions hydrated phenoxide salts were used. Attempts to react potassium pentafluorophenoxide with hexafluorobenzene in dimethylformamide, using anhydrous conditions and refluxing, resulted in the formation of pentafluoro-*N,N*-dimethylaniline. Apparently under this basic condition, cleavage of *N,N*-dimethylformamide occurs, liberating dimethylamine. The product obtained was confirmed by comparison with an authentic sample prepared by other means [5].

In tetrahydrofuran, no improvement in the yield of perfluorophenyl ether from hexafluorobenzene and potassium pentafluorophenoxide was observed, even though the reaction was carried out in a bomb at 120 °C for 18 hr.

When methanol was used as the reaction medium, pentafluoroanisole was obtained in a fair yield. Although the acid-base reaction (eq 1b)

$$C_6F_5OK + CH_3OH \underset{b}{\overset{a}{\rightleftarrows}} CH_3OK + C_6F_5OH \qquad (1)$$

$$c \downarrow C_6F_6$$

$$C_6F_5OCH_3 + KF$$

TABLE 1. *Infrared spectral bands of some fluoroaromatic ethers and phenols in the 1300 cm^{-1} to 1100 cm^{-1} region*

Compounds	Bands (cm^{-1})				
	C_6F_5—O—R	C_6H_5—O—R	OH	CF	Misc.
Phenols					
A. C_6F_5OH			1242(S)	1330(S)	1105(M)
B. $C_6F_4(OH)_2$			1235(S)	1300(S)	1138(M)
C. $C_6F_5OC_6F_4OH$	1171(S)		1237(S)	1315(S)	1116(M)
D. $C_6F_5O(C_6F_4O)_xC_6F_4OH$	1170(VS)		1237(S)	1315(S)	1117(M)
Ethers					
E. $C_6F_5OC_6F_5$	1170(S)			1310(S)	1125(W)
F. $C_6F_5OC_6H_5$	1169(S)	1205(VS)		1315(S)	1130(W)
G. $(C_6H_5O)_2C_6F_4$	1168(S)	1195VS)		1310(S)	1110(W)
Fluorocarbons					
H. C_6F_6				1300(M)	1157(M)
I. $(C_6F_5)_2$				1292(M)	1150(M)

S=strong. M=medium. W=weak.

should be the preferred reaction, the driving force of the reaction appears to be replacement of fluorine (eq 1c) in hexafluorobenzene by methoxide ion. Reactions of this type have been shown [11, 12] to occur quite rapidly.

4. Properties of Perfluorophenyl Ether

The perfluorophenyl ether [5] was usually isolated by diluting the reaction mixture with water and separating the fluorocarbon layer. After removal of the unreacted hexafluorobenzene by distillation, the residue solidified upon cooling. The initial fraction obtained from the sublimation of this residue was a white crystalline solid, mp 68–69 °C. The high melting point of this compound was unusual, as it was expected to be similar to that of phenyl ether, mp 27 °C. Chemical analysis indicated perfluorophenyl ether. The compound contained only carbon, fluorine, and oxygen. Analysis for hydrogen was negative. However, other verification of the structure was required since there are only small percentage differences of the elements in two- and three-ring compounds in this series. Confirmatory evidence was obtained from mass spectrometric analysis, which showed the parent peak at 350 mass units. Vapor-phase chromatographic analysis on a Viton-A column at 200 °C indicated an expected retention time slightly less than that of pentafluorophenyl phenyl ether.

The infrared spectra showed the characteristic ring vibration at 1520 cm^{-1}. The aryl ether band is usually found in the 1270–1230 cm^{-1} region [17], but in some cases, it may be as low as 1218 ± 10 cm^{-1} [18]. In perfluorophenyl ether there is a single strong band at 1170 cm^{-1} (table 1, E). This band appears in all spectra of the limited number of compounds investigated containing the C_6F_5—O—R ether grouping (C to G in table 1). It is of interest to note that the fluorophenols do not show this band. Similarly, the fluoroaryl ethers do not exhibit the band at 1235 cm^{-1}. However, both bands (1170 cm^{-1} and 1235 cm^{-1}) are shown by pentafluorophenoxy-tetrafluorophenol (table 1, C). In pentafluorophenyl phenyl ether (table 1, F) two distinct bands appear. The one at 1205 cm^{-1} is probably associated with the phenyl ether linkage (C_6H_5—O—R), whereas the other at 1169 cm^{-1} seems to be the pentafluorophenyl ether band. These same two bands appear in the spectra of 1,4-diphenoxytetrafluorobenzene. The bands in all of these compounds near 1100 cm^{-1} and 1300 cm^{-1} are probably carbon fluorine vibrations. Although there is some variance in the 1100 cm^{-1} region, the one at 1300 cm^{-1} remains fairly constant. Comparison bands in this 1100 cm^{-1} to 1300 cm^{-1} region are also listed for hexafluorobenzene and perfluorobiphenyl (table 1, H and I).

5. Reactions of Pentafluorophenoxide Salts in Water

The low reactivity of pentafluorophenoxide salts in *N,N*-dimethylformamide, tetrahydrofuran, and methanol, although they are soluble in these solvents, led to investigations in other media in which the reactivity of the salt could be enhanced. The excellent yields of pentafluorophenol and pentafluoroaniline obtained in aqueous medium, even though the reactions are heterogeneous in nature, suggested that water may be a useful reaction solvent for preparing the fluorophenylene ethers. Reactions performed in water would also yield important information on the hydrolytic stability of the ring fluorines as well as the ether linkages.

Hexafluorobenzene is stable to hydrolysis by water in the absence of base to at least 300 °C (limit of temperature range of equipment used), but as reported earlier in this article, in the presence of base, reaction can occur at a temperature as low as 120 °C in a closed system under autogenous pressure. Thus, it appeared feasible to consider the preparation of polyfluoroethers directly from hexafluorobenzene. In the first step, therefore, the usual conditions for preparing pentafluorophenol from hexafluorobenzene and potassium hydroxide were maintained (eq 2a), and after 5 hr the temperature was raised to

$$C_6F_6+2KOH+H_2O \xrightarrow[175\,^\circ C]{a} C_6F_5OK+KF+H_2O$$
$$\qquad\qquad\qquad\qquad\qquad\qquad\qquad\qquad\qquad\qquad b\,\big|\,225\,^\circ C \qquad (2)$$
$$\qquad\qquad\qquad\qquad\qquad\qquad\qquad\qquad\qquad\qquad \text{products}$$

225 °C for an additional 15 hr (eq 2b). The *p*H of the solution was then only slightly alkaline to alk-acid test paper, indicating almost complete reaction of the base. The experiment was designed to produce poly(perfluorophenylene ethers) in which there was no hydroxyl end group (eq 3),

$$xC_6F_5OK+C_6F_6 \rightarrow C_6F_5O(C_6F_4O)_xC_6F_5+xKF \qquad (3)$$

such as occurs in the thermal decomposition of sodium pentafluorophenoxide (eq 4).

$$xC_6F_5ONa \xrightarrow[345\,^\circ C]{} C_6F_5(OC_6F_4)xONa$$
$$\qquad\qquad\qquad\qquad\qquad\qquad\qquad\qquad +\text{other products} \qquad (4)$$

However, the reaction was observed to be rather complex in nature. Partial separation of the products was obtained by vacuum distillation. The volatile fraction solidified on cooling, mp 83 to 87 °C. This fraction was subdivided further into neutral and acid components by extraction with aqueous sodium carbonate. The neutral fraction was mainly perfluorophenyl ether, along with a trace of bis(pentafluorophenoxy)-tetrafluorobenzene, which were separated by vacuum sublimation. The perfluorophenyl ether obtained from this reaction was identical to the one prepared previously. The base-soluble component was shown to be pentafluorophenoxytetrafluorophenol by chemical and mass spectrometric (parent peak at 348 mass units) analyses. The near-infrared spectra of this compound showed the single

hydroxyl band at 3570 cm^{-1}, similar to other fluorophenols [5]. In the 1300 cm^{-1} to 1100 cm^{-1} region the compound showed both the ether band at 1171 cm^{-1} as well as the band due to the hydroxyl at 1237 cm^{-1} (table 1, C). This hydroxy ether was insoluble in water and failed to give a positive test for phenol in aqueous ferric chloride; however, a positive test can be obtained by the addition of ethanol.

From the nonvolatile fraction a green-tinted grease was obtained by sublimation; it showed a hydroxyl vibration in the near-infrared region. After removal of this material and upon cooling, the residue was a dark-brown brittle glass. Both compounds appear to be low molecular weight polyfluoroethers; they were not further investigated, except to observe that the brown glass was insoluble in benzene after this thermal treatment.

Attempts were made to increase the yield of perfluorophenyl ether by employing a large excess of hexafluorobenzene in relation to base, but a reaction in which a 16:1 ratio of hexafluorobenzene to potassium pentafluorophenoxide was used actually gave much smaller yield.

A complicating feature of this reaction is the fact that potassium pentafluorophenoxide alone in water under these conditions will react to produce tarry products. From this reaction pentafluorophenoxytetrafluorophenol was isolated. Althouth there is a slight discrepancy in melting points between this compound and the hydroxy ether obtained when hexafluorobenzene was used (no melting point depression on admixture), the infrared spectra of the two compounds were almost identical, with similar bands in the 1300 cm^{-1} to 1100 cm^{-1} region (table 1, C).

6. Reaction of Pentafluorophenoxide Salts in Pentafluorophenol, Poly(Perfluorophenylene Ethers)

This reaction was primarily designed to produce pentafluorophenoxytetrafluorophenol for comparison purposes with those compounds isolated previously. However, none of this compound was obtained; only polymeric material was formed. The main product was an amber-colored, tacky material (I), soluble in most organic solvents. The material was divided into two fractions (II and III) by dissolving the polymer in methanol and using water as a precipitant.

The precipitate (II), after drying in vacuo, was a clear light-brown gum which flowed freely on slight warming. The infrared spectrum of this fraction (II) (table 1, D) showed it to be a fluorophenylene ether containing a free hydroxyl group, probably as an end group. This spectrum was similar to those of pentafluorophenoxytetrafluorophenol (table 1, C). However, in the spectrum of fraction II, the relative intensity of the free hydroxyl group was very much less than that of the broad pentafluorophenyl ether band at 1170 cm^{-1}, indicating a polyfluorophenylene structure. No attempt was made to correlate these relative intensities with the molecular weight of the polymers.

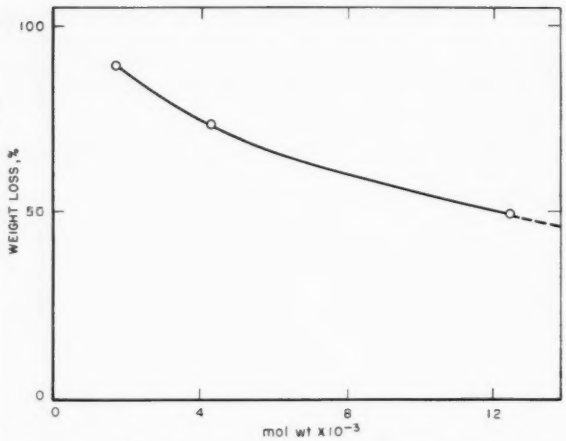

FIGURE 1. *Pyrolysis of poly(perfluorophenylene ethers) percent weight loss upon heating for ½ hr at 400 °C in a vacuum.*
Result for crosslinked sample, ——→.

The molecular weight of fraction II was found to be 1700, as determined by vapor-pressure osmometry. The average chain length was ten units, assuming the repeating unit to be—C_6F_4O—(formula weight 164). From pyrolysis data the polymer appeared to be a mixture of mers with varying chain lengths; 60 percent of the material sublimed as a white solid after 0.5 hours at 250 °C in vacuo and only 10 percent residue remained after 0.5 hours at 400 °C (see fig. 1).

Since the composition of the poly(perfluorophenylene ether) (II) was typical of condensation polymerization, several methods could be used to increase the molecular weight of the polymer. In one attempt potassium pentafluorophenoxide was added to a sample of the nonfractionated material (I) and the mixture was heated at 150 °C for 2 hours. The dark-brown, brittle glass obtained was still methanol soluble. The molecular weight was 1800; apparently the additional phenoxide ion reacts with itself or smaller chain molecules rather than adding onto longer existing chains.

One of the difficulties of condensation polymerization is the combining of the smaller chain units produced into one large polymeric unit. Since the poly(fluorophenylene ethers) isolated, as described above, all show a free hydroxyl group in their infrared spectra, a method for combining chains may be found which utilizes this hydroxyl group in the form of the potassium salt. The procedure involved was similar to other melt polymerization techniques [19]. Fraction III (methanol soluble) was converted to the potassium salt and heated for 0.5 hour at 175 °C and then at 200 °C. By this procedure a fraction was obtained which was benzene soluble but methanol insoluble. It was a light straw-colored glass, somewhat brittle, and had a low softening point (60–80 °C). The molecular weight of this material was 4300; it contained approximately 26 phenyl units. The infrared spectrum showed the poly-

fluorophenylene ether band at 1170 cm^{-1}. Since this fraction was still in the salt form, the hydroxyl bands were absent in their respective regions. Pyrolysis at 400 °C for 0.5 hour in vacuo volatilized 72.4 percent of the polymer. Of the total volatiles obtained, only 7.1 percent was volatile at room temperature. Since the polymer was not preheated before raising the temperature to 400 °C, this 7.1 percent fraction could be traces of solvent or low molecular weight material occluded in the polymer.

A higher molecular weight poly(perfluorophenylene ether) (mol wt 6500; average of 40 phenyl units) was obtained by simply recycling the above polymer (mol wt 4300) through the melt process. The polymer was still light colored and not so brittle. Very little decomposition occurred during the heating cycles. The amount of branching in the 4300 or 6500 molecular weight fractions was not determined.

A poly(perfluorophenylene ether) of 12,500 mol wt was obtained by heating excess potassium pentafluorophenoxide and pentafluorophenol at 200 °C for 72 hours. The polymer was a dark-brown glass which had a softening point of 80 °C and flowed freely at 100 °C. Pyrolysis at 400 °C for 0.5 hour gave a 50 percent weight loss. Heating at 260 °C for 18 hours appeared to crosslink this polymer; the product obtained was a hard brittle glass, insoluble in organic solvents. The polymer softened at 90 °C and possessed rubbery characteristics at temperatures up to 300 °C. Pyrolysis at 400 °C for 0.5 hour gave a 47 percent weight loss. After this treatment the specimen was smaller in size, but retained its original shape. The polymer itself is being evaluated as a potential high temperature rubber. The pyrolysis data of these polymers are shown in figure 1. The molecular weight of the crosslinked polymer is unknown, but from the weight loss we can obtain the general shape of the curve. The leveling off of the curve is interpreted as the breaking of phenyl to oxygen links, so that the thermal stability of these perfluorophenylene ethers is not much greater than 400 °C.

Some physical properties of these polyperfluorophenylene ethers are summarized in table 2. Two factors become apparent from the table. First, the softening point increases as the molecular weight increases. The range indicates where softening begins and complete melting occurs. For the crosslinked polymer the figure represents the point at which rubbery behavior appears. At no temperature up to 400 °C does this polymer "puddle."

The other point of interest is the change in solubility with increasing molecular weight. From this solubility behavior it is possible to obtain a qualitative estimate of the molecular weight of the polymers obtained from various experiments. For example, the 12,500 mol wt fraction is insoluble in ether whereas the lower molecular weight polymers are soluble.

The crosslinked polymer appears to be of the most interest. The nature of these crosslinks is obscure at the moment. At first it was believed that these links were caused by reaction of the polymer with the glass walls of the reaction vessel in which it was made, i.e., by stripping fluorine between the rings. However, it was recently reported [20] that the hydrocarbon phenoxylenes also crosslinked but at a much lower temperature (150 °C), so that the removal of a mole of fluorine does not appear to be an integral part of the crosslinking mechanisms. Also, Halpern [21] has also shown that 2,6-dimethylphenylene oxide polymers crosslink independent of the molecular weight of the polymer sample used, at 500 °F. The amount of branching in the crosslinked ether has not been determined; and from the carbon analysis of the polymer, branching does not appear to be extensive. The carbon analysis is compatible with a large cyclic structure, and it could occur by coupling remaining —OK end groups with a phenyl ring somewhere along the interior of the chain. Although the potassium residue remaining in the crosslinked polymer has not changed very much from that of the 12,500 mol wt fraction, it is difficult to determine at this stage whether this group, —OK, is still part of an end group, or whether because of the insolubility of the system, this residue is occluded in the polymer matrix. Perhaps, a better insight into the nature of these crosslinks will become apparent from an examination of the volatiles obtained from the pyrolysis of the polymers. These products are currently under investigation.

TABLE 2. *Some physical properties of PPPE*

Mol. Wt.	Appearance	Soft. pt. (°C)	Sol.	Insol.
1700	Amber gum	40–60	Most organic	H_2O
3700–6500	Amber, brittle glass.	60–80	Ether, CCl_3H, benzene.	CH_3OH, H_2O
12,500	Brown, brittle glass.	80–100	CCl_3H, Benzene	Ether, CH_3OH
X-link	Brown, brittle glass.	*90	None	

*Temperature at which rubbery behavior appears.

7. Discussion

It is evident that poly(perfluorophenylene ethers) are easier to obtain than the simple ether itself. This fact demonstrates that perfluorophenyl ether is a reactive intermediate, even with a weak nucleophile, such as pentafluorophenoxide ion, especially in aqueous systems. Tatlow [9] reported similar results in attempts to prepare perfluorophenyl thioether in pyridine, only polymers being formed. These fluorophenylene sulfide polymers are essentially para linked and high melting. Proof of the para structure was obtained by desulfurization with Raney nickel, which led to the isolation of pentafluorobenzene and 1,2,4,5-tetrafluorobenzene. In the case of polyperfluorophenylene ethers, structure determinations are more difficult since no simple reaction will convert the polymer into monomeric components. However, some insight into the structure of the polyethers may be obtained from examination of the simple compounds isolated from the reactions in aqueous medium. These compounds may be frag-

ments arising from cleavage of the fluoroaryl ethers under the basic conditions of the reaction, or they may be simply products which failed to propagate into polymers.

Perhaps the most significant compound isolated was tetrafluororesorcinol. The formation of this compound suggests the direct attack of hydroxyl ion on the pentafluorophenoxide ion. It has been shown previously [5] that even strong nucleophiles such as sodamide in liquid ammonia have failed to react with pentafluorophenoxide salts. Certainly, resonance structures similar to those for phenoxide ion can be written for pentafluorophenoxide as shown below:

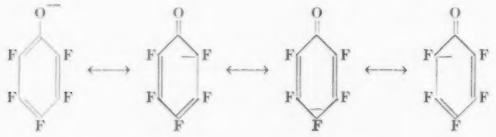

Therefore, the reaction conditions, i.e., excess base and high temperature and pressure, must have been sufficiently drastic for the incoming nucleophile to overcome the repulsion due to the negative charge of the pentafluorophenoxide. From these resonance structures the main reaction product would be expected to be the meta isomer, since these positions would be least negative and therefore vulnerable to attack. However, it was also shown that multiple replacement can occur by use of extreme conditions of base and temperature, in that only carbonlike solids were obtained at 190 °C and a 2 mole excess of potassium hydroxide. It could also be argued that tetrafluororesorcinol is the product obtained by cleavage of 1,3-bis(pentafluorophenoxy)-tetrafluorobenzene by hydroxide ion (eq 5).

$$C_6F_5OC_6F_4OC_6F_5+2KOH\rightarrow 2C_6F_5OK+C_6F_4(OH)_2 \quad (5)$$

In the presence of excess hydroxide it is doubtful that any of the 1,3-bis(pentafluorophenoxy)-tetrafluorobenzene even formed, since pentafluorophenoxide would be a weaker nucleophile than hydroxide ion and reaction of the latter ion would be expected to take precedence over the former. The isolation of perfluorophenyl ether and pentafluorophenoxytetrafluorophenol, from reactions of pentafluorophenoxide ion and hexafluorobenzene in water at high temperatures under autogenous pressure, would seem to indicate multiple modes of reaction. In the first case, pentafluorophenoxide and hexafluorobenzene react to give perfluorophenyl ether and subsequent reactions to lead to polymers (eq 6);

$$C_6F_5OC_6F_5+xC_6F_5OK\rightarrow C_6F_5(OC_6F_4)_xOC_6F_5+xKF \quad (6)$$

or, the pentafluorophenoxide ion (see resonance forms) may react with itself to produce pentafluorophenoxytetrafluorophenol and eventually to polymers (eq 7)

$$2C_6F_5OK\rightarrow C_6F_5OC_6F_5OK \quad . \quad . \quad . \quad (7)$$

A third possibility also exists in that the potassium pentafluorophenoxide is a salt of a weak acid and increased amounts of free pentafluorophenol may be obtained under these conditions according to eq 8:

$$C_6F_5OK+H_2O\rightarrow C_6F_5OH+KOH \quad (8)$$

This is similar to the exchange reaction observed in the methanol reaction (eq 1). If partial hydrolysis of the potassium pentafluorophenoxide does occur at these temperatures, then reaction between the pentafluorophenoxide and the pentafluorophenol thus formed would be expected to be faster because of the reduced charge on the free phenol oxygen than on the pentafluorophenoxide ion. The feasibility of this reaction occurring has been shown by the susceptibility of pentafluorophenoxide to react easily when pentafluorophenol was used both as a solvent and a reactant.

From consideration of the various foregoing reaction sequences, the polyperfluorophenylene ethers are probably composed of both *para* and *meta* linkages ($p>m$). This is not too surprising since evidence was previously [5] cited that the reactions of weak nucleophiles often yield *meta* derivatives. Kornblum [22, 23] and Le Noble [24] have recently shown the effects of solvation, temperature, and pressure on the reaction course of ambident [23] ions. Similar effects would be expected to alter the reaction course of pentafluorophenoxide. Nuclear magnetic resonance spectra, which proved effective in determining simple isomers, becomes complex and difficult to interpret, even for a small compound such as pentafluorophenoxytetrafluorophenol. Although the near infrared region has been useful in eliminating the *ortho*-hydroxyl compounds from further consideration, more data are needed to distinguish clearly between the amount of *para* and *meta* linkages in these polymers.

7.1. Thermal Stability of Small Molecules

The thermal stability of perfluorophenyl ether was determined by the same procedure as described previously [25]. For comparative purposes individual samples of phenyl ether, biphenyl, and decafluorobenzophenone were included in the test. From 0.1 to 0.5 g of the samples were sealed in evacuated thick-walled glass capillary tubes. After 1 hour at 500 °C, the samples were examined visually. The perfluorophenyl ether appeared to be completely charred, whereas the sample of decafluorobenzophenone showed approximately 50 percent decomposition. No change was observed in the tube containing biphenyl and only a slight coloration developed in the phenyl ether sample. The perfluorophenyl ether heated at 400 °C for 1 hour showed approximately 40 percent decomposition. The relative thermal stability of the small molecules

examined in the course of our work is as follows:

$$(C_6F_5)_2 \geq (C_6H_5)_2 \geq C_6F_6 > (C_6H_5)_4Si \geq (C_6H_5)_2O$$
$$> (C_6F_5)_2C{=}O \geq (C_6F_5)_4Si > (C_6F_5)_3P \geq (C_6F_5)_2O$$
$$> (C_6H_5)_3P > (C_6F_5)_3PO$$

The results indicate that increased thermal stability may be obtained in perfluorinated aromatic polymers by incorporating C=O or CX_2 groups between the rings instead of oxygen alone. However, the polyperfluorophenylene ethers may find considerable application where temperatures do not exceed 400 °C.

8. Experimental

Near-infrared spectra in the 2.5 to 3.2 μ range were obtained using 1 percent solutions in carbon tetrachloride. Infrared spectra of solids were obtained with pellets containing 1 to 2 mg of the compound and 300 mg of potassium bromide. Molecular weights were determined by osmometry using 1 percent solutions of the polymer in chloroform.

8.1. Pentafluorophenol and Tetrafluororesorcinol

A solution of 171 g (3 moles) of potassium hydroxide and 387 ml of distilled water, along with 181 g (0.97 mole) of hexafluorobenzene, were placed into an 800-ml capacity, silver-lined bomb. The bomb was rocked and heated at 150 °C for 5 hours, cooled, opened, and 139 g (77 percent) of unreacted hexafluorobenzene was recovered. The aqueous layer was acidified and extracted with two 100-ml portions of methylene chloride. After removal of the solvent by distillation there was obtained 12 g (28.8 percent) of pentafluorophenol (bp 144–145 °C) and 7 g (29.2 percent based on reacted C_6F_6) of tetrafluororesorcinol (bp 217–218 °C/760 mm; mp 95–96 °C). This latter compound is water soluble at 25 °C, and gives a typical blue ferric chloride test for phenols. Mass spectrometer analysis showed the parent peak at 182 mass units. Nuclear magnetic resonance data indicated the meta isomer. The melting point of the compound changes to 72–75 °C on standing in a moist atmosphere, indicating hydrate formation.

Analysis: Calculated for $C_6H_2F_4O_2$: C, 39.6; F, 41.7. Found: C, 40.15; F, 41.7.

When the same quantities as described above were heated at 190 °C for 20 hours, mostly carbon-like solids and very little phenolic material were obtained.

8.2. Perfluorophenyl Ether

a. Anhydrous Conditions in *N, N*-Dimethylformamide

To 6 g (0.027 mole) of potassium pentafluorophenoxide were added 14.4 g (0.077 mole) of hexafluorobenzene and 45 ml of *N,N*-dimethylformamide. No indications of reaction were observed at 25 °C for 24 hours. When heated at 70 °C for 48 hours, the color changed from yellow to dark brown. After cooling, the reaction products were poured into 200 ml of water and the aqueous layers extracted with several 50-ml portions of methylene chloride. After removal of the solvent, the residual liquid was distilled to yield 7.5 g (52 percent) of unreacted hexafluorobenzene and 2 g (25.7 percent based on reacted C_6F_6) of pentafluoro-*N,N*-dimethylaniline (bp 84–86 °C/1 mm; $n_D^{21}=1.4423$). This compound was identical to the pentafluoro-*N,N*-dimethylaniline prepared by a different method [5]. Only trace amounts of perfluorophenyl ether were formed.

b. Anhydrous Conditions in Tetrahydrofuran

To 21.7 g (0.098 mole) of potassium pentafluorophenoxide in a 188 ml capacity steel bomb was added 50 g (0.27 mole) of hexafluorobenzene and 25 ml of dried ($LiAlH_4$) tetrahydrofuran. The bomb was rocked and heated at 120 °C for 18 hours. After cooling, the contents were poured into 100 ml of 10 percent hydrochloric acid solution, extracted with two 500-ml portions of methylene chloride, and the combined extracts dried ($CaSO_4$) and distilled. There was recovered 28 g (56 percent) of hexafluorobenzene and 11 g (61 percent of pentafluorophenol. The residual liquid (1 g) solidified on cooling. Sublimation of this solid afforded two fractions: (1) mp 68–75 °C, probably a mixture of perfluorophenyl ether and pentafluorophenoxytetrafluorophenol and (2) mp 158–160 °C, appearing from analysis to be bis(pentafluorophenoxy)-tetrafluorobenzene.

Analysis: Calculated for $C_{18}F_{14}O_2$: C, 42.05; F, 51.8. Found: C, 42.46; F, 52.4; H, 0.0.

c. In Methanol

Eighteen grams (0.081 mole) of potassium pentafluorophenoxide, 40 g (0.22 mole) of hexafluorobenzene, and 40 ml of methanol were rocked and heated at 120 °C for 20 hours in a 188 ml capacity bomb, cooled, and poured into 100 ml of water. The usual workup yielded 22 g (55 percent) of unreacted hexafluorobenzene and 11 g (57 percent based on reacted C_6F_6) of pentafluoroanisole (bp 138–139 °C). Acidification of the aqueous solution gave 6 g (40 percent) of recovered pentafluorophenol.

8.3. Polyperfluorophenylene Ethers From Pentafluorophenoxide Salts

a. Thermal Decomposition of Sodium Pentafluorophenoxide

To 9.2 g (0.05 mole) of pentafluorophenol in 50 ml of anhydrous ether was added in small pieces 1.15 g (0.05 g-atom) of sodium metal. At the end of the evolution of hydrogen, the solvent was removed in vacuo. The white sodium salt was heated for 1 hour in vacuo at 150 °C to insure complete removal of the solvent. The flask was then placed in a Wood's metal bath and the temperature slowly raised to 345 °C at 1 mm pressure. The salt de-

composed, yielding mainly a volatile solid (mp 94–150 °C) and a glassy residue. The solid, after sublimation at 120 °C and 5 mm pressure, followed by recrystallization from ligroin-toluene solution, gave white colorless plates (mp 164–165.5 °C). The material was insoluble in base, and by chemical and mass spectrometric analyses (parent peak 328 mass units) was shown to be octafluorodiphenylene dioxide.

Analysis: Calculated for $C_{12}F_8O_2$: C, 43.95; F, 46.3. Found: C, 44.1; F, 44.5.

The glassy brownish residue was soluble in ether, and some purification could be effected in this manner. Analysis of the residue showed it to be polymeric in nature.

Analysis: Calculated for C_6F_4O: C, 43.9; F, 46.3. Found C, 44.0; F, 42.8; H, 0.3.

b. With Hexafluorobenzene in Water

This reaction was done in two heating steps. In the first step, 40 g (0.21 mole) of hexafluorobenzene, 12.5 g (0.189 mole) of potassium hydroxide, 0.5 g copper oxide, and 75 ml of distilled water were placed in a 188 ml capacity bomb that was rocked and heated at 175 °C for 5 hours. The second step consisted in raising the temperature to 225 °C and maintaining this temperature for 15 hours. After cooling, the contents were poured into 150 ml of water and showed only slight alkalinity to alk-acid *p*H paper. After filtration, the aqueous layer was extracted with methylene chloride. The extracts were combined with the organic layer, dried ($CaSO_4$) and distilled. After removal of the unreacted hexafluorobenzene (8.1 g; 20 percent), the residue was distilled in vacuo. It was divided into a volatile liquid (3.4 g; bp 120 °C/1 mm), which on cooling solidified (mp 83–87 °C), and a nondistillable fraction. The volatile fraction (solid) was treated with aqueous sodium carbonate, and the neutral insoluble material separated by filtration. Sublimation of the filter cake showed it to contain two compounds: (1) perfluorophenyl ether (1.5 g, mp 67–69 °C) identical with the perfluorophenyl ether described previously, and (2) probably bis(pentafluorophenoxy)-tetrafluorobenzene (0.5 g, mp 154–158 °C). The aqueous carbonate solution was acidified, and the precipitate filtered, dried, and sublimed. There was obtained 1 g of pentafluorophenoxytetrafluorophenol (mp 93–94 °C). This compound was further identified by chemical, mass spectrometer (parent peak at 348 mass units) and infrared analyses (see table 1). The The compound gives a ferric chloride phenol test in alcoholic solution.

Analysis: Calculated for $C_{12}HF_9O_2$: C, 41.39; F., 49.3; H, 0.29. Found: C, 41.9; F, 49.4; F, 0.29.

From the nondistillable fraction there was obtained 2 g of a sublimed white solid (mp 40–85 °C) which probably contains varying amounts of the above compounds, 2.7 g of a milky grease (softening point 30 °C), and 2 g of a dark-brown brittle residue.

c. In the Absence of Hexafluorobenzene in Water

In a 188-ml bomb, 10 g of potassium pentafluorophenoxide and 60 ml of distilled water were rocked and heated at 200 °C for 20 hours. After cooling, the contents consisted mainly of a tarry mass. From the aqueous layer, however, 0.4 g of a white solid was separated by filtration, and purified by sublimation (mp 96–97 °C). Mass spectrometer (parent peak at 348 mass units) and infrared analyses indicate the compound to be a pentafluorophenoxytetrafluorophenol. The tar was not investigated.

d. In Pentafluorophenol

In a 100-ml flask, fitted with an air-cooled condenser and protected from atmospheric moisture with a drying tube, 20 g (0.109 mole) of pentafluorophenol and 2 g (0.009 mole) of potassium pentafluorophenoxide were refluxed for 3 hours. A white precipitate (potassium fluoride) began to appear after 2 hours and increased with time. At the end of 3 hours, the contents were cooled to 90 °C and distilled under vacuum. There was recovered 8 g (40 percent) of pentafluorophenol. No volatile solids were obtained at this stage. On cooling, the organic portion of the residue was dissolved in 100 ml ether and filtered from the white salts. Evaporation of the ether solution gave 10 g of a tacky, light-brown, viscous oil (I). Three and one-half grams of this oil (I) were dissolved in 5 ml of methanol, after which 1 ml of water was added and the oily layer (II) allowed to settle. The aqueous methanol layer was decanted from the oil (II) and further diluted with 2 ml of water, which precipitated an additional 2.3 g of a less viscous oil (III). Traces of solvent were removed from fraction II in vacuo by heating at 100 °C. During this treatment, 0.1 g of a white sublimate was obtained which was not further investigated. On cooling, fraction II hardened to a clear, light-brown gum and flowed freely on slight warming (40 °C). The molecular weight of fraction II was 1700.

Analysis: Calculated for C_6F_4O: C, 43.9; F, 46.7. Found: C, 43.6; H, 0.3; F, 41.8.

Infrared characteristics are similar to compound D as listed in table 1.

e. From Low Molecular Weight Polyperfluorophenylene Ethers

(1) *From Fraction I*—To 7 g of fraction I (as described above) was added 2 g of potassium pentafluorophenoxide. On heating, the salt appeared to dissolve in the oil. It was heated at 150 °C at atmospheric pressure for 2 hours, during which the contents darkened considerably. After cooling, the dark-brown, organic material was dissolved in 100 ml ether and filtered from the salts. The ether was evaporated in vacuo, and there was obtained 6 g of a dark-brown, tacky gum, which was dissolved partially in 50 ml of methanol leaving 0.5 g of insoluble material. To the methanol solution was added 5 ml of water, the oily layer was allowed to settle, and the methanolic layer was decanted. Traces of solvent were removed from the oil in vacuo at 100 °C, leaving 1.5 g of a dark-brown, brittle glass having a molecular weight of 1800. Infrared spectra still showed a free hydroxyl group in the

3600 cm^{-1} region, as well as the broad ether band at 1170 cm^{-1}.

(2) *From Fraction III*—To 2.3 g of fraction III was added 10 ml of a solution containing 3 g of potassium hydroxide and 25 ml of water. The oil (III) coagulated into a milky tacky gum. The aqueous solution was decanted and the gum was dried overnight (16 hours) in vacuo at room temperature, yielding a straw colored, fluffy, easily powdered solid (1.2 g; mp 60–80 °C). The powder was degassed in a tube attached to a high-vacuum line, heated at 175 °C for 0.5 hours and then at 200 °C for an additional 0.5 hours. The material turned brown and the formation of potassium fluoride increased with time. On cooling, the contents solidified into a hard mass. Benzene (20 ml) was used to extract the polymer from the inorganic salts. A light-brown, viscous liquid was precipitated from the benzene solution with methanol (5 ml). On drying in vacuo, a light straw-colored, brittle glass (0.4 g) was obtained, very little changed in melting point. The molecular weight of this poly(fluorophenylene ether) was 4300. Since this fraction was still in the form of the potassium salt, no hydroxyl bands were observed in the infrared spectra. The spectra still showed the broad aromatic and pentafluorophenyl ether bands.

A higher molecular weight polymer (6500) was obtained by recycling the polymer through the melt polymerization again. The polymer (0.1 g) obtained in this fashion was still light-colored, more tacky, and not as brittle as the 4300 mol wt polymer.

f. An Insoluble Poly(perfluorophenylene Ether)

Thirteen grams of potassium pentafluorophenoxide and 2.5 g of pentafluorophenol were sealed in thick-walled, glass tube after degassing. The tube was heated for 72 hours at 200 °C. Initially, the contents became fluid at 180 °C and changed to a deep-red color. At the end of the heating period the contents no longer flowed and were dark brown in color. The tube was precooled in liquid nitrogen before opening. The contents were dissolved in 75 ml of benzene, filtered to remove potassium fluoride, and 40 ml of methanol added to the filtrate. The dark-brown precipitate was allowed to settle, the mother liquor decanted, the remaining precipitate after extraction with 25 ml of ether was a polymeric dark-brown glass (2.5 g; mp 80 °C) which flowed freely at 100 °C and had a molecular weight of 12,500. The infrared spectrum still showed the broad fluorophenyl ether band at 1170 cm^{-1}. Pyrolysis gave a 50 percent weight loss after 0.5 hours at 400 °C; of the total volatiles, 20 percent were volatile at 25 °C.

Analysis: Calculated for C_6F_4O: C, 43.9. Found: C, 44.2; H, 0.1; K, 0.12.

From the ether-soluble fraction there was obtained 2.1 g of a polymer having a molecular weight of 3700. Characteristics of this polymer were similar to the 4300 mol wt polymer described previously.

The 12,500 mol wt fraction (2.3 g) was placed in a thick-walled tube and heated at 260 °C for 18 hours in vacuo, after which the contents no longer flowed. The tube was cooled, and the dark-brown, hard, brittle glass (2.1 g) was removed from the tube. The material was insoluble in benzene, hexafluorobenzene, ether, chloroform, acetone, and 2,5-dichlorobenzotrifluoride. The polymer softened and became rubbery at 90 °C and maintained this property up to 300 °C. Although the polymer suffered a 47 percent weight loss after 0.5 hours at 400 °C, the specimen still retained its shape but became smaller in size. As yet, the molecular weight of this polymer has not been determined.

Analysis: Calculated for C_6F_4O: C, 43.9. Found: C, 44.1; H, 0.1; K, 0.09.

The authors wish to express their appreciation and thanks to R. A. Paulson for chemical analysis, James Brown for mass spectrometer analysis, Harold Finegold for nuclear magnetic resonance spectra, Max Tryon for helpful suggestions concerning the infrared spectra, and to Sidney Straus for pyrolysis data of the poly(perfluorophenylene ethers). Our thanks are also extended to Professor J. C. Tatlow, University of Birmingham, Birmingham, England, for furnishing a sample of decafluorobenzophenone.

9. References

[1] M. Hellmann, A. J. Bilbo, and W. J. Pummer, J. Am. Chem. Soc. **77,** 3650 (1955).
[2] S. Aftergut, R. J. Blackinton, and G. P. Brown, Chem. Ind. **1959,** 1090.
[3] E. S. Blake and W. C. Hammann, Abstracts of the 140th Meeting of the American Chemical Society, Boston, Massachusetts, April 1959, p. 11L.
[4] R. L. Huang, J. Chem. Soc. **1958,** 3725.
[5] L. A. Wall, W. J. Pummer, J. E. Fearn, and J. M. Antonucci, J. Research NBS **67A,** 481 (1963).
[6] G. C. Finger and W. C. Kruse, J. Am. Chem. Soc. **78,** 6034 (1956).
[7] A. E. Pavlath and A. J. Leffler, Aromatic fluorine compounds, p. 141. (Reinhold Publishing Corporation, New York, N.Y., 1962.)
[8] W. J. Pummer and L. A. Wall, NBS Tech. News Bull. **43,** 78 (1959).
[9] P. Robson, M. Stacey, R. Stephens, and J. C. Tatlow, J. Chem. Soc. **1960,** 4754.
[10] J. M. Birchall and R. N. Haszeldine, J. Chem. Soc. **1961,** 3721.
[11] W. J. Pummer and L. A. Wall, Science **127,** 643 (1958).
[12] E. J. Forbes, R. D. Richardson, M. Stacey, and J. C. Tatlow, J. Chem. Soc. **1959,** 2019.
[13] J. M. Birchall and R. N. Haszeldine, J. Chem. Soc. **1959,** 14.
[14] K. Wallenfels and W. Draber, Chem. Ber. **90,** 2819 (1957).
[15] E. Nield and J. C. Tatlow, Tetrahedron **8,** 39–40 (1960).
[16] L. J. Bellamy, Infrared spectra of complex molecules, p. 96. (John Wiley & Sons, Inc., New York, N.Y 1954.)
[17] Ibid., p. 102.
[18] K. J. Sax, W. S. Saari, G. C. Mahoney, and J. M. Gordon, J. Org. Chem. **25,** 1590 (1960).
[19] W. R. Sorenson and T. W. Campbell, Preparative methods of polymer chemistry, pp. 61–63. (Interscience Publishers, Inc., New York, 1961.)

[20] G. P. Brown and A. Goldman, Preprints of papers presented before the Polymers Division at the 145th Meeting of the American Chemical Society, New York, September 1963, p. 45.
[21] K. C. Tsou, H. E. Hoyt, and B. D. Halpern, ibid., p. 583.
[22] N. Kornblum, P. J. Berrigan, and W. J. Le Noble, J. Am. Chem. Soc. **85,** 1141 (1963).
[23] N. Kornblum, R. Seltzer, and P. Haberfield, ibid., 1148.
[24] W. J. Le Noble, ibid., 1470.
[25] L. A. Wall, R. E. Donadio, and W. J. Pummer, J. Am. Chem. Soc. **82,** 4846 (1960).

(Paper 68A3–274)

JOURNAL OF RESEARCH of the National Bureau of Standards—A. Physics and Chemistry
Vol. 68A, No. 3, May–June 1964

Cyclic Polyhydroxy Ketones II. *xylo*-Trihydroxycyclohexenediolic Acid and Keto-Inositols

Alexander J. Fatiadi and Horace S. Isbell

(January 30, 1964)

A new crystalline compound, DL-*xylo*-trihydroxycyclohexenediolic acid (DL-*xylo*-pentahydroxy-2-cyclohexen-1-one) (I), has been isolated from the products of oxidation of *myo*-inositol with nitric acid, and its structure has been established. Compound (I) reduces Tillmans reagent, reacts with iodine in neutral or slightly acidic solution, produces a blue color with ferric chloride solution, and exhibits other properties characteristic of an enediolic acid. On catalytic reduction, it gives both *scyllo*-inositol and *myo*-inositol. On oxidation, it yields a new triketo-inositol, *xylo*-4,5,6-trihydroxycyclohexane-1,2,3-trione (II).

Under acidic conditions, catalytic acetylation of I gives two pentaacetates, the infrared spectra of which are similar but not identical. One of these acetates exists in two forms, both of which, on deacetylation, yield the parent acid I. The product formed by deacetylation of the other pentaacetate has not been identified. Benzoylation of I gives a crystalline pentabenzoate.

Under basic conditions, acetylation of I proceeds with simultaneous aromatization, resulting in the formation of pentaacetoxybenzene, from which pentahydroxybenzene is obtained by hydrolysis.

xylo-4,5,6-Trihydroxycyclohexane-1,2,3-trione (II) gives a crystalline bis(phenylhydrazone). By acetylation under basic conditions, it yields hexaacetoxybenzene.

Mechanisms are presented for the aromatization of keto-inositols by enolization and *beta* elimination-reactions, and certain observations reported in the literature are rationalized. Infrared and ultraviolet absorption spectra are reported for the new compounds.

1. Introduction

Cyclic polyhydroxy ketones, obtained by the oxidation of inositols, yield enolic compounds of value in the study of oxidation–reduction phenomena and molecular structure. Prior workers have established that oxidation of *myo*-inositol (III) with nitric acid gives DL-*epi*-inosose-2 (V), tetrahydroxy-*p*-benzoquinone, rhodizonic acid, and a residue weighing approximately half the weight of the parent *myo*-inositol [1 to 5].[3] It has now been found that, after treatment with potassium carbonate, this residue gives a crystalline potassium salt of a new enediolic acid (I)[4] in a yield of 10 percent (based on the weight of *myo*-inositol taken). On oxidation, the salt gives a new crystalline trihydroxycyclohexanetrione (II). The structures and properties of I and II have been investigated, and certain characteristic derivatives have been prepared.

[1] This work was supported, in part, by the Division of Air Pollution, Public Health Service, U.S. Department of Health, Education, and Welfare.

[2] Presented, in part, before the Division of Carbohydrate Chemistry at the 141st Meeting of the American Chemical Society, Washington, D.C., March 26, 1962. Abstracts Papers, Am. Chem. Soc. **141,** 6D (1962). Paper I was published in J. Res. NBS **67A,** (Phys. and Chem.) No. 2, 153 (1963).

[3] Figures in brackets indicate the literature references at the end of this paper.

[4] The term "enediolic acid" is used here for α,β-unsaturated, dihydroxy aldehydes and ketones having the structure R—C(HO)=C(OH)—C(=O)—R′. The compounds belong to the group that have been classified by their chemical reactions as "aci-reductones" [6, p. 3]. The enediolic acids are related to the carboxylic acids in that they have a carbonyl group in conjugation with a hydroxyl group. Typical examples are

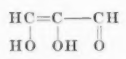

Propenediolic acid
(2,3-dihydroxy-2-propenal, reductone)

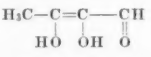

Butenediolic acid
(2,3-dihydroxy-2-butenal)

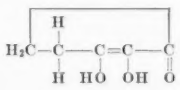

Cyclopentenediolic acid
(2,3-dihydroxy-2-cyclopenten-1-one, reductic acid)

Enediolic derivatives of tetrahydrofuran are more conveniently named as ascorbic acids, for example:

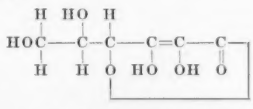

L-*threo*-Hexoascorbic acid [7]
(L-*threo*-hexono-2-ene-1,4-lactone)

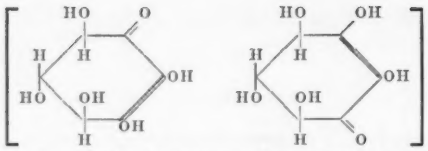

I DL-*xylo*-4,5,6-Trihydroxycyclohexenediolic acid

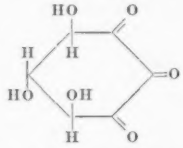

II *xylo*-4,5,6-Trihydroxycyclohexane-1,2,3-trione

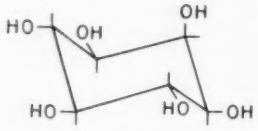

III *myo*-Inositol

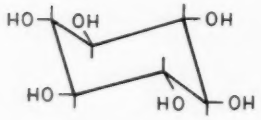

IV *scyllo*-Inositol

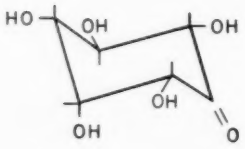

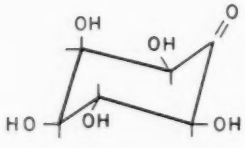

V DL-*epi*-Inosose-2

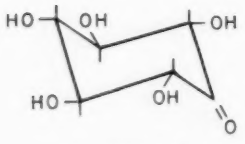

VI *myo*-Inosose-2

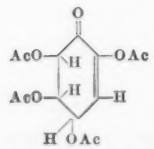

VII 2,4,5,6-Tetraacetoxy-2-cyclohexen-1-one

2. DL-*xylo*-4,5,6-Trihydroxycyclohexenediolic Acid (I)

The structure of (I) was established from the following considerations: The equivalent weight and chemical analysis of the acid correspond to the formula $C_6H_8O_6$; analysis of the potassium salt of the acid is in agreement with the formula $C_6H_7KO_6 \cdot H_2O$; both the acid and the salt react with two equivalents of either iodine or Tillmans reagent and give a deep-blue color on admixture with methanolic ferric chloride.

A compound having structure I may arise by enolization of either an *ortho*- or a *meta*-diketo-inositol.[5] Compound I might have any one of several configurations: the actual configuration was established by studying the reduction products. On catalytic reduction with hydrogen, I gave a mixture of *myo*-inositol (III) and *scyllo*-inositol (IV). The latter has an alternating arrangement of the hydroxyl groups around the ring ([9], p. 138; [10]). Hence, the new enediolic acid (I) likewise must have an alternating arrangement of its three hydroxyl groups and must be DL-*xylo*-trihydroxycyclohexenediolic acid. In nonionic derivatives formed from the acid, the configuration is D- and L-*xylo* (racemic, unless diastereomers are formed). However, in the anion (fig. 1), C1 and C3 are identical because of resonance, and the configuration is *meso*.

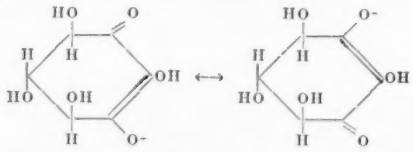

FIGURE 1. *Anion of* xylo-*4, 5, 6-trihydroxycyclohexenediolic acid.*

The potassium salt is particularly suitable for isolating and purifying the compound.

The isolation of I does not establish the structure of the parent diketo-inositol. Thus, as depicted in figure 2, all of the diketo-inositols are theoretically interconvertible by reversible enolizations, to yield a mixture of isomeric trihydroxycyclohexenediolic acids. Compound I is the only isomer thus far isolated.

Acetylation of I, catalyzed by mild acidic catalysts, gave a pentaacetate, mp 111 to 113 °C, which solidified above 113° and then remelted at 134 to 136 °C. Recrystallization of the higher-melting acetate from ethanol produced the lower melting. The infrared spectra of the two compounds are identical, and hence they are polymorphic modifications of the same compound. Deacetylation of both modifications regenerated I; therefore, the acetylation had not altered the configuration, and the compound is

[5] After oxidizing (the D isomer of) DL-*epi*-inosose-2 with *Acetobacter suboxydans*, Magasanik and Chargaff [8] found that the oxidation product had "acidic properties . . . in agreement with the expected behavior of an enolized *β*-di-ketone." This compound, which was not isolated, may have been the enediolic acid described here.

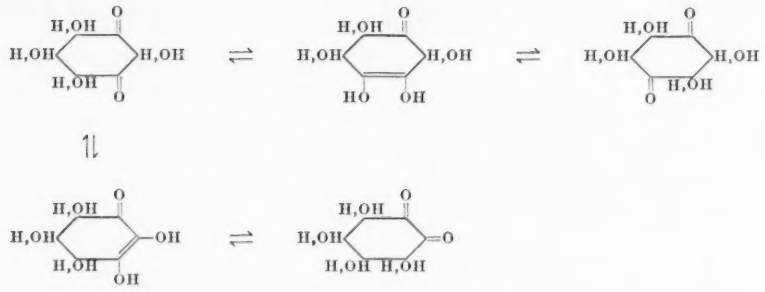

FIGURE 2. *Interconversion of diketo-inositols by enolization.*

DL-*xylo*-pentaacetoxy-2-cyclohexen-1-one. Benzoylation of I, with zinc chloride as catalyst, gave a pentabenzoate shown to be DL-*xylo*-pentabenzoyloxy-2-cyclohexen-1-one.

Acetylation of I, catalyzed by sulfuric acid, gave a pentaacetate (mp 154 to 155 °C) presumably having an altered configuration. The substance differs from that described above in its melting point, in its infrared spectrum, and in the fact that, on deacetylation, it does not yield I. However, it has essentially the same ultraviolet spectrum.

Acetylation of I under basic conditions gave pentaacetoxybenzene, presumably by the series of enolization and *beta*-elimination reactions depicted in figure 3 [11, 12]. On deacetylation, the pentaacetate gave pentahydroxybenzene, an important substance neither generally available nor closely investigated [13, 14].

3. *xylo*-4,5,6-Trihydroxycyclohexane-1,2,3-trione (II)

When oxidized with concentrated nitric acid, the new enediolic acid (I) gave a crystalline product (II). The analysis, molecular weight, and other properties of the latter show that it is *xylo*-4,5,6-trihydroxycyclohexane-1,2,3-trione. Crystalline II, the first triketo-inositol to be isolated, provides a promising new area for investigation. The relationship of I to II is the same as that of ascorbic acid to dehydroascorbic acid.

Acetylation of II under basic conditions gave hexaacetoxybenzene [15, 16, 17], presumably by the process depicted in figure 4. Compound II yielded a crystalline bis(phenylhydrazone) whose structure is being investigated.

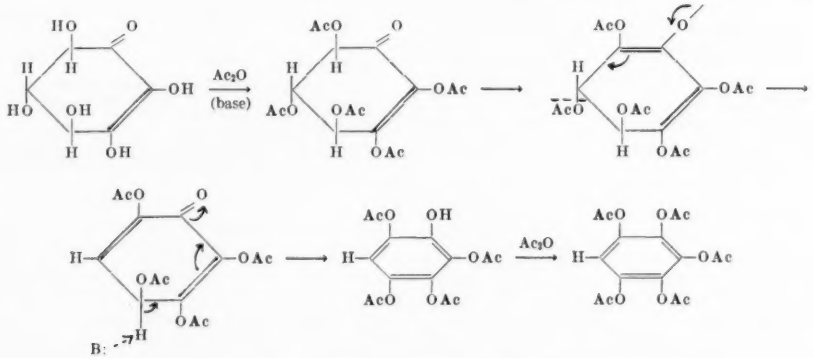

FIGURE 3. *Mechanism for the formation of pentaacetoxybenzene from I.*

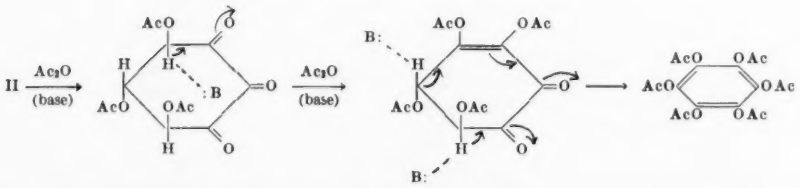

FIGURE 4. *Mechanism for the formation of hexaacetoxybenzene from II.*

4. Mechanisms for Aromatization of Keto-Inositols [11, 12]

For many years, inositols have been considered to be possible precursors of certain naturally occurring, aromatic compounds. In 1936, Posternak [3] showed that, following treatment with sodium acetate and acetic anhydride, or with pyridine and acetic anhydride, the pentaacetates and pentabenzoates of DL-*epi*-inosose-2 (V) and *myo*-inosose-2 (VI) yield 1,2,3,5-tetrahydroxybenzene. Under milder conditions, the pentabenzoate of *myo*-inosose-2 gives 1-hydroxy-2,3,5-tribenzoyloxybenzene (2,3,5-tribenzoyloxyphenol). Posternak [4] suggested that the aromatization of the inosose takes place through an enolic intermediate. Isbell [11, 12] depicted the process as involving successive enolization reactions with cleavage of acyloxy groups *beta* to the enolic hydroxyl groups (fig. 5). He predicted that the reaction would lead to 2-hydroxy-1,3,5-tribenzoyloxybenzene (2,4,6-tribenzoyloxyphenol) instead of the 1-hydroxy-2,3,5-tribenzoyloxybenzene actually found. In 1959, Angyal and Anderson ([9], p. 179) reported that heating penta-*O*-acetyl-*myo*-inosose-2 in soft glass yields 2,4,5,6-tetraacetoxy-2-cyclohexen-1-one (VII), one of the intermediates postulated by Isbell. Later, Stanacev and Kates [18] isolated VII by treating the acetates of *myo*-inosose-2 and DL-*epi*-inosose-2 with platinum oxide and hydrogen. These authors accounted for a number of discrepancies in the literature by showing that the pentaacetates and pentabenzoates of inososes are easily altered by alkali-catalyzed reactions. Posternak and Peshusses [19] also isolated VII. They suggested that the 1-hydroxy-2,3,5-tribenzoyloxybenzene previously reported arises by migration of a benzoyl group from the oxygen of C1 to that of C2 by a neighboring-group mechanism. Thus, Isbell's postulated mechanism for the aromatization has largely been confirmed, and the unexpected formation of the 1-hydroxy-2,3,5-tribenzoyloxybenzene has now been explained.

5. Experimental Procedures

5.1. Oxidation of *myo*-Inositol With Nitric Acid, and Separation of Products

Commercial *myo*-inositol (100 g) was added, with stirring, to 300 ml of 5-*N* nitric acid[6] in a large evaporating dish, and the stirred mixture was heated to boiling. Heating and stirring were continued until a sample of the material taken on a glass rod was a milky-white, viscous sirup; this required about 70 min. During the final stage, the mixture was heated cautiously, to avoid charring. The mixture was placed over moistened sodium hydroxide in a desiccator, and concentrated under reduced pressure to a semisolid, foamy residue (about 60 min) which was triturated with 90 ml of hot water and kept in a refrigerator for 24 hr. The resulting crude, crystalline DL-*epi*-inosose-2 was collected by filtration and washed with ice water; wt, 10 g (air-dried). A sample of the inosose, purified through its phenylhydrazone by the method of Posternak [20], melted at 206 to 208 °C dec.

The mother liquor (about 150 ml) was stirred and gradually brought to *p*H 7 to 7.5 by addition of potassium carbonate (40 to 43 g), heated for 15 min on a boiling water-bath, allowed to stand at room temperature for 15 min, and kept in ice for 45 min, with occasional stirring. The resulting dark, greenish-blue crystals were collected on a filter, successively washed with ice water and cold, 50-percent aqueous methanol, and air-dried; wt, 15 to 18 g. The crude product contained approximately equal quantities of the dipotassium salts of rhodizonic acid and tetrahydroxy-*p*-benzoquinone.[7]

---

[6] By treatment of *myo*-inositol with concentrated nitric acid according to Posternak [3, 20, 21], it is possible to obtain the same product (I) reported here, but in lower yield and more contaminated with byproducts.

[7] When the mother liquor, after separation of the inosose, was neutralized with potassium bicarbonate instead of potassium carbonate, about 80 percent of the resulting product was the dipotassium salt of tetrahydoxy-*p*-benzoquinone. This compound can be oxidized in air to dipotassium rhodizonate [17].

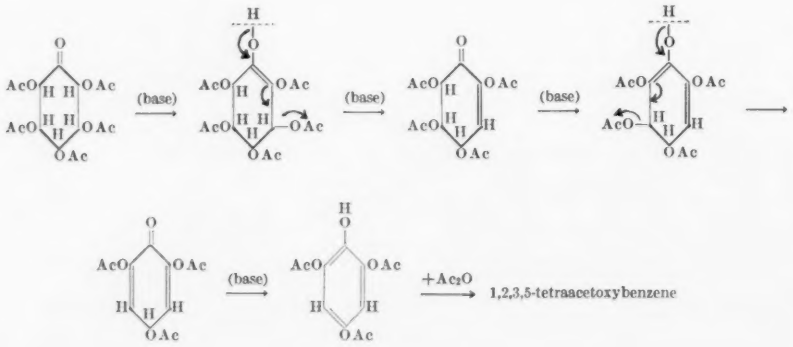

FIGURE 5. *Mechanism for the formation of 2-hydroxy-1,3,5-triacetoxybenzene from inososes by acetylation [11, 12].*

The mother liquor was concentrated at 40 °C under reduced pressure to about 100 ml, at which point crystallization began; the mixture was stored overnight in a refrigerator. The resulting prismatic crystals were collected by filtration (polyethylene dam) and successively washed with ice water, 50-percent methanol, and anhydrous methanol. A small second crop was obtained by concentrating and cooling the filtrate. The combined, crude, light-yellow product was dried; wt, 25 g. By analysis, it contained about 75 percent of the potassium salt of I.

For purification, the crude salt was dissolved in 300 ml of freshly boiled, distilled water at 55 °C. The solution was treated with 5 g of acid-washed, activated carbon,[8] the suspension was filtered, and the residue was washed with freshly boiled water. The combined, light-brown filtrate and washings were saturated with acetone (about 500 ml) and gradually cooled. The resulting, reddish-orange crystals[9] were collected by filtration, washed successively with cold, 75-percent aqueous acetone and anhydrous acetone, and dried; wt, 17.5 g. By analysis, they contained 98 percent of potassium trihydroxycyclohexenediolate monohydrate.

From the residue, after separation of the potassium salt of I, the following were isolated through their copper complexes: compound I (small proportion); rhodizonic acid; tetrahydroxy-*p*-benzoquinone; and croconic acid. Oxalic acid was separated from the original residue as the bis(phenylhydrazide).

The potassium salt of I was also obtained by precipitation of the oxidation products (after separation of DL-*epi*-inosose-2) with excess glacial acetic acid. On neutralizing the resulting colorless, amorphous products with potassium carbonate and treating the solution as described above, the potassium salts of tetrahydroxybenzoquinone, rhodizonic acid, and the enediolic acid (I) were crystallized in approximately the yields reported above.

5.2. DL-*xylo*-Trihydroxycyclohexenediolic Acid (I)

a. Preparation and Properties

A solution of 35 g of the recrystallized potassium salt of I in 650 ml of freshly boiled water was passed through 500 ml of a cation-exchange resin (Amberlite IR120–H) into 200 ml of 50-percent, aqueous acetic acid. The resin was washed with 1 liter of freshly boiled water. The combined effluent and washings were concentrated under reduced pressure to about 850 ml, treated with 25 g of acid-washed decolorizing carbon, and filtered. The colorless filtrate was mixed with 50 ml of acetic acid and concentrated under reduced pressure to about 400 ml, whereupon crystallization commenced. The mixture was diluted with 50 ml of acetic acid and stored overnight in a refrigerator; the resulting lustrous crystals were separated by filtration, washed with 50-percent, aqueous acetic acid, and dried in a vacuum desiccator over sodium hydroxide. The mother liquor, after concentration and dilution with acetic acid, gave a second crop of I; total wt, 18 to 20 g; mp, 210 to 211 °C dec., with darkening at 205 °C.

The crude product was dissolved in 600 ml of 10-percent aqueous acetic acid at 60 °C, 60 ml of glacial acetic acid and 15 g of acid-washed decolorizing carbon were added, and the suspension was filtered. The colorless filtrate was concentrated under reduced pressure to about 450 ml, whereupon crystallization began. The mixture was diluted with 50 ml of acetic acid, kept overnight in a refrigerator, and filtered. The crystals were washed with 50-percent, aqueous acetic acid, and dried; wt, 15 to 18 g; mp, 211 to 212 °C dec.

Anal. Calcd. for $C_6H_8O_6$: C, 40.9; H, 4.6. Found: C, 41.0; H, 4.5.

The enediolic acid was also obtained by treating 10 g of the potassium salt with 50 g of warm, glacial acetic acid. After several hours, the difficultly soluble acid was separated by filtration and recrystallized from aqueous acetic acid; wt, 5 to 6 g.

A 74.1-mg sample of I required 4.20 ml of 0.1-*N* sodium hydroxide for neutralization; hence, the equivalent weight is 176, in agreement with the calculated molecular weight.

Furthermore, an 84.4-mg sample of I reacted with 9.57 ml of 0.1-*N* iodine, in agreement with an equivalent weight of 88.0 and a molecular weight of 176.

The enediolic acid reduces Benedict solution, silver nitrate, and periodic acid, gives a transitory blue color with methanolic ferric chloride, reacts with an equimolecular proportion of Tillmans reagent and of iodine, and forms an insoluble copper complex when added to a solution of cupric acetate ([6], p. 16).

b. Potassium Salt

Purified I (1 g) was dissolved at room temperature in 150 ml of freshly boiled water. The solution was neutralized under nitrogen with aqueous potassium hydroxide, cooled in an ice bath, and treated with cold acetone (about 300 ml) to incipient turbidity. The resulting colorless crystals were separated under nitrogen, washed with acetone, and dried over phosphorus pentoxide in a vacuum desiccator; the yield was nearly quantitative.

Anal. Calcd. for $C_6H_7KO_6 \cdot H_2O$: C, 31.0; H, 3.9; K, 16.8. Found: C, 30.9; H, 3.9; K, 17.3.

A sample (108.1 mg) of the potassium salt reacted with 9.29 ml of 0.1-*N* iodine, in agreement with a molecular weight of 232.7 (calcd. M.W. 232.2). An aqueous solution of the salt gave a stable, deep-blue color with methanolic ferric chloride.

When the purified potassium salt of I was heated with 1-*N* potassium hydroxide and active manganese dioxide by the procedure of reference [17], croconic acid was isolated (as the barium salt) in a yield of about 10 percent.

[8] A slurry of Darco 60 (Atlas Chemical Industries Inc., Wilmington, Del.) in 15-percent, aqueous hydrochloric acid was heated at 80 °C for 24 hr. The carbon was collected by filtration, washed with distilled water until free from chloride ion, and dried at 85 °C in a vacuum oven.

[9] The colored potassium salt obtained here is adequate for preparing the free enediolic acid (sec. 5.2a). The preparation of the pure potassium salt, which is colorless, is described in section 5.2b.

722–641—64——3

c. Ammonium Salt

A solution of 200 mg of I in 10 ml of freshly boiled water at 10 °C was mixed, under nitrogen, with 300 mg of ammonium carbonate. After treatment with a small amount of acid-washed decolorizing carbon, the solution was filtered, saturated with cold acetone, and cooled in ice. The ammonium salt of I crystallized in nearly colorless needles. The product was recrystallized three times from aqueous acetone, and dried for 12 hr at 25 °C/0.1 mm; wt, 150 mg; mp 170 to 172 °C dec.

Anal. Calcd. for $C_6H_{11}NO_6 \cdot H_2O$: C, 34.1; H, 6.2; N, 6.6. Found: C, 34.1; H, 6.0; N, 6.6.

d. Catalytic Hydrogenation of I, and Separation of Cyclitols

A mixture of 2 g of I, 150 ml of water, 50 ml of ethanol, and about 5 g of freshly prepared Raney nickel T–4 [22] was treated with hydrogen at 1350 psi, and the temperature was gradually raised to 100 °C. After 6 hr, the pressure was released, the mixture was filtered, and the filtrate was concentrated under reduced pressure to about half volume. The solution was treated with decolorizing carbon, refiltered, concentrated to about 10 ml, treated with acetone to incipient turbidity, and kept in a refrigerator for 18 hr. The resulting crystals were separated and dried; wt, 1.8 g.

A 500-mg sample of the cyclitol mixture was dissolved, with slight heating, in a mixture of 8 ml of acetic anhydride and 2 ml of 100-percent phosphoric acid, kept 30 min, and poured into ice water; the resulting crystals were collected on a filter, washed with water, and dried; wt, 0.8 g. A 300-mg sample of the crude product was extracted with 50 ml of boiling absolute ethanol, and the extract was concentrated, giving a crystalline product which was recrystallized several times from ethanol; mp 214 to 215 °C.

The ethanol-insoluble residue was recrystallized from 2:1 ethanol—acetic acid, to give colorless crystals, mp 300 to 301 °C. The melting points and infrared spectra agreed with those of the authentic hexaacetates of *myo*-inositol and *scyllo*-inositol, respectively.

e. Acylation

(1) *Benzoylation.* A mixture of I (0.5 g), 3 ml of benzoyl chloride, and 3 g of fused zinc chloride, in a test tube protected by a drying-tube, was heated at 110° for 2 hr and allowed to cool to room temperature. It was then diluted with 8 ml of absolute ethanol and kept in an ice bath for 2 hr. The resulting crystals (0.2 g) were separated and were recrystallized by suspending them in 40 ml of stirred, hot ethanol, gradually adding nitromethane until most of the product had dissolved, filtering, and cooling; mp 234 to 236 °C.

Anal. Calcd. for $C_{41}H_{28}O_{11}$: C, 70.7; H, 4.1. Found: C, 70.4; H, 4.0.

(2) *Acetylation without isomerization.* Acetic anhydride (10 ml, containing 5 drops of perchloric acid) was added in small portions to a suspension of 1 g of I in 40 ml of ethyl acetate in a bath at 65 °C [23]. After the crystals had dissolved, the solution was kept at room temperature for 30 min, and poured into ice water. The mixture was extracted with chloroform, and the extract was successively washed with 5-percent aqueous sodium bicarbonate and water, dried with sodium sulfate, and concentrated to a sirup which was diluted with 8 ml of absolute ethanol to give colorless, glistening plates; these were recrystallized from 15 ml of hot ethanol; wt 1.5 g. The product melted at 111 to 113 °C, solidified above 113°, and again melted at 134 to 136 °C. The higher-melting form was converted to the lower-melting by recrystallization from ethanol; the lower-melting was converted to the higher-melting by recrystallization from benzene.

Anal. Calcd. for $C_{16}H_{18}O_{11}$: C, 49.8; H, 4.7: CH_3CO, 55.7. Found, for the product of mp 111 to 113 °C; C, 49.8; H, 4.7; CH_3CO, 55.3. Found, for the product of mp 134 to 136 °C; C, 49.7; H, 4.8.

The analyses and infrared spectra of the two pentaacetates showed that the two materials are different crystal forms of the same substance.

A solution of the lower-melting form in methanol containing a few drops of concentrated hydrochloric acid, kept at room temperature for 2 hr and in a refrigerator for 3 days, deposited crystals of I. Hence, the compound is DL-*xylo*-pentaacetoxy-2-cyclohexen-1-one.

The pentaacetate was also obtained by acetylation of I with (a) acetic anhydride and zinc chloride, (b) acetic anhydride and 100-percent phosphoric acid, and (c) isopropenyl acetate and *p*-toluenesulfonic acid. Acetylation of I with acetic anhydride and sulfuric acid, however, gave a different pentaacetate, described below.

(3) *Acetylation with isomerization.* I (1 g) was added to a stirred mixture of 19 ml of acetic anhydride and 1 ml of concentrated sulfuric acid at 50 °C. After the crystals had dissolved (about 5 min), the mixture was cooled, kept at 20 °C for 1 hr, and poured into a mixture of ice and water. The mixture was extracted with chloroform, and the extract was washed, dried, and evaporated. The residue was recrystallized from absolute ethanol; yield, 1.2 g; mp 150 to 152 °C. By repeated recrystallization from ethanol, the melting point was raised to 154 to 155 °C.

Anal. Calcd. for $C_{16}H_{18}O_{11}$: C, 49.8; H, 4.7; CH_3CO, 55.7. Found: C, 49.6; H, 4.6; CH_3CO, 56.1.

When this acetate was hydrolyzed by the method in the preceding section, it failed to yield the parent compound (I).

f. Aromatization

(1) *Simultaneous acetylation and aromatization.* I (1 g) was added in small portions to a hot, stirred mixture of 25 ml of acetic anhydride and 5 g of fused sodium acetate. After 15 min, the mixture was cooled, kept for 1 hr at room temperature, and poured into a mixture of ice and water, from which crude pentaacetoxybenzene crystallized; wt, 1.9 g. A

solution of this in a hot mixture of 180 ml of absolute ethanol and 20 ml of glacial acetic acid was treated with decolorizing carbon, filtered, and kept for 18 hr in a refrigerator. The resulting crystals were separated and dried; wt, 1.5 g: mp 165 to 166 °C, in agreement with the value reported for pentaacetoxybenzene [14]. By recrystallization from hot, glacial acetic acid, the melting point was raised to 166 to 168 °C. The once-recrystallized material was used for preparing pentahydroxybenzene (section 5.3).

(2) *Aromatization of acetates.* For each of the three pentaacetates described in section 5.2e, a 250-mg sample was dissolved in a mixture of 10 ml of pyridine and 5 ml of acetic anhydride. The solution was heated to boiling, kept at room temperature for 2 hr, and poured into ice water. The product (approximately 200 mg) was separated and recrystallized from ethanol, or from a mixture of ethanol and acetic acid. Each of the products melted at 169 to 171 °C and showed an infrared spectrum identical with that of the product derived from I by simultaneous acetylation and aromatization.

5.3. Pentahydroxybenzene

A mixture of 1 g of pentaacetoxybenzene, 50 ml of methanol, and 5 ml of concentrated hydrochloric acid was placed in a 200-ml flask equipped with a reflux condenser. Under a stream of nitrogen, the mixture was gently boiled for 15 min; the light-yellow solution was then filtered, and concentrated under reduced pressure (40 °C). The resulting pale-yellow crystals were separated by filtration, washed with 25 ml of cold ether, and dried in a vacuum desiccator; wt, 325 mg. For recrystallization, 100 mg was dissolved in 10 ml of boiling absolute ethanol; the solution was concentrated to about 2 ml, and pentane (about 2 ml) was added to incipient turbidity. The slightly pinkish crystals that separated on cooling were collected by filtration, washed with pentane, and dried; wt, 60 mg. The substance does not melt, but decomposes slowly at 255 to 265 °C. The analysis of the product did not correspond exactly with that of anhydrous pentahydroxybenzene, but was sufficiently close to show that the material was, indeed, pentahydroxybenzene.

Anal. Calcd. for $C_6H_6O_5$: C, 45.6; H, 3.8. Found: C, 44.4; H, 3.8.

Freshly prepared methanolic solutions of pentahydroxybenzene are usually slightly yellow; they turn deep red on exposure to air. Ferric chloride solution imparts a pink color that rapidly deepens to magenta. Pentahydroxybenzene is sensitive to oxidation; even acid-washed decolorizing carbon causes a solution of the compound to turn deep red. At room temperature, the substance reduces Benedict solution and also silver nitrate, the latter almost instantaneously.

5.4. *xylo*-Trihydroxycyclohexane-1,2,3,-trione (II)

a. Preparation and Properties

A solution of I (1 g) in 10 ml of stirred, concentrated nitric acid was heated for 5 min on a steam bath, at which point II began to crystallize. The reaction mixture was cooled in ice, diluted with 25 ml of cold methanol, and kept 5 min. The resulting crystals were separated on a fritted-glass filter and washed with methanol; the filtrate was discarded.[10] The fairly pure product began to darken at 200 °C and decomposed, without melting, at 220 to 225 °C.[11]

The compound may be recrystallized in low yield from hot water. II (1.5 g) was dissolved in 125 ml of hot water, and the solution was decolorized, filtered, and concentrated under reduced pressure to a sirup which was diluted with 50-percent aqueous methanol and kept at room temperature for 3 days. The resulting crystals were collected by filtration, washed with methanol, and dried; yield, 0.25 g. The infrared spectrum was unchanged by recrystallization. After being dried for 4 hr at 25 °C/0.1 mm, the compound was analyzed.

Anal. Calcd. for $C_6H_6O_6+1{\cdot}5H_2O$: C, 35.8; H, 4.5. Found: C, 35.8: H, 4.6.

After being dried 1 hr at 110 °C/0.1 mm, it was reanalyzed. Calcd. for $C_6H_6O_6{\cdot}H_2O$: C, 37.5; H, 4.2. Found: C, 38.0; H, 4.2.

A warm solution of II reduced Benedict solution instantaneously. On being heated, an aqueous solution of II decomposes slowly, giving oxalic acid as one of the decomposition products. An aqueous solution, treated at 60 °C, in air, with a solution of ammonium carbonate, changes color to deep yellow and finally deposits dark-blue needles of ammonium rhodizonate [17].

b. Simultaneous Acetylation and Aromatization

II (500 mg) was added to a hot, stirred mixture of 25 ml of acetic anhydride and 5 g of anhydrous sodium acetate. After 5 min, the mixture was cooled and poured into 100 ml of ice water. The solid that separated was collected by filtration, washed with water, and recrystallized from 15 ml of boiling acetic acid containing decolorizing carbon. The suspension was filtered and the filtrate cooled; the resulting crystals were separated, washed with acetic acid, and dried over sodium hydroxide in a vacuum desiccator; wt, 0.3 g; mp 203 to 205 °C. The product was identical, in melting point and infrared spectrum, with an authentic sample of hexaacetoxybenzene [24].

On hydrolysis with warm, 85-percent phosphoric acid, the acetate yielded needlelike crystals identical with those of hexahydroxybenzene [17].

c. Bis(phenylhydrazone)

II (300 mg) was dissolved in 75 ml of 7.5-percent aqueous acetic acid by warming slightly. To the stirred solution were added 50 g of crushed ice and 5 ml of phenylhydrazine. After 1 hr, the resulting

[10] Mixtures of nitric acid and methanol should not, of course, be concentrated with heating because of the danger of violent decomposition.

[11] Compound II can also be obtained by oxidation of I with iodine, neutral potassium permanganate, or a cold solution of silver nitrate.

red crystals were separated by filtration, washed with water, and dried; wt, 300 mg. The crude product was twice recrystallized from boiling methanol; dark-red needles, mp 184 to 186 °C (dec). Purified on a column of neutral alumina by elution with a 4:1 mixture of benzene and methanol, it melted at 186 to 187 °C.

The same bis(phenylhydrazone) was prepared from I as follows: A solution of 5 ml of phenylhydrazine in 12 ml of 50-percent aqueous acetic acid was added to a stirred solution of I (1.2 g) in 50 ml of water at 70 °C; the deep-red bis(phenylhydrazone) of II crystallized almost immediately. After 30 min, it was separated, washed with cold water, and dried wt; 1.2 g.

Anal. Calcd. for $C_{18}H_{18}N_4O_4$: C, 61.0; H, 5.1; N, 15.8. Found: C, 61.3; H, 5.0; N, 15.9.

5.5. Spectrophotometric Measurements

a. Apparatus and Techniques

The infrared spectra were recorded for the freshly prepared crystalline compounds, in Nujol mulls and in potassium chloride pellets, with a Perkin-Elmer Infracord Model 137 (double beam) spectrophotometer equipped with a prism of sodium chloride for the 2- to 15-μ range.

The ultraviolet spectra were determined with a Beckman DK–2 spectrophotometer having matched 1-cm quartz cells, with the relevant solvent as the reference standard. Molecular extinction coefficients are reported for those compounds for which the intensity of absorption did not change appreciably with time.

b. Discussion of Spectra

The ultraviolet absorption spectrum of the *enediolic acid I* varies with the solvent and the hydrogen-ion concentration. A freshly prepared, dilute aqueous solution of I exhibits a rapidly changing R-band ([25], p. 111; [26], p. 204) at λ_{max} near 309 mμ, almost identical with an absorption band at λ_{max} 307 mμ shown by the *potassium and the ammonium salt of I* (fig. 6, *1* to *3*). Hence, in dilute aqueous solution, I is present largely as the anion. The free acid and its potassium and ammonium salts are unstable in aqueous solution (in the presence of light and air), as evidenced by the rapid decrease in intensity of the absorption maxima.

The characteristic absorption of an aqueous solution ($3.7\times10^{-5}M$) of the potassium salt disappears in about 30 min at room temperature.

In acid solution (5-percent aqueous acetic acid or 2.5-*N* hydrochloric acid), the maximum of I shifts to shorter wavelengths, to provide a relatively stable band at λ_{max} near 279 mμ (fig. 6, *4*). The presence of an acid stronger than I suppresses ionization and favors the nonionized form of I over the anion. Table 1 gives ultraviolet absorption maxima for several enediolic acids, including compound I. In each instance, the maximum for the nonionized form is at a shorter wavelength than that for the ionized form.

TABLE 1. *Ultraviolet absorption maxima of some enediolic acids*

Compound	Approximate maxima		References
	In aq HCl	In aq NaOH	
DL-*xylo*-Trihydroxycyclohexanediolic acid	mμ 279	mμ 307	
L-Ascorbic acid	242	300	[1]
Reductic acid	*(266)	293	[2]
Croconic acid	295	365	[3]
Triose reductone	*(271)	292	[2]

* In ethanol.
[1] P. Karrer, H. Salomon, R. Morf, and K. Schöpp, Biochem. Z. **258,** 4 (1933).
[2] G. Hesse and F. Urbanek, Ann. **604,** 47 (1957).
[3] K. Yamada, N. Mizuno, and Y. Hirata, Bull. Chem. Soc. Japan **31,** 543 (1958).

The *pentaacetate and pentabenzoate of I* show a K-band near 237 mμ and 232 mμ, respectively (fig. 6, *5*, *6*, and *7*). It is of interest to compare these observed maxima with values calculated for the K-bands of α,β-unsaturated ketones by the empirical substitution rules of Woodward [27] and the Fiesers ([28], p. 19).[12] If it is assumed that the effect of an acyloxy group is the same as that of an alkyl substituent (10 mμ), then, starting with methyl vinyl ketone (3-buten-2-one) (λ_{max} 215 mμ), the calculated absorption maximum for the pentaacetate and pentabenzoate of I should be 245 mμ. Although the agreement with the observed values is not particularly good, it seems probable that the effect of the acyloxy substituent is not 10 mμ, but of the order of 5 mμ ([25], p. 99; [29]). Use of the latter value gives a calculated absorption maximum of 235 mμ. The difference in the observed maxima for the pentaacetate and pentabenzoate may arise from steric effects ([30], p. 66).

Additional information concerning the structure of I and its derivatives can be obtained from their infrared spectra. Because of the low solubility of I in carbon tetrachloride, dilution studies to elucidate the type of hydrogen bonding present were not feasible. Either in potassium chloride pellets or Nujol mulls, with careful exclusion of moisture, I showed bands at 2.74 and 2.96 μ that can be attributed to hydroxyl groups (fig. 7, *1*). The spectrum also showed a moderately strong absorption band at 5.88 μ (C=O) and a strong band at 6.08 μ (α,β-unsaturated ketone).

The absence of a keto C=O band in the infrared spectrum of the potassium salt of I (fig. 7, *2*) is attributed to the fact that, in the anion, the carbonyl group is part of a resonance system involving C1 and C3, as shown in figure 1. A band at 6.45μ is assumed to arise from the anion of I, and is in fair agreement with a band at 6.35μ reported ([31], p. 68) for the anion of 5,5-dimethyl-1,3-cyclohexanedione (dimedone). An absorption band at 6.15μ is due, at least in part, to water ([32], p. 430; [33], p. 150; [34]).

The spectrum of the ammonium salt of I (fig. 7, *3*), like that of the potassium salt, fails to show a keto C=O band; it shows bands at 6.45 and 6.20μ,

[12] See summary by Jaffe and Orchin ([26], pp. 218, 219).

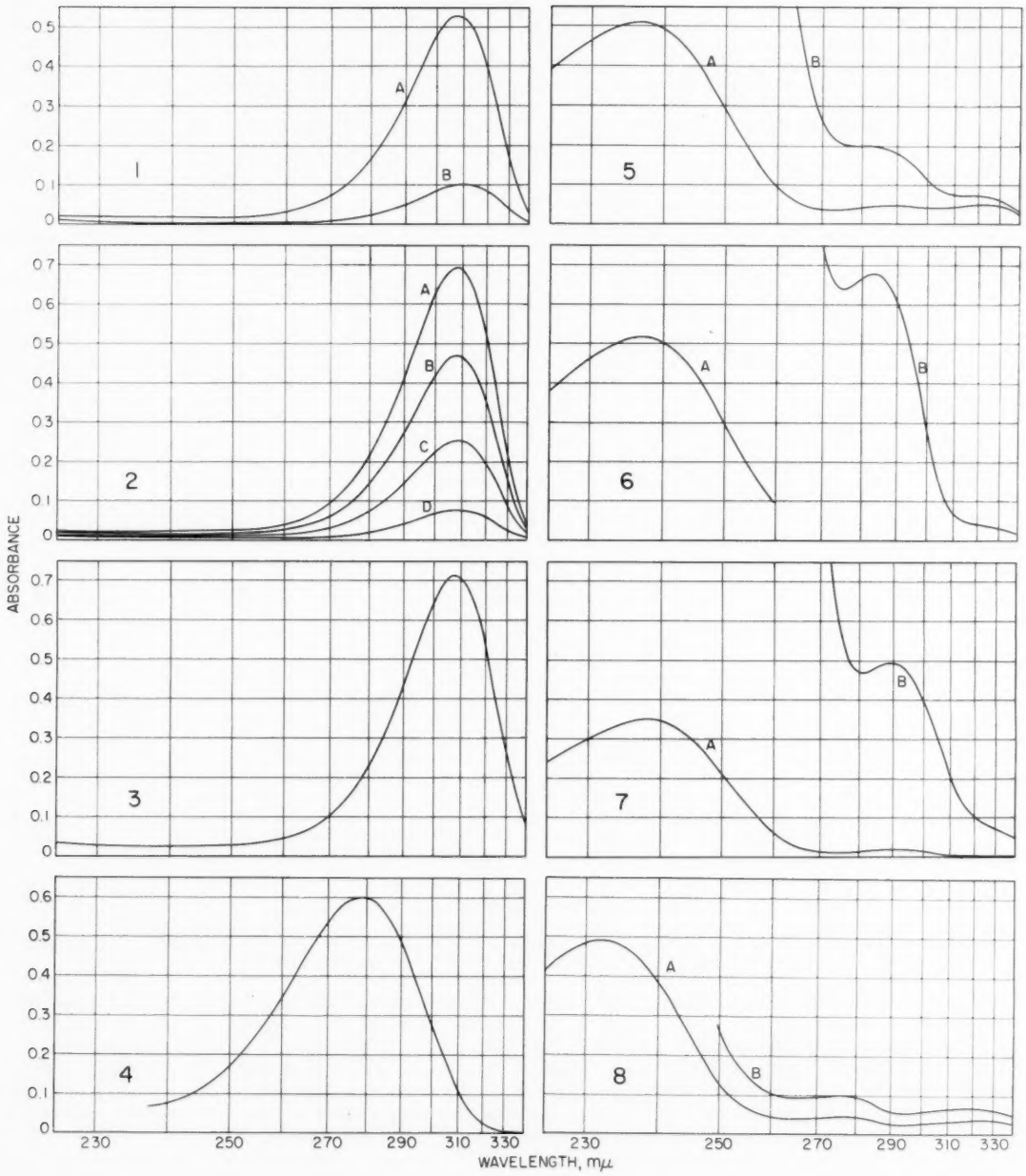

FIGURE 6. *Ultraviolet spectrograms.*

1. DL-*xylo*-4, 5,6-Trihydroxycyclohexenediolic acid (I) in water, $3.6\times10^{-5}M$, λ_{max} near 309mμ. A, 3 min after dissolution; B, 25 min after dissolution; 2. potassium DL-*xylo*-4,5,6-trihydroxycyclohexenediolate monohydrate in water, $3.9\times10^{-5}M$, λ_{max} near 308mμ. A to D, respectively, 10, 16, 22, and 28 min after dissoultion; 3. ammonium DL-*xylo*-4,5,6-trihydroxycyclohexenediolate monohydrate in water, $7.4\times10^{-5}M$, 15 min after dissolution, λ_{max} near 307mμ; 4. DL-*xylo*-4,5,6-trihydroxycyclohexenediolic acid (I) in 5-percent aqueous acetic acid, $4.8\times10^{-5}M$, λ_{max} near 279mμ, ε~12,500; 5. DL-*xylo*-pentaacetoxy-2-cyclohexene-1-one, mp 111 to 113 °C (see sec. 5.2 e2) in methanol. A, $4.3\times10^{-5}M$, λ_{max} near 237mμ, ε~12,400; B, $3.1\times10^{-4}M$, λ_{max} near 283mμ, ε~700; 6. DL-*xylo*-pentaacetoxy-2-cyclohexene-1-one, mp 134 to 136 °C (see sec. 5.2 e2) in methanol. A, $4.3\times10^{-5}M$, λ_{max} near 237mμ, ε~12,400; B, $1\times10^{-4}M$, λ_{max} near 283mμ, ε~700; 7. pentaacetoxy-2-cyclohexene-1-one, mp 154 to 155 °C (see sec. 5.2 e3) in methanol. A, $20.\times10^{-5}M$, λ_{max} near 238mμ, ε~17,500; B, $2.0\times10^{-5}M$, λ_{max} near 288mμ, ε~250; 8. DL-*xylo*-pentabenzoyloxy-2-cyclohexene-1-one; (see sec. 5.2 e1) in methanol. A, $8.3\times10^{-5}M$, λ_{max} near 232mμ; B, $1.65\times10^{-4}M$, λ_{max} near 275mμ.

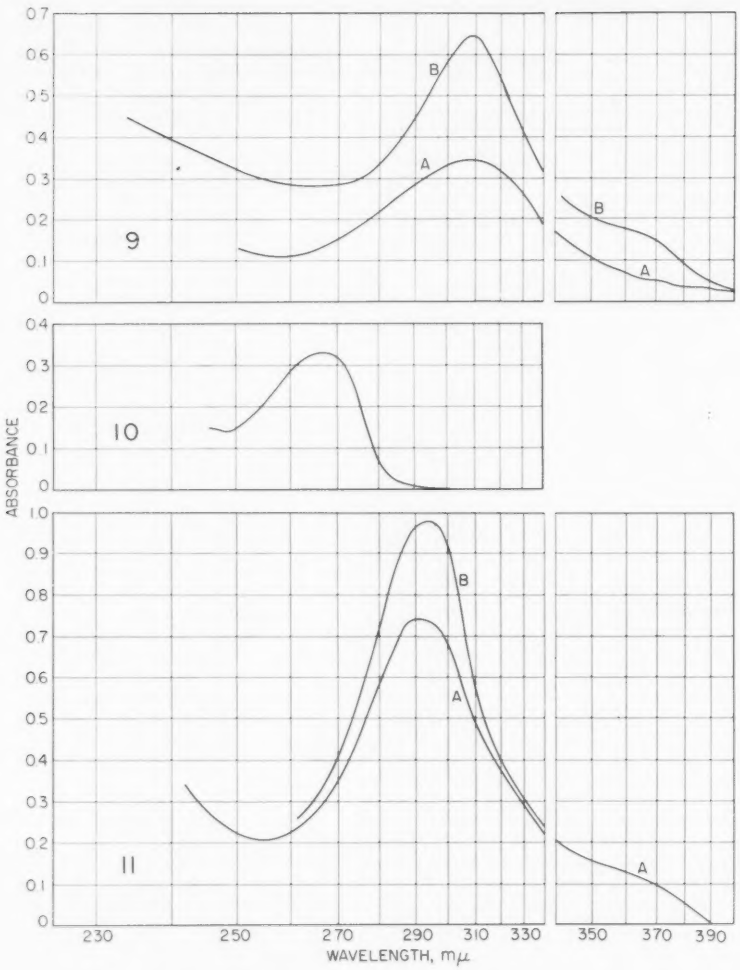

FIGURE 6. *Ultraviolet spectrograms*—Continued

9. *xylo*-4,5,6-trihydroxycyclohexane-1,2,3-trione (II). A, in 5-percent aqueous acetic acid, $4.5\times10^{-3}M$, 5 min after dissolution, λ_{max} near 306mμ. B, in warm water $9.1\times10^{-3}M$, 10 min after dissolution, λ_{max} near 309mμ; 10. pentaacetoxybenzene (see sec. 5.2 f1) in glacial acetic acid, $4.7\times10^{-4}M$, λ_{max} near 267mμ, $\epsilon\sim580$; 11. pentahydroxybenzene in methanol, $1.4\times10^{-4}M$. A, 3 min after dissolution, λ_{max} near 292; B, 9 min after dissolution λ_{max} near 294mμ.

presumably characteristic of the anion and of water of crystallization, respectively.

The infrared spectra of the acetates of I, mp 111 to 113 °C, 134 to 136 °C, and 154 to 155 °C, are given in figure 7, Curves *4*, *5*, and *6*, respectively. They are similar in the region from 2.5 to 7.5μ, showing (a) a doublet near 5.63 and 5.70μ attributed to the presence of both vinyl and saturated acetates, (b) a band near 5.81μ (α,β-unsaturated ester), and (c) a band near 6.02μ (α,β-unsaturated ketone). In the "fingerprint" region, two bands are common to all three, 8.02μ (acetate) and 8.33μ (vinyl acetate) ([35], p. 182; [36], p. 64; [32], pp. 483, 484). However, curve *6* differs markedly from curves *4* and *5* at 7.5 to 7.7, 8.9, 10.2, 11.4, and 13.0μ. Some samples of the crude acetate (mp 111 to 113°C and 134 to 135 °C) of I, showed a strong absorption band at 13.0 μ, as did the acetate of mp 154 to 155 °C; on further purification of the acetate of mp 111 to 113 °C, particularly by change of solvent, the band disappeared. It thus appears that small proportions of the isomer of mp 154 to 155 °C are formed, even in the preparation of the low-melting acetate with "mild" catalysts (see p. 288).

The infrared spectrum of the benzoate of I (fig. 7, 7) shows the bands characteristic of an α,β-unsaturated ester: a doublet at 5.69μ (vinyl ester) and 5.78μ (C=0); and a band at 6.00μ (C=C). Other bands are present at 6.22 and 6.70μ (phenyl) 6.90μ (C—H asymmetric deformation); and 7.95μ (aromatic ester ([36], p. 64)).

The *triketone* (II), unlike the enediolic acid (I), has almost the same ultraviolet spectrum in water, aqueous acetic acid, and methanol; the intensity of

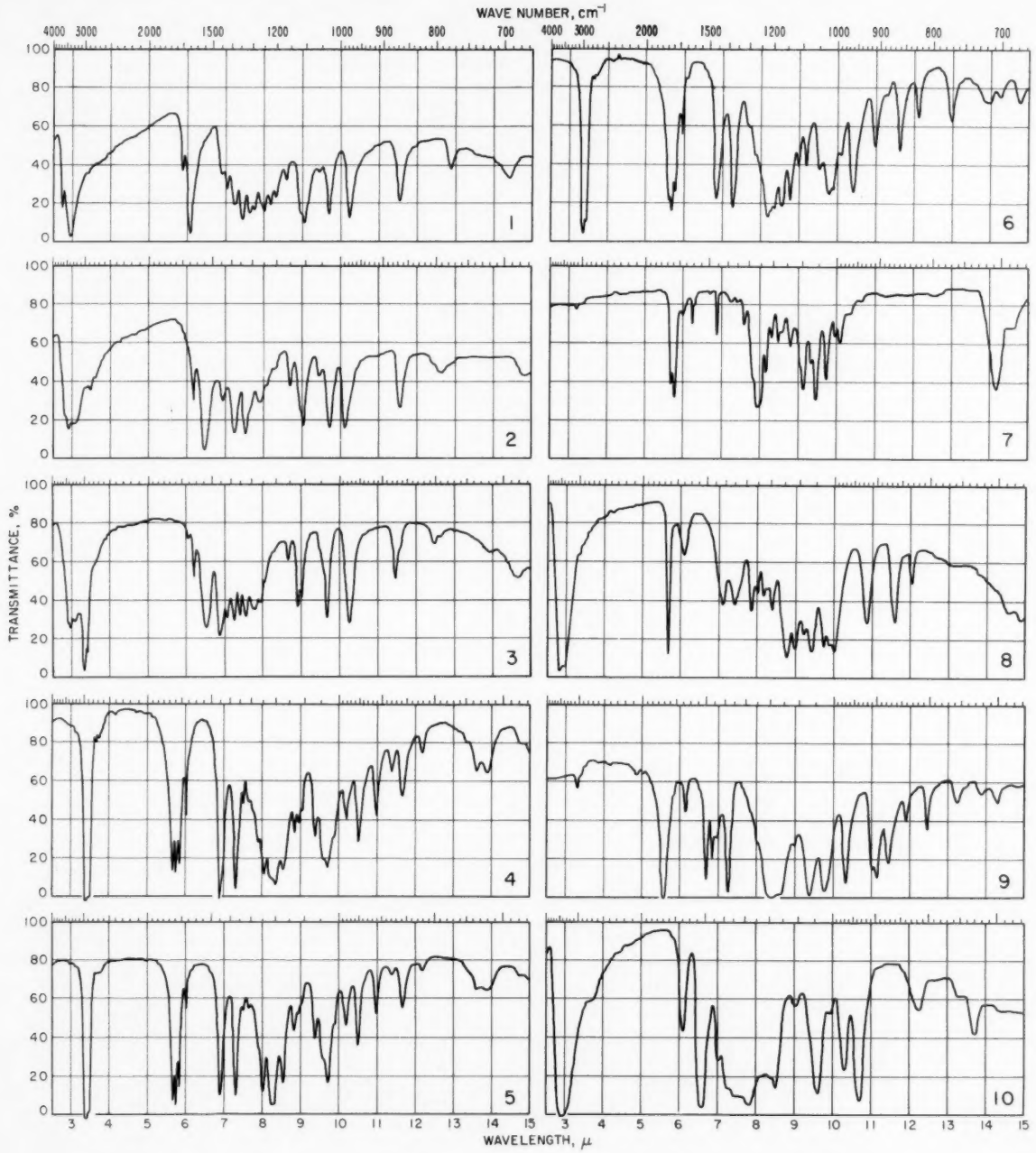

FIGURE 7. *Infrared spectrograms of compounds in Nujol mulls and in potassium chloride pellets.*

1, DL-*xylo*-4,5,6-Trihydroxycyclohexenediolic acid (I) in potassium chloride pellet; 2, potassium salt of I in potassium chloride pellet; 3, ammonium salt of I in Nujol mull; 4, pentaacetate of I (mp 111–113 °C) in Nujol mull; 5, pentaacetate of I (mp 134–136 °C) in Nujol mull; 6, isomeric pentaacetate of I (mp 154–155 °C) in Nujol mull; 7, pentabenzoate of I in potassium chloride pellet; 8, *xylo*-4,5,6-trihydroxycyclohexane-1,2,3-trione in potassium chloride pellet; 9, pentaacetoxybenzene in potassium chloride pellet; 10, pentahydroxybenzene in potassium chloride pellet.

absorption at the observed λ_{max} at 302 to 306 mμ decreases with time (fig. 6, *8*). The identity of the spectra in water and aqueous acetic acid indicates that this band can be attributed to nonenolized carbonyl groups. The observed maximum is in approximate agreement with the maxima (295 to 301 mμ) reported for two isolated carbonyl groups [37]. Aqueous solutions of II show a weak band at about 365 mμ, in addition to the band at 302 to 306 mμ.

If the aqueous solution of II is treated with sodium carbonate, the solution becomes deep yellow, presumably through successive enolization and *beta*-elimination reactions, as represented for the acetates of II in figure 4. Bands appear in the ultraviolet and visible spectra near 296, 368, 422 (sh), and 482 mμ. The band at 368 mμ can be assigned to the anion of an enolized keto group [38]. The bands at 296, 422, and 482 mμ are similar to those observed for tetrahydroxy-*p*-benzoquinone in methanol at 312, 441, and 482 mμ[13] [39] and for *p*-benzoquinone at 296 and 435 mμ. The bands for *p*-benzoquinone have been ascribed to a conjugated keto group [40]. Absorption by quinones in the region of 410 to 440 mμ has been ascribed to an n-π^* transition [41, 42, 43].

When the alkaline solution of II is acidified with acetic acid, a broad band is produced with λ_{max} at 269 to 275 mμ; this band corresponds to a benzenoid structure ([25], pp. 116–120), in agreement with the expected aromatization and formation of *hexahydroxybenzene*. The solution, on treatment with methanolic ferric chloride, gave the magenta color typical of the reaction of phenols. Thus, the spectra and chemical properties indicate that II, in alkaline solution, undergoes aromatization and complex oxidation–reduction reactions.

The infrared spectrum of II (fig. 7, *8*) shows a single band at 5.70 μ, that is, at a somewhat shorter wavelength than that to be expected for dicarbonyl compounds (5.78 to 5.85 μ [36], p. 62, [32], pp. 483–484). A band at 6.12 μ can be attributed to water ([32], p. 430, [34], [33], p. 150).

The ultraviolet spectrum of pentaacetoxybenzene, either in glacial acetic acid or in methanol (fig. 6, *9*), shows a single band, λ_{max} 267 to 268 mμ, within the region characteristic of benzenoid compounds ([25], p. 116).

The infrared spectrum of pentaacetoxybenzene (fig. 7, *9*) is consistent with the aromatic structure. Bands were observed at: 2.31 μ (C—H aromatic stretching); 6.15 μ (olefinic bond); 6.70 μ (aromatic ring); and 11.18 and 11.48 μ (C—H out-of-plane deformation of the isolated hydrogen atom on a pentasubstituted benzene ring). The strong band at 11.95 μ is probably *also* associated with an isolated hydrogen atom on the benzene ring ([35], pp. 69–79, [32], p. 394, [31], pp. 26, 27).

The methyl groups of the acetoxy substituents are associated with absorption at: 6.85 μ (C—H asymmetric deformation); 7.28 μ (C—H symmetrical deformation); 13.22 and 13.85 μ (C—H skeletal vibration) [36], p. 57). Ester bands were observed at 5.60 μ (phenolic acetate), and 8.00 μ (sh) (acetate). A strong band at 8.50 μ is probably associated with the acetoxy substituent ([36], p. 64).

Freshly prepared pentahydroxybenzene, when dissolved in methanol, shows a band at λ_{max} near 292 mμ whose intensity increases with time (fig. 6, *10*). Pentahydroxybenzene is extremely sensitive to oxidation by air. A methanolic solution, exposed to air, quickly acquires a red color and shows absorption bands at 288, 358, and 490 mμ. In comparison, 2,3,5-trimethoxy-*p*-benzoquinone absorbs at 288 mμ in ethanol [44], and hydroquinone absorbs at 294 mμ ([25], p. 119).

The infrared spectrum of pentahydroxybenzene (fig. 7, *10*) is also consistent with an aromatic structure. It shows a band at 6.10 μ (C=C) and at 6.55 μ (substituted benzene ring [35], pp. 71, 72). Characteristic strong bands observed at 12.25 and 13.70 μ are indicative of C—H out-of-plane deformation and of the presence of one free hydrogen atom on the ring. However, a band was not observed in the region of 3.4 to 3.5 μ, characteristic of C—H stretching. Bands found at 9.62, 10.30, and 10.80 μ are apparently associated with pentasubstitution on the ring ([35], p. 79; [36], p. 59; [32], p. 394).

[13] In addition, there is a strong band in the visible region, at 510 mμ.

The authors express their appreciation to H. L. Frush and R. S. Tipson for highly valued counsel and assistance in preparing the manuscript.

6. References

[1] J. Scherer, Ann. **73,** 322 (1850), **81,** 375 (1852).
[2] L. Maquenne, Compt. Rend. **104,** 297 (1887).
[3] T. Posternak, Helv. Chim. Acta **19,** 1333 (1936).
[4] T. Posternak, Helv. Chim. Acta **24,** 1045 (1941).
[5] P. W. Preisler and L. Berger, J. Am. Chem. Soc. **64,** 67 (1942).
[6] H. von Euler and B. Eistert, Chemie und Biochemie der Reduktone and Reduktonate (Ferdinand Enke Verlag, Stuttgart, Germany, 1957).
[7] W. Pigman, The Carbohydrates, p. 329 (Academic Press Inc., New York, N.Y., 1957).
[8] B. Magasanik and E. Chargaff, J. Biol. Chem. **174,** 173 (1948).
[9] S. J. Angyal and L. Anderson, Advan. Carbohydrate Chem. **14,** 135 (1959).
[10] H. G. Fletcher, Jr., Advan. Carbohydrate Chem. **3,** 45 (1948.)
[11] H. S. Isbell, Ann. Rev. Biochem. **12,** 213 (1943).
[12] H. S. Isbell, J. Res. NBS **32,** 45 (1944) RP 1573.
[13] W. Baker, J. Chem. Soc. **1941,** 662.
[14] A. Einhorn, J. Cobliner, and H. Pfeiffer, Ber. **37,** 100 (1904).
[15] R. Nietski and T. Benckiser, Ber. **18,** 1833 (1885).
[16] A. J. Fatiadi and W. Sager, Org. Syn. **42,** 66 (1962).
[17] A. J. Fatiadi, H. S. Isbell, and W. F. Sager, J. Res. NBS **67A,** (Phys. and Chem.) No. 2, 153 (1963).
[18] N. Z. Stanacev and M. Kates, J. Org. Chem. **26,** 912 (1961).
[19] T. Posternak and J. Deshusses, Helv. Chim. Acta **44,** 2088 (1961).
[20] T. Posternak, Biochem. Prep. **2,** 57 (1952).
[21] T. Posternak, Methods Carbohydrate Chem. **1,** 289 (1962).

[22] S. Nishimura and Y. Urushibara, Bull. Chem. Soc. Japan **30,** 199 (1957).
[23] J. S. Fritz and G. H. Schenk, Anal. Chem. **31,** 1808 (1959).
[24] R. Nietzki and T. Benckiser, Ber. **18,** 499 (1885).
[25] A. E. Gillam and E. S. Stern, An Introduction to Electronic Absorption Spectroscopy in Organic Chemistry (Edward Arnold, London, 1954).
[26] H. H. Jaffe and M. Orchin, Theory and Applications of Ultraviolet Spectroscopy (John Wiley & Sons, Inc., New York, N. Y., 1962).
[27] R. Woodward, J. Am. Chem. Soc. **63,** 1123 (1941); **64,** 72, 76 (1942).
[28] L. F. Fieser and M. Fieser, Steroids (Reinhold Publishing Co., New York, N.Y., 1959).
[29] A. M. Cragg, F. M. Dean, and G. Winfield, J. Chem. Soc. **1959,** 2431.
[30] W. F. Forbes, in Steric Effects in Conjugated Systems, G. W. Gray, ed. (Academic Press Inc., New York, N.Y., 1958).
[31] K. Nakanishi, Infrared Absorption Spectroscopy, (Holden-Day, Inc., San Francisco, 1962).
[32] R. N. Jones and C. Sandorfy, in Technique of Organic Chemistry, Vol. **IX,** A. Weissberger, ed. (Interscience Publishers, Inc., New York, N.Y., 1956).
[33] F. A. Miller, in Organic Chemistry, Vol. **III,** H. Gilman ed. (John Wiley & Sons, Inc., New York, N.Y. 1953).
[34] R. J. Morris, Anal. Chem. **35,** 1489 (1963).
[35] L. J. Bellamy, The Infra-red Spectra of Complex Molecules (John Wiley & Sons, Inc., New York, N.Y., 1958).
[36] A. D. Cross, An Introduction to Practical Infra-red Spectroscopy (Butterworths Scientific Publications, London, 1960).
[37] C. Tamm and R. Albrecht, Helv. Chim. Acta **43,** 768 (1960).
[38] K. Yamada, N. Mizuro, and Y. Hirata, Bull. Chem. Soc. Japan **31,** 543 (1958).
[39] A. J. Fatiadi and H. S. Isbell, unpublished work.
[40] E. A. Braude, J. Chem. Soc. **1945,** 490.
[41] L. E. Orgel, Trans. Faraday Soc. **52,** 1172 (1956).
[42] S. E. Hunt and A. S. Lindsey, J. Chem. Soc. **1962,** 4550.
[43] J. W. Sidman, Chem. Rev. **58,** 689 (1958).
[44] K. Yamada and Y. Hirata, Bull. Chem. Soc. Japan **31,** 550 (1958).

(Paper 68A3–275)

JOURNAL OF RESEARCH of the National Bureau of Standards—A. Physics and Chemistry
Vol. 68A, No. 3, May–June 1964

Tritium-Labeled Compounds. XI. Mechanism for the Oxidation of Aldehydes and Aldoses-*1-t* With Sodium Chlorite[1]

Horace S. Isbell and Lorna T. Sniegoski

(February 3, 1964)

Measurements of kinetic isotope-effects (k^*/k) for the oxidation of ten aldoses-*1-t* with sodium chlorite in acid solution gave values ranging from 0.56 to 0.75, with an average of 0.66. The values show that the C1—H* bond is not ruptured in the rate-determining step. For the reaction, a mechanism is proposed which accounts for this fact and for the dependence of the rate of reaction on the concentration of chlorous acid. The mechanism involves formation of a chlorous acid—aldehyde intermediate; this decomposes, giving the aldonic acid and hypochlorous acid. The latter then reacts with more chlorous acid, affording the chlorine dioxide and hydrogen chloride found experimentally.

1. Introduction

Sodium chlorite is widely used for the technological treatment of carbohydrates [1],[2] but the basic chemistry of the reactions involved has not been adequately developed. Jeanes and Isbell [2] showed that (a) nonreducing saccharides, alditols, ketoses, and aldonic acids are inert to chlorites in acid solution, whereas aldoses are oxidized to aldonic acids; (b) the first detectable product from the aldose is the free aldonic acid, and not the lactone; (c) aldopentoses are oxidized more rapidly than aldohexoses, and monosaccharides more rapidly than disaccharides; and (d) the anomer of D-glucopyranose that, in its most stable conformation, is now known to have an axial C1-hydroxyl group is oxidized more rapidly than the anomer having an equatorial C1-hydroxyl group. Formation of the free acid as an initial product, and the more-rapid oxidation of the anomer having an axial C1-hydroxyl group, indicate that the reaction does *not* involve the direct oxidation of a pyranose intermediate, in contrast to the oxidation of an aldose with bromine [3].

Launer, Wilson, and Flynn [4] established that the oxidation is first-order with respect to both aldose and chlorous acid, and they developed a procedure for the quantitative determination of aldoses from the amount of chlorine dioxide formed in the reaction. For D-glucose, D-galactose, and D-mannose, Wilson [5] found an approximate parallelism between the rates of oxidation and the rates of transformation of the ring form of the aldose to the aldehyde form. Previously, White, Taylor, and Vincent [1] had reported that sodium chlorite in acid solution rapidly oxidizes formaldehyde, acetaldehyde, and benzaldehyde, with the formation of chlorine dioxide. Thus, it seems likely that the oxidation of aldoses takes place through the aldehyde form. The situation is complicated by concurrent decomposition of chlorous acid and by certain disproportionation reactions involving chlorine dioxide, chlorous acid, and chlorates. After making allowance for these complications, Jeanes and Isbell [2] found that the oxidation follows eq (1).

$$RCHO + 3\,HClO_2 \rightarrow RCO_2H + HCl + 2\,ClO_2 + H_2O. \quad (1)$$

A satisfactory mechanism for the oxidation of the aldose (or aldehyde) must account for the utilization of 3 moles of chlorous acid per mole, in a process that is first-order with respect to chlorous acid and the aldehyde. In the reaction of an aldehyde with a chlorite in acid solution, one possibility would be a nucleophilic addition of the chlorite ion to the conjugate acid as shown in eq (2). Formation of this

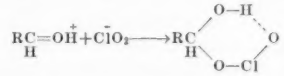

(2)

intermediate would account for the fact that the reaction is first-order with respect to chlorous acid and aldehyde. The intermediate would be similar to an aldehyde bisulfite compound and, by hydrogen bonding, could have a cyclic structure. The intermediate would be unstable, because of the electron deficiency of the chlorine atom and the presence of a potential source of electrons at the C1—hydrogen bond. Release of the C1—hydrogen atom, with the redistribution of electrons as indicated in eq (3), would give a carboxylic acid and hypochlorous acid.

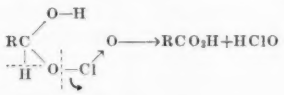

(3)

One mole of the nascent hypochlorous acid would then react with two moles of chlorous acid in the

[1] Presented, in part, before the Division of Carbohydrate Chemistry at the 145th Meeting of the American Chemical Society, New York, N.Y., September 10, 1963. Abstracts Papers, Am. Chem. Soc. **145,** 5p (1963).
[2] Figures in brackets indicate the literature references at the end of this paper.

known manner, according to eq (4).

$$HClO + 2\ HClO_2 \rightarrow 2\ ClO_2 + HCl + H_2O \quad (4)$$

The overall process (eq (3) plus eq (4)) corresponds to eq (1).

With aldoses, the reaction includes the following steps: (1) formation of the aldehyde intermediate from the pyranose; (2) combination of chlorite ion with the aldehyde cation; (3) decomposition of the aldehyde—chlorite complex, yielding aldonic acid and hypochlorous acid; and (4) reaction of 1 mole of the resulting hypochlorous acid with 2 moles of chlorous acid, affording 2 moles of chlorine dioxide and 1 mole of hydrogen chloride. Side reactions give small proportions of chlorate and oxalic acid, as noted and explained by Jeanes and Isbell [2].

Formation of a chlorous acid—aldose intermediate accounts for the first-order kinetics found by Launer, Wilson, and Flynn [4], but, from the kinetics, it is not possible to predict which step is rate determining. The problem can be attacked, however, by the use of isotope effects in the oxidation of aldoses-*1-t*.

In the oxidation of aldoses-*1-t* by bromine and iodine, we have shown [6, 7] that the isotope effect is about 0.14 for reactions in which cleavage of the C1—hydrogen bond is rate determining, and about 0.8 for reactions in which isomerization is rate determining. Hence, an isotope effect of about 0.8 would be expected if steps 1 or 2 are rate determining and of about 0.14 if step 3 is rate determining.

Results for the oxidation of ten aldoses-*1-t* with sodium chlorite, in slightly acid solution at 0 °C, are given in table 1. The values [3] of k^*/k average 0.66.

The magnitude of the isotope effect clearly shows that the C1—hydrogen bond is not broken in the rate-determining step. Presumably the aldehyde—chlorous acid complex forms slowly (steps 1 and 2) and collapses rapidly (step 3). The rate of formation of the aldehyde intermediate from the pyranose by the mutarotation reaction (step 1) depends on the presence of acid and base catalysts and on the particular aldose involved. Step 2 is sensitive to *p*H and to the concentration of chlorite. Hence, the relative rates for steps 1 and 2 would be expected to depend on the experimental conditions and on the particular aldose involved.

The difference in the rates of reaction for the α and β anomers of D-glucopyranose, reported by Jeanes and Isbell [2], shows that reaction of the intermediate aldehyde with chlorous acid is sufficiently fast to preclude maintenance of a steady state in which the aldehyde is in equilibrium with all modifications of the sugar. According to the transition-state theory [8], the rate of reaction depends on the difference in free energy ($\Delta F^{\ddagger}$) for the reactants in the ground state and in the transition state. The higher rate of reaction for α-D-glucopyranose indicates that the difference in free energy is less for the reaction of α-D-glucopyranose than for the reaction of β-D-glucopyranose. This might be expected, because, in the ground state, β-D-glucopyranose is at a lower energy level than α-D-glucopyranose, and the difference in the transition states is small.

At present, there are few data for the chlorite oxidation of the anomers of the other aldoses. For different aldoses, there is an approximate parallelism between the rates of oxidation and the rates of isomerization [5]. Quantitative correlations are not feasible, however, because the reactions are complex and because, in most instances, the isomerization and oxidation reactions have not been measured under like conditions.

2. Experimental Procedures

2.1. Materials and Apparatus

a. Labeled Aldoses

Aldoses-*1-t* were prepared by the procedures given in reference [9]. D-Glucose-*6-t* and D-glucose-*6-*C^{14} were prepared by the procedures given in references [10] and [11], respectively. The "doubly labeled" aldoses D-glucose-*1-*C^{14}*-6-t* and D-glucose-*1-t-6-*C^{14} were prepared by mixing suitable quantities of the singly labeled sugars. The mixtures were recrystallized from water with the addition of methanol and 2-propanol. Before use of each sugar, the purity was checked by paper chromatography.

b. Chlorous Acid Solution

A *1-M* solution of sodium chlorite was prepared by dissolving 9.5 g of commercial sodium chlorite in 100 ml of water. The solution of chlorous acid for the oxidation was prepared immediately before use by mixing one volume of ice-cold, *1-M* sodium chlorite with 1.1 volumes of *1-M* acetic acid; the freshly prepared solution had a *p*H of 3.4.

TABLE 1. *Isotope effects for the oxidation of aldoses*-1-t *with sodium chlorite at* pH *3.4 and 0 °C*

Aldose-*1-t*	Reaction time	Extent of oxidation (*f*)	Isotope effect, k^*/k	Average
	min			
L-Arabinose-*1-t*	10	0.279	0.69	
	15	.254	.73	0.71
D-Galactose-*1-t*	60	.302	.56	
	70	.302	.67	
	80	.297	.76	.66
D-Glucose-*1-t*	180	.243	.64	
	240	.285	.70	.67
D-Lyxose-*1-t*	7	.248	.66	
	10	.463	.71	.68
D-Mannose-*1-t*	45	.399	.59	
	60	.446	.57	.58
L-Rhamnose-*1-t*·H_2O	30	.273	.53	
	60	.342	.61	
	90	.447	.67	.60
D-Ribose-*1-t*	3	.209	.70	
	5	.338	.73	.72
D-Talose-*1-t*	10	.330	.73	
	15	.394	.77	.75
D-Xylose-*1-t*	20	.281	.52	
	25	.263	.60	.56
Average				0.66

[3] The variation in the values (0.56 to 0.75) found for different aldoses-*1-t* is not significant, because it does not differ widely from that found in replicate measurements with a single aldose-*1-t* (for example, 0.56 to 0.76 for D-galactose-*1-t*). The relatively large variation arises from the difficulty in determining small quantities of reducing sugar in mixtures containing sodium chlorite.

TABLE 2. *Isotope effects for the oxidation of* D-*glucose*-1-C^{14}-6-t *and of* D-*glucose*-1-t-6-C^{14} *with sodium chlorite at* pH *3.4 and 0 °C*

Labeled aldose	Sample		$HClO_2$	Reaction time	Carrier added	f	$p°$	p	k^*/k	k^*/k (average)
	mg	*m mole*	*m mole*	*hr*	*mg*					
D-Glucose-*1*-C^{14}-*6-t*	11.370	0.063	0.170	20	100.2	0.752	0.1144	0.1105	1.02	
	9.481	.053	.120	20	100.4	.656	.1144	.1164	0.98	1.00
D-Glucose-*1-t-6*-C^{14}	9.825	.055	.147	20	100.1	.764	9.12	14.40	.68	
	9.155	.051	.120	20	100.4	.695	9.12	13.84	.65	
	[a] 9.043	.050	.151	1	99.9	.306	9.12	10.00	.75	
	9.190	.052	.294	5.5	100.1	.437	9.12	11.12	.66	
	9.807	.054	.147	20	100.8	.680	8.02	11.12	.71	
	9.545	.053	.127	20	100.8	.640	8.02	10.78	.71	
	11.030	.061	.918	8.5	100.6	.611	8.02	9.88	.78	
	10.217	.057	.851	7.5	100.8	.596	8.02	10.10	.75	0.72

[a] Phosphoric acid was used in the reaction mixture, instead of acetic acid.

c. Counting Equipment

Carbon 14 or tritium, or both, were determined by measurements of radioactivity, either with a liquid scintillation spectrometer or with a windowless, gas-flow, proportional counter. The measurements given in table 1 were made with the liquid scintillation spectrometer by the procedure given in reference [12]. Those given in table 2 were made, in films, with the gas-flow, proportional counter by the procedure described in [13], and with the liquid scintillation spectrometer by the procedure described in [6] and [12].

2.2. Chlorous Acid Oxidation of Aldoses-*1-t*

a. Determination of k^*/k by the H_2O-*t* Method

A 0.05-mmole sample of aldose-*1-t* was weighed into a 10-ml volumetric flask. The aldose-*1-t* was dissolved in three drops of water, and the solution was allowed to stand overnight. The flask was then cooled in an ice bath, and 1.58 ml (a fivefold excess) of ice-cold, chlorous acid solution was added. The reaction was allowed to proceed for sufficient time to oxidize 20 to 45 percent of the aldose-*1-t*, the solution was diluted to 10 ml with ice water, and aliquots were taken for analysis. A 5-ml aliquot was transferred to a 25-ml volumetric flask containing 0.83 ml of 2.11-*N* potassium iodide. A 2-ml aliquot was removed to a 50-ml standard-tapered, male-joint flask containing 20 mg of anhydrous sodium carbonate. This solution was frozen and the water-*t* was sublimed by the procedure described in [6]. Duplicate samples of the tritiated water were analyzed with the Packard Tri-Carb counter, using 100 μl of distillate and 10 ml of the scintillator solution. Each sample was counted to a total of 10,000 counts, to give a statistical accuracy of ±1 percent.

The 5-ml aliquot in the 25-ml flask was used for the determination of the residual aldose-*1-t*. The iodine formed by reaction of the excess chlorous acid with the potassium iodide was reduced by the addition of 6 to 8 ml of a 6-percent, aqueous solution of sulfur dioxide. The solution was allowed to stand for at least half an hour, and was then boiled to remove all sulfur dioxide and to concentrate the solution. After the solution had cooled, it was neutralized with aqueous sodium hydroxide to the Phenol Red endpoint. The volume was adjusted to 25 ml, and three 5-ml aliquots were analyzed for reducing sugar by the Somogyi method [14]. The method was standardized, for each aldose, and the factor so obtained was used for calculating the amount of aldose in the sample.

The isotope effect, k^*/k, was calculated from eq (5),

$$k^*/k = \log\,(1-rf)/\log\,(1-f) \qquad (5)$$

where f is the ratio of the weight of aldose consumed to the initial weight, and rf is the ratio of the total μc of tritiated water formed to the μc of tritium in the initial sample (calculated from the specific activity of the sample).

b. Determination of k^*/k by the Double-Labeled Method [15]

Samples of doubly labeled D-glucose of about 9 mg (0.05 mmole) were weighed into separate, small, test tubes on the microbalance. The tubes were placed on a shaker in an ice-water bath, and the quantities of ice-cold chlorous acid solution listed in table 2 were added. The reactions were allowed to proceed for the times given.

After elapse of the recorded reaction time, 100 mg of D-glucose carrier and 50 mg of a decolorizing carbon were added to each tube, the mixture was filtered, and the filtrate was passed through mixed anion-cation resin. The eluate and washings were concentrated, and filtered into a standard-tapered test tube. The solution was concentrated and the labeled D-glucose was crystallized three times from water, with the addition of methanol and 2-propanol. The purified, doubly labeled D-glucose was assayed for radioactivity, either in solution with the liquid scintillation counter, or in films with the proportional counter.

The isotope effect, k^*/k, was calculated by eq (6) [15],

$$k^*/k = 1+[\log\,(p/p°)/\log\,(1-f)] \qquad (6)$$

where p is the ratio of the functional to the reference isotope in the residual reactant, $p°$ is the ratio in the initial reactant, and f and k^*/k have the same meanings as before. The data are recorded in table 2.

3. References

[1] J. F. White, M. C. Taylor, and G. P. Vincent, Ind. Eng. Chem. **34,** 782 (1942).

[2] A. Jeanes and H. S. Isbell, J. Res. NBS **27,** 125 (1941) RP1408.

[3] H. S. Isbell, J. Res. NBS **66A** (Phys. and Chem.) No. 3, 233 (1962).

[4] H. F. Launer, W. K. Wilson, and J. H. Flynn, J. Res. NBS **51,** 237 (1953) RP2456.

[5] W. K. Wilson, Tappi **38,** 274 (1955).

[6] H. S. Isbell and L. T. Sniegoski, J. Res. NBS **67A** (Phys. and Chem.) No. 6, 569 (1963).

[7] H. S. Isbell and L. T. Sniegoski, J. Res. NBS **68A** (Phys. and Chem.) No. 2, 145 (1964).

[8] H. Eyring, Chem. Rev. **17,** 65 (1935).

[9] H. S. Isbell, H. L. Frush, N. B. Holt, and J. D. Moyer, J. Res. NBS **64A** (Phys. and Chem.) No. 3, 233 (1962).

[10] H. S. Isbell, H. L. Frush, and J. D. Moyer, J. Res. NBS **64A** (Phys. and Chem.) No. 4, 359 (1960).

[11] R. Schaffer and H. S. Isbell, J. Res. NBS **56,** 191 (1956) RP2667.

[12] F. N. Hayes, Packard Technical Bulletin, January, 1962, Packard Operation Manual, Tri-Carb Liquid Scintillation Spectrometer, Series 314 E. Packard Instrument Company Inc., La Grange, Ill.

[13] H. S. Isbell, H. L. Frush, and N. B. Holt, J. Res. NBS **64A** (Phys. and Chem.) No. 2, 171 (1960).

[14] F. J. Bates and Associates, Polarimetry, saccharimetry and the sugars, NBS Circ. 440, p. 196.

[15] H. S. Isbell, L. T. Sniegoski, and H. L. Frush, Anal. Chem. **34,** 982 (1962).

(Paper 68A3–276)

JOURNAL OF RESEARCH of the National Bureau of Standards—A. Physics and Chemistry
Vol. 68A, No. 3, May–June 1964

Medium Effects on the Dissociation of Weak Acids in Methanol-Water Solvents

E. E. Sager, R. A. Robinson, and R. G. Bates

(February 5, 1964)

A spectrophotometric method has been used to determine the dissociation constants of *o*-chloroanilinium ion, *m*-nitroanilinium ion, and 4-chloro-2,6-dinitrophenol in methanol-water solvents at 25 °C. The ranges of solvent compositions (in weight percent methanol) were as follows: *o*-chloroanilinium ion, 0 to 99.9; *m*-nitroanilinium ion, 0 to 93.7; and 4-chloro-2,6-dinitrophenol, 0 to 33.4. The pK of the first two acids falls with addition of methanol and passes through a minimum when the mole fraction of methanol in the solvent mixture is about 0.7. The pK of the substituted phenol, however, rises as the dielectric constant of the solvent is decreased by addition of methanol. It is suggested that the total medium effect for both types of acid can be explained by the superposition of an electrostatic effect and a nonelectrostatic effect. The latter is a constant for each particular solvent composition and probably characterizes the acid-base property of the medium itself.

1. Introduction

The nature of the parameters that describe the effect of a changing medium on the free energy of electrolytes is not yet well understood. There is considerable agreement, however, that two effects, one electrostatic and the other chemical, can be identified [1].[1] The electrostatic effect is more easily estimated than is the chemical term. The Born equation [2] furnishes an estimate of the former by contrasting the work required to charge spherical ions in the two media of different dielectric constant. This simple approach ignores specific chemical effects and second-order interactions and treats the medium as a dielectric continuum. Nevertheless, it may furnish estimates of medium effects that are completely reasonable and, when a comparison with experiment is possible, also qualitatively correct.

The effects of changes in the composition of a solution on an acid-base equilibrium in that solution

$$\mathrm{A} \rightleftharpoons \mathrm{B} + \mathrm{H}^+ \tag{1}$$

are embodied in the activity coefficients, γ_i, which are part of the thermodynamic formulation of the expression for the equilibrium constant K, in this special case the acidic dissociation constant of A. On the molal (m) scale,

$$K = \frac{m_{\mathrm{H}} m_{\mathrm{B}}}{m_{\mathrm{A}}} \frac{\gamma_{\mathrm{H}} \gamma_{\mathrm{B}}}{\gamma_{\mathrm{A}}}. \tag{2}$$

The numerical value of K is fixed by choice of a standard state in which the activity coefficients are assigned values of unity. In aqueous solutions, the customary standard state is chosen so that γ_i approaches unity as m approaches 0.

When the composition of the solvent medium changes as well as the solute concentration (and ionic strength), it is convenient to separate each activity coefficient, γ_i, into two factors,

$$\gamma_i \equiv {}_{\mathrm{m}}\gamma_i \cdot {}_{\mathrm{s}}\gamma_i. \tag{3}$$

γ_i is measured relative to the standard state in pure water and becomes unity only in an infinitely dilute *aqueous* solution. On the contrary, the activity coefficient ${}_{\mathrm{s}}\gamma_i$ in eq (3) becomes unity when $m=0$ in the solvent s, whereas ${}_{\mathrm{m}}\gamma_i$ has a value different from unity whenever the solvent differs from pure water.

The "salt effect" ${}_{\mathrm{s}}\gamma_i$ varies with the solute concentration, but the "medium effect" ${}_{\mathrm{m}}\gamma_i$ is a function only of the free energy of the species i in the two standard states (namely those in the medium s and in water). When ionic species are involved, ${}_{\mathrm{s}}\gamma_i$ can be estimated by the Debye-Hückel equation with appropriate allowance for the effect of altering the dielectric constant of the medium s on the interionic forces.

The activity coefficient ${}_{\mathrm{m}}\gamma_i$ measures the difference in the standard free energy of i in the two media:

$$\Delta G_i^0 = {}_{\mathrm{s}}G_i^0 - {}_{\mathrm{w}}G_i^0 = RT \ln {}_{\mathrm{m}}\gamma_i. \tag{4}$$

Electrostatic considerations show that there will be a change of free energy when free ions are transferred from one medium to another of different dielectric constant, even though the ions remain free in the second medium also. Yet chemical interactions, of which solvation is the most important, must surely influence the medium effect as well. For this reason, the nonelectrostatic contribution to the free energy may change considerably as the solvent composition is altered.

The reaction of the solvent with the acid A and the base B in eq (1) (solvation) is a manifestation of the acid-base property of the solvent. Hence, the electrostatic treatment accounts satisfactorily for the change of the equilibrium constant of eq (1) with dielectric constant only when the change of dielectric constant is accomplished without a change

[1] Figures in brackets indicate the literature references at the end of this paper.

in the acid-base properties of the solvent. This condition is evidently difficult to achieve, but the essential correctness of these concepts is attested by the observation that the ratios of the dissociation constants of different acids A to that of a chosen reference acid of the same charge type are often nearly independent of the dielectric constant of the solvent.

In view of the complexity of the medium effect on acid-base dissociation, it is not surprising that the Born electrostatic treatment alone is incapable of yielding useful quantitative data. It is indeed rather remarkable that the predictions of the Born equation are so often qualitatively correct. Considering only the electrostatic contribution to the free energy, one can write, by combining the Born equation with eq (4),

$$\ln {}_{\mathrm{m}}\gamma_i = \frac{Nz_i^2e^2}{2RTr}\left(\frac{1}{\epsilon_s}-\frac{1}{\epsilon_w}\right), \tag{5}$$

where N is the Avogadro number, z_i is the number of charges borne by the species i, e is the electronic charge, r is the radius of the (spherical) ion or molecule i, ϵ_s and ϵ_w are the dielectric constants of the two solvent media, R is the gas constant, and T is the temperature in degrees Kelvin. The mass law expression, eq (2), for equilibrium (1) yields

$${}_sK = {}_wK \cdot \frac{{}_{\mathrm{m}}\gamma_{\mathrm{A}}}{{}_{\mathrm{m}}\gamma_{\mathrm{H}} \cdot {}_{\mathrm{m}}\gamma_{\mathrm{B}}}, \tag{6}$$

where ${}_wK$ and ${}_sK$ are the dissociation constants referred to the standard states in water and in solvent s, respectively.

By combination with eq (5) we obtain

$$p({}_sK)-p({}_wK) = \frac{Ne^2}{4.6052RT}\left(\frac{1}{\epsilon_s}-\frac{1}{\epsilon_w}\right)\left(\frac{z_{\mathrm{B}}^2}{r_{\mathrm{B}}}-\frac{z_{\mathrm{A}}^2}{r_{\mathrm{A}}}+\frac{1}{r_{\mathrm{H}}}\right). \tag{7}$$

When the dissociation equilibrium (1) is of the charge type A^0B^- (for example, A^0= uncharged acetic acid, B^-= acetate anion; $z_A=0$), eq (7) predicts that $p({}_sK)$ will be greater than $p({}_wK)$ if the dielectric constant ϵ_s is lower than that of water (as it is in methanol-water solvents and in pure methanol). Actually the pK for acids of this charge type has been found to be from 3 to 5 units higher in methanol than in water.[2]

If the equilibrium is of the charge type A^+B^0 (for example, A^+= anilinium cation, B^0= uncharged aniline; $z_B=0$) and r_H is about equal to r_A, however, the electrostatic treatment alone would lead one to expect pK to be almost unaffected by changes in the dielectric constant of the solvent. It is unlikely that r_A will often be less than r_H, and therefore an increase in pK would be more easily explained on electrostatic grounds than would a decrease. In actuality, there are several instances where pK for acids of this charge type has been found to be nearly the same in pure methanol as in water [3]. There is evidence, however, that the pK of amines decreases when methanol is added to the water solvent; it passes through a minimum at a solvent composition in the region 60 to 80 wt percent methanol and rises again at high methanol concentrations.[3]

This type of shift of the equilibrium constant of an isoelectric process with composition of the solvent is of interest for its implications concerning the relative basicities of water and methanol in the mixed solvents, about which there is as yet no general agreement. For example, the conductance of hydrochloric acid in methanol-water mixtures appears to indicate that protons are bound more tightly to water molecules than to methanol [8], and equilibrium studies have led to the same result [9]. On the other hand, Feakins and Watson [10] have concluded that the standard free energies of transfer of the halogen acids from water to the mixed solvent (10 or 43.12 wt percent methanol) indicate that the proton is in a state of lower energy in the methanol-water solvents than in pure water. Similar conclusions have been drawn by Wells [11] from the behavior of *p*-nitroaniline in solutions of strong acids in methanol and isopropanol.

The dissociation constants of two substituted anilinium acids, namely *o*-chloroanilinium ion and *m*-nitroanilinium ion, have been determined in solutions of hydrochloric acid by spectrophotometric methods in methanol-water solvents of composition varying from 0 to 93.7 wt percent methanol (*m*-nitroanilinium) or 99.9 wt percent (*o*-chloroanilinium). The pK of both acids has been found to decrease as the solvent is enriched with methanol up to a composition of about 70 mole percent, where it passes through a minimum and rises rapidly as the last 10 percent of water is removed from the mixed solvent. The contrasting behavior of an acid of the charge type A^0B^- has also been demonstrated by parallel measurements on 4-chloro-2,6-dinitrophenol at three methanol concentrations between 0 and 33.5 wt percent.

2. Experimental Methods

2.1. Materials

o-Chloroaniline was purified by distillation at reduced pressure (about 16 mm Hg) and was stored in the dark. *m*-Nitroaniline was recrystallized once from methanol, and 4-chloro-2,6-dinitrophenol was crystallized three times from methanol.

The spectro grade methanol used in the study of *o*-chloroaniline was distilled and the first fraction collected was discarded. The lot used in the measurements was found by Karl Fischer titration to contain 0.09 percent water. This grade of methanol was of sufficiently high quality that it was used without distillation in the study of the other two indicators.

[2] See, for example, references 3 and 4.

[3] See, for example, references 5, 6, and 7

Hydrochloric acid, purified by distillation, was used to prepare the solutions in solvents containing at least 10 wt percent of water, but diluted reagent grade acid was used without further purification to obtain the limiting absorptions of the acidic forms of the three substances studied.

For solvents of high methanol concentration, a reagent solution was prepared by passing gaseous hydrogen chloride (generated by adding concentrated aqueous hydrochloric acid dropwise to concentrated sulfuric acid) into methanol. The hydrochloric acid solutions were standardized by titration with a standard aqueous solution of sodium hydroxide. At the highest methanol concentrations, the limiting absorption of the alkaline form of the indicator was measured in a solution of sodium methoxide formed by dissolving a piece of clean sodium metal in methanol. The concentration of this solution was determined by titration with a standard aqueous solution of hydrochloric acid.

2.2. Procedures

The several components of the solutions were weighed so that the weight composition of the solvent and the molality of each constituent could be calculated. The spectral absorbance of the solutions containing *o*-chloroaniline was measured by a Beckman Model DU spectrophotometer the cell compartment of which was controlled at 25 °C. In general, the absorbance was determined at 10 to 12 different wavelengths extending from 10 mμ below the maximum of the absorption band to 10 mμ above. The value of α, the fraction of the indicator present in the base form, was computed from each measurement, and the results were averaged.

An Optica single-beam spectrophotometer was employed for the measurements with *m*-nitroaniline and 4-chloro-2,6-dinitrophenol. The room in which the instrument was located was maintained at a temperature close to 25 °C. The measurements were made at the wavelength at which the absorptions of the base forms (the free aniline and the phenolate ion) were at a maximum in water. These wavelengths were 360 mμ and 450 mμ, respectively. The solvents used in the study of *m*-nitroanilinium ion varied in composition from pure water to 93.7 wt percent methanol, while the dissociation of 4-chloro-2,6-dinitrophenol was studied in pure water, 16.2 percent methanol, and 33.5 percent methanol.

3. Results. Calculation of pK

The spectrophotometric data for *o*-chloroanilinium ion are summarized in table 1. The values of log $\frac{\alpha}{1-\alpha}$ for mixtures of *o*-chloroaniline and hydrochloric acid (third column) are the averages of about 10 measurements made at wavelengths near the maximum of the absorption band. This quantity is log $[(D-D_1)/(D_2-D)]$, where D_1, D_2, and D are respectively the absorbance of the acid form of the indicator molecule, of the base form, and of the solution of the partially transformed indicator, determined in the same or identical cells at identical total concentrations of the absorbing substance. The molality of

TABLE 1. *Determination of* $p(_aK)$ *for o-chloroanilinium ion in water and in methanol-water solvents by the spectrophotometric method at 25 °C*

m_{HCl}	$-\log m_H$	$\log \frac{\alpha}{1-\alpha}$	$p(_aK)'$
Water; indicator $3.46\times10^{-4}M$			
0.000404	3.445	0.825	2.620
.001616	2.828	.215	2.613
.002522	2.629	.004	2.625
.003533	2.477	−0.139	2.616
.006062	2.235	−.373	2.608
.01010	2.008	−.624	2.632
			$p(_aK)=2.615$
			S.D.=0.008
8.0 wt percent MeOH; indicator $3.72\times10^{-4}M$			
0.001041	3.025	0.469	2.556
.002083	2.715	.168	2.547
.003124	2.533	−0.027	2.560
.005208	2.304	−.254	2.558
.01041	1.995	−.567	2.562
			$p(_aK)=2.552$
			S.D.=0.005
16.2 wt percent MeOH; indicator $3.72\times10^{-4}M$, $3.43\times10^{-4}M$			
0.002112	2.703	0.237	2.466
.003167	2.523	.055	2.468
.004223	2.395	−0.073	2.468
.005278	2.296	−.175	2.471
.01056	1.989	−.498	2.486
			$p(_aK)=2.459$
			S.D.=0.001
24.6 wt percent MeOH; indicator $3.72\times10^{-4}M$, $3.43\times10^{-4}M$			
0.001070	3.003	0.631	2.372
.002138	2.693	.342	2.351
.003209	2.514	.151	2.363
.004280	2.387	.025	2.362
.005344	2.288	−0.079	2.367
.01070	1.982	−.405	2.387
			$p(_aK)=2.355$
			S.D.=0.008
33.4 wt percent MeOH; indicator $3.43\times10^{-4}M$			
0.002173	2.683	0.458	2.225
.003256	2.504	.285	2.219
.004348	2.377	.159	2.218
.005432	2.279	.057	2.222
.008694	2.072	−0.143	2.215
.01086	1.974	−.240	2.214
.02176	1.671	−.545	2.216
			$p(_aK)=2.221$
			S.D.=0.003
42.4 wt percent MeOH; indicator $3.43\times10^{-4}M$			
0.002211	2.670	0.633	2.037
.003315	2.493	.447	2.046
.004419	2.367	.321	2.046
.005525	2.269	.220	2.049
.01105	1.965	−0.081	2.046
.02211	1.661	−.398	2.059
			$p(_aK)=2.041$
			S.D.=0.003
52.0 wt percent MeOH; indicator $3.43\times10^{-4}M$			
0.001128	2.960	1.064	1.896
.002254	2.658	.764	1.894
.003386	2.481	.578	1.903
.004507	2.355	.464	1.891
.005645	2.258	.365	1.893
.02250	1.651	−0.250	1.901
			$p(_aK)=1.895$
			S.D.=0.004

TABLE 1. *Determination of* $p(_sK)$ *for o-chloroanilinium ion in water and in methanol-water solvents by the spectrophotometric method at 25 °C*—Continued

m_{HCl}	$-\log m_H$	$\log \frac{\alpha}{1-\alpha}$	$p(_sK)'$
62.3 wt percent MeOH; indicator $3.43\times10^{-4}M$			
0.002313	2.645	0.869	1.776
.005790	2.243	.484	1.759
.008095	2.098	.333	1.765
.01158	1.952	.182	1.770
.01388	1.863	.097	1.767
.01737	1.766	−.005	1.771
.02315	1.640	−.128	1.768
.03473	1.463	−.300	1.763
			$p(_sK)=1.769$
			S.D.$=0.005$
73.4 wt percent MeOH; indicator $3.72\times10^{-4}M$			
0.01192	1.939	0.241	1.698
.01792	1.753	.059	1.694
.02386	1.627	−.069	1.696
.02729	1.568	−.137	1.705
			$p(_sK)=1.691$
			S.D.$=0.004$
82.1 wt percent MeOH; indicator $3.72\times10^{-4}M$			
0.002456	2.619	0.940	1.679
.006144	2.220	.535	1.685
.01223	1.918	.219	1.699
.01814	1.747	.038	1.709
.02376	1.629	−.079	1.708
.03005	1.452	−.252	1.704
			$p(_sK)=1.685$
			S.D.$=0.008$
87.8 wt percent MeOH; indicator $3.82\times10^{-4}M$			
0.002481	2.617	0.800	1.817
.003105	2.520	.715	1.805
.003730	2.440	.633	1.807
.004969	2.315	.507	1.808
.006216	2.217	.420	1.797
.01242	1.914	.104	1.810
.01693	1.778	−.040	1.818
.02412	1.623	−.191	1.814
.04810	1.321	−.519	1.840
			$p(_sK)=1.804$
			S.D.$=0.006$
99.9 wt percent MeOH; indicator $3.82\times10^{-4}M$			
0.000426	3.570	0.228	3.342
.000788	3.281	−.073	3.354
.001420	2.967	−.377	3.344
.001607	2.904	−.459	3.363
.002979	2.591	−.747	3.338
.008764	2.081	−1.345	3.426
			$p(_sK)=3.336$
			S.D.$=0.014$

hydrochloric acid is given in the first column, and the logarithm of the molality of the hydrogen ion at equilibrium (taking into account the acid-base reaction with the aniline) is given in the second column.

The values of $p(_sK)'$ for *o*-chloroanilinium ion were calculated by the equation

$$p(_sK)' \equiv p(_sK) + \log_s \left(\frac{\gamma_H \gamma_B}{\gamma_{HB^+}}\right)$$

$$= -\log m_H - \log \frac{\alpha}{1-\alpha}, \quad (8)$$

where B represents the free aniline base and γ_i is the activity coefficient on the molal basis, here referred to the standard state in the methanolic solvent s.

Activity coefficient terms of this form and charge type have been found to vary in proportion to the ionic strength in 33.4 wt percent methanol, as they do in water [12]. Hence, $p(_sK)$ is the intercept at $I=0$ of the best straight line through the several values of $p(_sK)'$. The values of $p(_sK)$ are given at the end of each section of the table. The estimates of the standard deviation of a point from the extrapolation line are marked "S.D."

Similar but less extensive data were obtained for the acids *m*-nitroanilinium ion and 4-chloro-2,6-dinitrophenol. The total concentration of the indicator (sum of the concentrations of the acid and base forms) was $4\times10^{-4}M$ for *m*-nitroanlinium ion and 1×10^{-4} for 4-chloro-2,6-dinitrophenol. The molar extinction coefficient of *m*-nitroaniline (the base form) remained constant at 1,390 up to a methanol concentration of 87.8 wt percent but rose to 1,410 in 93.7 percent methanol. The corresponding extinction coefficient for the chloro-dinitrophenolate ion was 6,880 in water and increased to 6,920 and 7,070 in 16.2 and 33.5 wt percent methanol, respectively.

The values of $p(_sK)'$ for *m*-nitroanilinium ion were calculated by eq (8). For 4-chloro-2,6-dinitrophenol they were calculated by the equation

$$p(_sK)' \equiv p(_sK) + bm = -\log m_H - \log \frac{\alpha}{1-\alpha}$$

$$+ \frac{A\sqrt{m}}{1+1.5(78.30/\epsilon_s)\sqrt{m}} \quad (9)$$

where the activity coefficient term $\gamma_H\gamma_{B^-}/\gamma_{HB}$ has been expressed by a form of the Debye-Hückel equation; m is the molality of hydrochloric acid and A is the Debye-Hückel slope at the dielectric constant (ϵ_s) of the methanolic solvent [13]. For *m*-nitroanilinium ion in solvents of methanolic content from 0 to 42.6 wt percent, there was no apparent trend of $p(_sK)'$ with m (that is, b was zero). At the higher concentrations of methanol, however, the thermodynamic $p(_sK)$ was determined by extrapolation of $p(_sK)'$ to $m=0$. Likewise the values of $p(_sK)'$ for 4-chloro-2,6-dinitrophenol did not appear, within the error of the experiments, to change with m. The $p(_sK)$ for this acid was therefore obtained by averaging the separate values of $p(_sK)'$.

The results for these two acids are given in table 2, together with the estimates of the standard deviations (S.D.) of a single point. The pK values found in pure water are in excellent agreement with earlier results, for example *m*-nitroanilinium, 2.46_1 at 25° (Biggs and Robinson [14]), and 4-chloro-2,6-dinitrophenol, 2.97 at 25° (Bates and Schwarzenbach [15]). The $p(_sK)$ values in the methanolic solvents were plotted as a function of N_2, the mole fraction of methanol, and the values given in table 3 were interpolated for round values of the weight percentage of methanol. The values of $p(_sK)-p(_wK)$ at round values of the mole fraction (N_2) of methanol are given in table 4.

TABLE 2. p($_s$K) *for m-nitroanilinium ion and 4-chloro-2,6-dinitrophenol in methanol-water solvents at 25 °C*

Wt % MeOH	0	8.0	16.2	24.6	33.4	42.6	59.0	80.0	87.8	93.7
m-Nitroanilinium ion										
$p(_sK)$	2.460	2.402	2.267	2.132	1.944	1.790	1.505	1.393	1.428	1.679
S.D.	0.003	0.004	0.011	0.012	0.005	0.012	0.004	0.010	0.010	0.011
4-Chloro-2,6-dinitrophenol										
$p(_sK)$	2.969		3.089		[a]3.177					
S.D.	0.007		0.004		0.004					

[a] In 33.5 wt % methanol.

TABLE 3. *Interpolated values of* p($_s$K) *for o-chloroanilinium ion, m-nitroanilinium ion, and 4-chloro-2,6-dinitrophenol in methanol-water solvents at 25 °C*

Wt % MeOH	*o*-Chloroanilinium	*m*-Nitroaniiinium	4-Chloro-2,6-dinitrophenol
0	2.61_5	2.46_0	2.96_9
10	2.53	2.37	3.05
20	2.42	2.22	3.11
30	2.27	2.03	3.16
40	2.09	1.83	
50	1.92	1.63	
60	1.79	1.50	
70	1.71	1.43	
80	1.68	1.39	
90	1.92	1.48	
99.9	3.34		

TABLE 4. *Medium effects on* pK *for o-chloroanilinium ion, m-nitroanilinium ion, and 4-chloro-2,6-dinitrophenol in methanol-water solvents at 25 °C*

N_2	$p(_sK)-p(_wK)$ for		
	o-Chloroanilinium	*m*-Nitroanilinium	4-Chloro-2,6-dinitrophenol
0	0	0	0
0.1	−0.15	−0.17	+0.12
0.2	−.35	−.45	+.19
0.3	−.58	−.69	+.25
0.4	−.75	−.90	
0.5	−.86	−1.00	
0.6	−.92	−1.05	
0.7	−.93	−1.07	
0.8	−.81	−1.03	
0.9	−.42	−0.74	
0.999	+0.75		

4. Discussion

The medium effect of methanol on the dissociation of the three acids studied is easily seen in figure 1, where $p(_sK)-p(_wK)$ is plotted as a function of the weight percentage of methanol. The values of $p(_sK)$ for the two anilinium ions decrease as the solvent is enriched with methanol and pass through a minimum at a solvent composition of about 70 mole percent methanol. This composition is close to that at which the conductance of hydrochloric acid in methanol-water solvents is also at a minimum [4].

It is apparent that the behavior of the dissociation constants of the two anilinium ions (charge type A^+B^0) as the composition of the solvent is changed is not consistent with the simple Born electrostatic

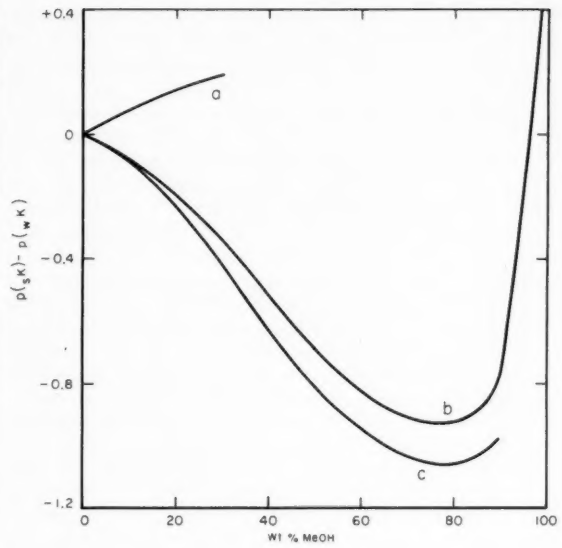

FIGURE 1. *Change of* pK *for three acids plotted as a function of the weight percent of methanol in the solvent.*

a, 4-chloro-2,6-dinitrophenol; b, *o*-chloroanilinium ion; c, *m*-nitroanilinium ion. The ordinate represents the difference between the pK in the methanolic solvent, $p(_sK)$, and that in pure water $p(_wK)$.

treatment of eq (7), which is based on the work of charging spherical ions in a dielectric continuum. This equation, together with reasonable values of the ionic radii, cannot explain either the decrease in pK or the minimum observed at about 70 mole percent methanol. On the contrary, the increase in $p(_sK)$ for 4-chloro-2,6-dinitrophenol (charge type A^0B^-) as the dielectric constant of the medium decreases is in qualitative agreement with the predictions of eq (7).

It is therefore of interest to compare the observed increase of $p(_sK)$ for 4-chloro-2,6-dinitrophenol (table 4) on addition of methanol to the solvent with the predictions of the Born electrostatic treatment, eq (7). On substitution of appropriate values of N, e, R, T, z_A, z_B, and ϵ_w, we obtain for 25 °C

$$p(_sK)-p(_wK)=121.6\left(\frac{1}{\epsilon_s}-0.0128\right)\left(\frac{1}{r_B}+\frac{1}{r_H}\right) \quad (10)$$

where r_i is in angstrom units. The spherical radii in solution are, of course, not known. That for hydrogen ion can be estimated to be 0.86 Å by interpolation in Pauling's table [16] of crystal radii for a univalent cation of mass 19. The radius of the phenolate ion is certainly greater than that of the hydrogen ion. From molecular models, a figure of 2.0 Å would seem to be reasonable.

When these values of r_{H^+} and r_{B^-} are substituted in eq (10), the predicted increase in pK on passing from the water solvent to a methanolic solvent of $N_2=0.3$ is 0.82 unit as compared with 0.25 unit observed. Even if the radius of the phenolate ion were taken as infinity, the predicted value of

$p({}_sK)-p({}_wK)$ would be reduced only to 0.58 unit. Values for the radii which are consistent with the observed result are equally unreasonable, for example $r_{H^+}=r_{B^-}=4.0$ Å and $r_{H^+}=2.4$ Å, $r_{B^-}=11$ Å. Furthermore, a decrease in pK for the two anilines (charge type A^+B^0) as the solvent is enriched with methanol (lowering the dielectric constant) can be accounted for on electrostatic grounds only if the radii of the anilinium ions are smaller than that of the hydrogen ion, as shown by eq (7).

In actuality, dissociation constants on the molal scale in solvents of different compositions are not strictly comparable unless an allowance is made for the variation in the total number of moles in 1000 g of solvent when the composition of the solvent changes. In other words, unit activity of solvent (in terms of which the values of pK are expressed) is 55.51 moles/1000 g in the pure aqueous medium and (55.51−24.30 N_2) moles/1000 g in mixed methanol-water solvents. For a comparison at the same number of solvent molecules as are present in 1000 g of pure water, therefore, one should reduce the values of $p({}_sK)$ in methanolic solvents by log (1−0.438 N_2), that is, by amounts varying from 0.02 unit at $N_2=0.1$ to 0.25 unit at $N_2=1$. This effect amounts to only 0.06 unit at $N_2=0.3$, and so cannot explain the wide disparity between the observed medium effect on the dissociation of 4-chloro-2,6-dinitrophenol and that predicted by the Born equation. Furthermore, this correction actually enhances the decrease found for the pK of the two anilinium ions.

It seems evident, therefore, that nonelectrostatic factors exert a considerable influence on the dissociation of acids of both charge types as the composition of the methanol-water solvent changes. The dissociation equilibrium $A+SH\rightleftharpoons B+SH_2^+$ (where SH represents the amphiprotic solvent) is shifted toward the right by an amount greater than can be accounted for by electrostatic considerations alone. This observation applies with equal force to acid-base pairs of the charge types A^0B^- and A^+B^0. It is tempting to conclude that the total basicity of the medium is increased by the addition of methanol. However, it is impossible to say whether this increase stems from a higher intrinsic basicity of methanol molecules than of water molecules or whether the addition of methanol provides a larger number of basic water molecules through a breakdown of the complex water structure [17], although the latter view seems the more reasonable.

It is clear that the effect of a decreased dielectric constant will tend to shift an equilibrium of the charge type A^0B^-,

$$HA+SH\rightleftharpoons SH_2^+ + A^-$$

toward the left, increasing the value of $p({}_sK_{HA})$. If, in addition, the solvent basicity decreases as methanol is added this increase in pK will be accentuated, whereas it will be lessened if the solvent basicity increases. When the acid-base equilibrium is of the charge type A^+B^0,

$$HA^+ + SH\rightleftharpoons SH_2^+ + A$$

the effect of a change in basicity will be the same as before (that is, a decrease of solvent basicity will tend to shift the equilibrium to the left, increasing pK) but the effect of a decreased dielectric constant will be much smaller and probably will tend also to increase pK, for the radius of the ion HA^+ will usually exceed that of SH_2^+.

Although the Born equation alone quite evidently is unable to account successfully for the change in the free energy of dissociation for acids of the two charge types on addition of methanol, there remains the possibility that this equation furnishes reasonably accurate values of the electrostatic term, ΔG^0_{el}. However, a nonelectrostatic term, ΔG^0_{non}, characteristic largely of the basicity[4] of the medium, would have to be added to it:

$$\Delta G^0_{diss}=\Delta G^0_{el}+\Delta G^0_{non}. \qquad (11)$$

In the same way, we may regard the observed change of pK, $(\Delta pK)_{obs}$, to be the sum of two terms $(\Delta pK)_{el}$ and $(\Delta pK)_{non}$. The validity of this view can be tested by determining whether the data for all three of the acids studied will furnish consistent values of $(\Delta pK)_{non}$ for the methanolic solvents when reasonable values for the radii of the ions are used.

The values of $(\Delta pK)_{obs}$, that is $p({}_sK)-p({}_wK)$, were corrected as described above for mass law effects resulting from the different numbers of solvent molecules present. The dielectric constants were taken from the paper of Albright and Gosting [13],[5] and r_{H^+} was taken to be 0.86 Å. When $(\Delta pK)_{el}$ was calculated by eq (7) with reasonable radii for the substituted anilinium and phenolate ions and subtracted from $(\Delta pK)_{obs}$, the values of $(\Delta pK)_{non}$ given in table 5 were obtained.

TABLE 5. *Values of the nonelectrostatic contribution to the medium effect* $p({}_sK)-p({}_wK)$ *in methanol-water solvents*

Mole fraction methanol N_2	$(\Delta pK)_{non}$ from measurements of—			
	o-Chloroanilinium ion [a]	*m*-Nitroanilinium ion [b]	4-Chloro-2,6-dinitrophenol [c]	Acetic acid [d]
0.1	−0.3	−0.3	−0.2	−0.2
.2	−0.6	−0.6	−0.4	−0.4
.3	−1.0	−1.0	−0.7	−0.7
.4	−1.3	−1.3	.....	−1.0
.5	−1.5	−1.5	.....	−1.3
.6	−1.8	−1.7	.....	−1.6
.7	−2.0	−1.9	.....	−1.9
.8	−2.0	−2.0	.....	−2.2
.9	−1.9	−1.9	.....	−2.2
1.0	−1.0	.....	.....	−1.5

[a] $r_{A^+}=2$Å. [b] $r_{A^+}=1.5$Å. [c] $r_{B^-}=1.5$Å. [d] $r_{Ac^-}=0.63$Å.

[4] The term *nonelectrostatic* is used for want of a satisfactory one-word designation for basicity effects and interactions involving the solvent in general. The electrostatic term connotes the ion-ion interaction of long-range coulombic forces as well as ion-charging effects; it is this interaction which is the subject of Bjerrum's description of dibasic acids [18] and its subsequent refinement by Kirkwood and Westheimer [19]. Interactions other than those of the ion-ion type, designated here as "basicity effect" or "nonelectrostatic term" may also be electrical in origin, as in the interaction of an ion with the dipole of a solvent molecule.

[5] See also reference 4.

The values found by Shedlovsky and Kay [4] for the dissociation constant of acetic acid in methanol-water solvents have been similarly treated and the results are given in the last column of table 5. The pK values of Shedlovsky and Kay were based on the volume concentration scale and were accordingly corrected to the molal scale for comparison with the data reported here. Although the agreement in the values of $(\Delta pK)_{non}$ derived from the four sets of data is satisfactory, it was necessary to choose a very small radius (0.63 Å) for the acetate ion in order to bring the results into essential harmony.

Tabagua [20] has shown that addition of methanol to aqueous solutions of trichloroacetic acid, benzoic acid, salicylic acid, or diethylbarbituric acid produces an increment in pK comparable with that found for acetic acid. The broad distinction between the effect of methanol on the dissociation of an acid of the A^0B^- type and on an acid of the A^+B^0 type is further supported by the work of Everett and Wynne-Jones [21], who determined the dissociation constants of ammonia and methylamine in 60 wt percent methanol over a range of temperatures.

Nevertheless, the values of $(\Delta pK)_{non}$ for acids of different charge types agree approximately in spite of the restrictions of the Born treatment and the arbitrary choice of ionic radii. The validity of separating medium effects on pK values into two parts: (a) an electrostatic part characteristic of the ion sizes, the dielectric constant of the medium, and the charge type of the acid-base equilibrium, and (b) a nonelectrostatic part characteristic of the chemical properties of the solvent, thus seems to be supported by these results. In our opinion, this approach may provide a means of assigning acid-base reaction parameters to solvent mixtures and warrants further study. The fact that $(\Delta pK)_{non}$ has a negative sign would suggest that the effective basicity of most methanol-water mixtures is greater than that of water itself.

Although the minimum in $p(_sK)$ for the two cation acids at a mole fraction of methanol of about 0.7 is probably attributable to the change in the total basicity of solvent molecules, it seemed desirable to ascertain whether the formation of ion pairs in the solvents of lowest dielectric constant might explain this phenomenon. The estimate was made at 87.8 and 100 wt percent methanol using values of 0.23 and 0.059, respectively, for the dissociation constant of hydrochloric acid in these solvents [4]. The effect of ion pairing is to make m_H in eq (8) less than the stoichiometric molality of hydrocholric acid. In the extreme case, the reduction was found to be sufficient to change $p(_sK)$ by only 0.03 unit in the two solvents of highest methanol content. The general conclusions are thus unaffected by ignoring the ion-pair equilibrium.

It is well known that solutions of the strong acids appear stronger in methanol and ethanol than in pure water itself,[6] and the same seems to be true for methanol-water solvents and ethanol-water solvents as well [24, 25]. An increase in acidity or "proton activity" might signify a *decrease* in solvent basicity, for the binding between solvent molecules and protons seems to be weakened. As Hammett has shown [26], this is not necessarily the case. The basicity of the solvent can be expressed in terms of K_{SH}, the acidity constant of the solvent. If leveling of monobasic strong acids (molality m) is complete in the solvent SH,

$$a_H = mK_{SH}\frac{\gamma_{SH_2^+}}{\gamma_{SH}}. \tag{12}$$

As the solvent basicity increases, K_{SH} decreases, but a lowering of the dielectric constant increases the activity coefficient term sharply. From the data of Gutbezahl and Grunwald [24], log (γ_{BH^+}/γ_B) for B=ammonia or aniline is estimated to be about 0.8 in 30 mole percent ethanol. Thus it is quite possible that the increase in the activity coefficient ratio may outweigh the decrease in K_{SH}. The increase in the acidity of the solution is thus not necessarily inconsistent with the indicator results which seem to suggest that addition of methanol to water initially increases the total basicity of the medium. After a mole fraction of about 0.8 methanol is reached, the basicity of the solvent mixture begins to decrease and may fall to a value less than that of water itself.

5. References

[1] I. M. Kolthoff and S. Bruckenstein, in Treatise on Analytical Chemistry, I. M. Kolthoff and P. J. Elving (ed), Pt. I, Vol. 1, ch. 13 (The Interscience Encyclopedia, Inc., New York, N.Y., 1959).
[2] M. Born, Z. Physik. **1,** 45, 221 (1920).
[3] I. M. Kolthoff, J. J. Lingane, and W. D. Larson, J. Am. Chem. Soc. **60,** 2512 (1938).
[4] T. Shedlovsky and R. L. Kay, J. Phys. Chem. **60,** 151 (1956).
[5] A. L. Bacarella, E. Grunwald, H. P. Marshall, and E. L. Purlee, J. Org. Chem. **20,** 747 (1955).
[6] C. L. de Ligny, Rec. Trav. Chim. **79,** 731 (1960).
[7] C. L. de Ligny, H. Loriaux, and A. Ruiter, Rec. Trav. Chim. **80,** 725 (1961).
[8] H. Strehlow, Z. Phys. Chem. (Frankfurt) **24,** 240 (1960).
[9] C. E. Newall and A. M. Eastham, Can. J. Chem. **39,** 1752 (1961).
[10] D. Feakins and P. Watson, Chem. Ind. (London), 2008 (1962).
[11] C. F. Wells, Nature **196,** 770 (1962).
[12] D. Rosenthal, H. B. Hetzer, and R. G. Bates, J. Am. Chem. Soc. **86,** 549 (1964).
[13] P. S. Albright and L. J. Gosting, J. Am. Chem. Soc. **68,** 1061 (1946).
[14] A. I. Biggs and R. A. Robinson, J. Chem. Soc. (London), 388 (1961).
[15] R. G. Bates and G. Schwarzenbach, Helv. Chim. Acta **37,** 1069 (1954).
[16] L. Pauling, The nature of the chemical bond, 3d ed., p. 514 (Cornell Univ. Press, Ithaca, N.Y., 1960).
[17] E. A. Braude and E. S. Stern, Nature **161,** 169 (1948); J. Chem. Soc. (London), 1976 (1948).
[18] N. Bjerrum, Z. Physik. Chem. **106,** 219 (1923).
[19] J. G. Kirkwood and R. H. Westheimer, J. Chem. Phys **6,** 506, 513 (1938).
[20] I. D. Tabagua, Zh. Fiz. Khim. **37,** 1545 (1963).

[6] See, for example, references 22 and 23.

[21] D. H. Everett and W. F. K. Wynne-Jones, Trans. Faraday Soc. **48,** 531 (1952).
[22] R. T. Hardman and A. Lapworth, J. Chem. Soc. **99,** 2242 (1911).
[23] R. G. Bates and G. Schwarzenbach, Helv. Chim. Acta **38,** 699 (1955).
[24] B. Gutbezahl and E. Grunwald, J. Am. Chem. Soc. **75,** 559, 565 (1953).
[25] N. A. Izmailov, Dokl. Akad. Nauk SSSR **127,** 104 (1959).
[26] L. P. Hammett, J. Am. Chem. Soc. **50,** 2666 (1928).

(Paper 68A3–277)

JOURNAL OF RESEARCH of the National Bureau of Standards—A. Physics and Chemistry
Vol. 68A, No. 3, May–June 1964

Crystallization of Anhydrous Copper Sulfate From Sulfuric Acid—Ammonium Sulfate Mixtures

Paul M. Gruzensky*

(November 26, 1962)

The growth of $CuSO_4$ crystals from a nonaqueous solvent, composed of $(NH_4)_2SO_4$ and H_2SO_4 is described. Solubility of $CuSO_4$ in solvents of varying $(NH_4)_2SO_4$ to H_2SO_4 ratio, at 200 °C, has been determined, as well as the temperature dependence of the solubility in $0.35(NH_4)_2SO_4-0.65H_2SO_4$. Single crystal specimens, weighing up to 150 mg have been obtained.

1. Introduction

Anhydrous $CuSO_4$, isostructural with orthorhombic $ZnSO_4$, is of particular interest because of its antiferromagnetic properties at low temperatures. Fundamental investigations on this compound would be greatly enhanced if single crystal specimens were readily available. Kokkoros and Rentzeperis [1][1] obtained $CuSO_4$ single crystals up to 1 mm in length by evaporation of an aqueous solution obtained by dissolving $CuSO_4 \cdot 5H_2O$ in water and adding H_2SO_4. Conditions under which the anhydrous salt may be obtained from an aqueous solution have been described in the early literature [2]. Kreines [3], in an effort to prepare crystal specimens of this salt for magnetic susceptibility and anisotropy studies, dissolved $CuSO_4$ in molten $(NH_4)_2SO_4$; then, by controlling the rate of decomposition of the solvent, he was able to obtain single crystals of $CuSO_4$ weighing up to 2 mg. Like many other sulfates, $CuSO_4$ undergoes decomposition before the melting point is reached so that growth from the melt under normal laboratory conditions is precluded. The use of a nonaqueous solvent appears to be the most promising approach, and experiments in our laboratory indicate that a sulfuric acid-ammonium sulfate mixture offers some definite advantages over the single components as a solvent for $CuSO_4$ single crystal growth.

2. Experimental Results and Discussion

Starting reagents used throughout this work were Baker "Analyzed Reagent" grade. The $CuSO_4 \cdot 5H_2O$ was further purified by recrystallization from distilled and demineralized water, then dehydrated by heating in a muffle furnace at 350 °C for 24 hr under a dry nitrogen atmosphere. The anhydrous powdered salt was stored in a dessicator over phosphorous pentoxide.

The sulfuric acid was adjusted to 100 percent composition by adding fuming sulfuric acid to the commercial 96 percent reagent, the freezing point method [4] being used to determine when the 100 percent composition point was reached.

Solvents of various compositions were then prepared by heating a measured quantity of H_2SO_4 to 150 °C and adding a weighed amount of $(NH_4)_2SO_4$ to give the desired composition.

The solubility of $CuSO_4$ in solvents of varying $(NH_4)_2SO_4$–H_2SO_4 ratios, at 200 °C, is indicated in figure 1. The experimental points were determined by adding powdered $CuSO_4$ to the solvent, maintaining the temperature at 200 °C ±2 °C for 24 hr to assure equilibrium, sampling the solution, and determining the copper content and sulfate content iodometrically and gravimetrically, respectively. The sulfate analysis was corrected for the amount of sulfate present as $CuSO_4$ so that the ordinates of figures 1 and 2 show the ratio of copper to solvent sulfate in the solution.

As figure 1 indicates, the solubility of $CuSO_4$ in pure H_2SO_4 is relatively low, but increases rapidly as the $(NH_4)_2SO_4$ content of the solvent increases. However, increasing the $(NH_4)_2SO_4$ ratio also increases the viscosity of the solvent at any given temperature, so that higher temperatures are necessary to maintain the solvent in a fluid state. Practical working temperatures are limited by the fact that $(NH_4)_2SO_4$ undergoes considerable decomposition above 300 °C. Since crystal growth is dependent on diffusion through the solution and since higher viscosities affect diffusion adversely, solvents of higher mole ratio than 0.35 $(NH_4)_2SO_4$ were not considered.

The temperature dependence of $CuSO_4$ solubility in $0.35(NH_4)_2SO_4$–$0.65H_2SO_4$ is shown in figure 2. In determining the experimental points, the temperature of the solution was controlled at the given value ±2 °C and maintained for 24 hr with occasional stirrings before sampling. A study of the copper content of the solution as a function of time, at the lowest temperature shown in figure 2, indicated that 24 hr was an adequate period to achieve equilibrium. Analyses for copper and sulfate were made as indicated above.

*National Bureau of Standards, Boulder, Colo.
[1] Figures in brackets indicate the literature references at the end of this paper.

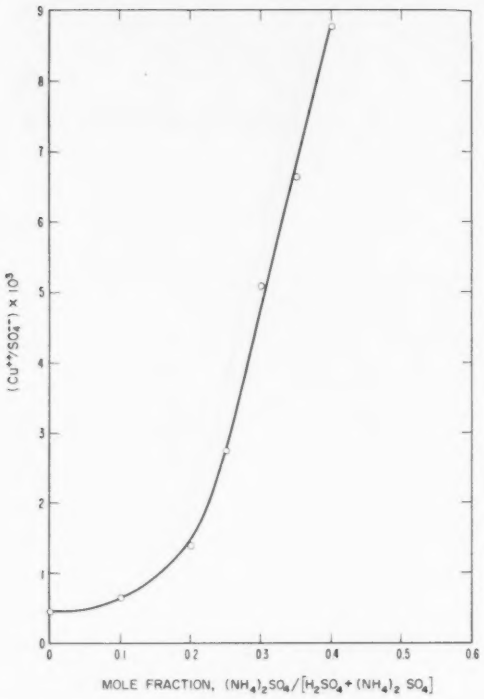

FIGURE 1. *Solubility of* $CuSO_4$ *in* $(NH_4)_2SO_4$–H_2SO_4 *of varying composition at 200 °C.*

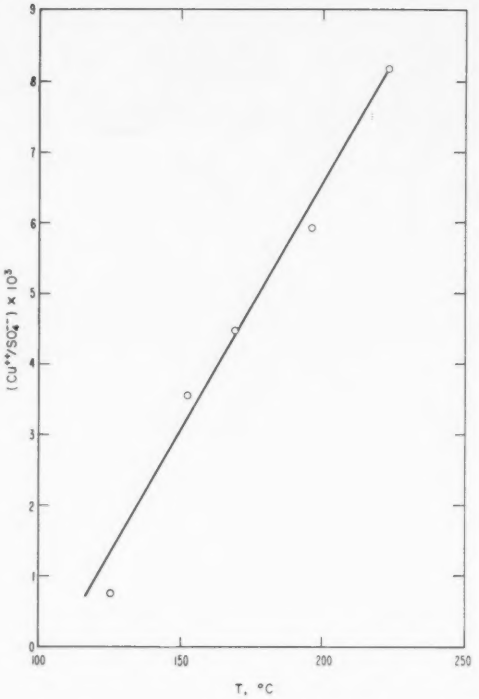

FIGURE 2. *Temperature dependence of* $CuSO_4$ *solubility in* $0.35(NH_4)_2SO_4$–$0.65H_2SO_4$.

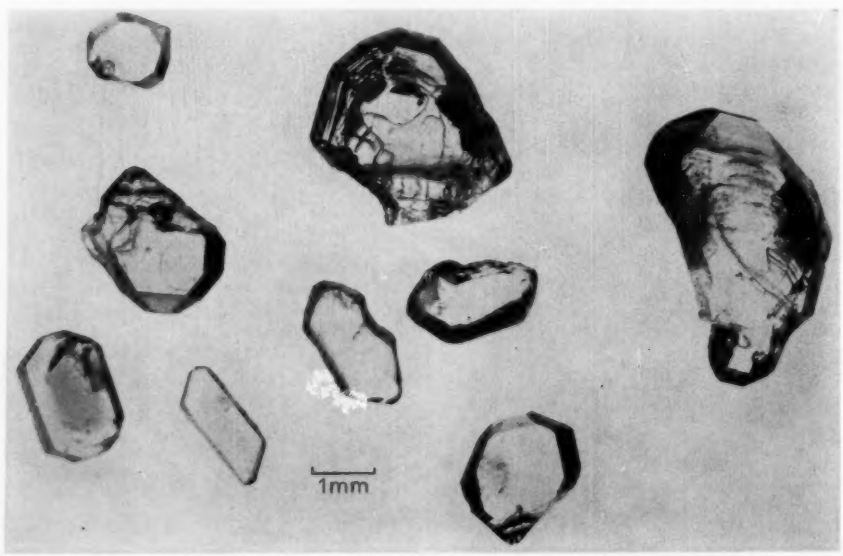

FIGURE 3. $CuSO_4$ *single crystals.*

To carry out the crystal growth, approximately 500 ml of solution were placed in a large borosilicate glass test tube, heated by a conventional hot plate. An excess of $CuSO_4$ powder was added to the solution, and a tantalum sheet, rotating at 10 rpm, was suspended in the solution near the surface. The test tube was loosely covered. The solution temperature was approximately 200 °C with a temperature gradient between the bottom of the container and the tantalum sheet of approximately 5 °C. Single crystals of $CuSO_4$ grew predominantly at the edges of the tantalum sheet, but occasionally also on the flat surfaces. In three or four days, crystals weighing up to 150 mg have been obtained. Excess solvent was removed from the crystal surfaces by washing in 100 percent H_2SO_4 and heating to 400 °C.

Figure 3 is a photograph of several $CuSO_4$ crystals. The specimens, which were transparent with a slight greenish tinge, were verified to be single crystals by Laue backscatter x-ray diffraction. Chemical analysis of the crystals indicated a composition of 99.7 percent $CuSO_4$.

3. References

[1] P. A. Kokkoros and P. J. Rentzeperis, Acta Cryst. **11,** 361 (1958).

[2] J. W. Mellor, A Comprehensive Treatise on Inorganic and Theoretical Chemistry, **3,** 234–251 (Longmans, Green & Co., London, 1923).

[3] N. M. Kreines, Soviet Phys. JETP **35,** 972 (1959).

[4] L. P. Hammett and A. J. Deyrup, J. Am. Chem. Soc. **55,** 1900 (1933).

(Paper 68A3–278)

JOURNAL OF RESEARCH of the National Bureau of Standards—A. Physics and Chemistry
Vol. 68A, No. 3, May–June 1964

Detection of Lattice Deformation and Recovery in Epsilon Phase Silver-Tin Alloys

R. M. Waterstrat and G. E. Hicho

(February 3, 1964)

A line-broadening effect has been observed in x-ray diffraction patterns from powdered epsilon phase silver-tin base alloys which have been subjected to cold work. The line breadth is reduced when the alloy ingots have received a prior homogenization treatment at 400° C and is also reduced when cold-worked alloy particles are annealed at 100° C. It is shown that the reduction in line breadth which occurs at 100° C is the result of a recovery process which significantly reduces the amount of internal deformation present in the alloy particles. The presence of internal deformation in these cold-worked alloy particles has also been associated with a dimensional expansion which occurs when the silver-tin particles are reacted with mercury at room temperature. Spherical alloy powders produced by an atomization process were found to be relatively free of internal deformation but were not chemically homogeneous. Metallographic and x-ray diffraction data indicated, however, that the spherical alloy particles can be homogenized by a high temperature heat treatment.

1. Introduction

X-ray diffraction measurements of line broadening may be used to detect lattice strains and other defects in cold-worked metals. As yet no such measurements have been reported for epsilon phase silver-tin alloys. The purpose of the present investigation was to observe the effects of cold working and also to follow the recovery process which may occur during the annealing of these alloys. The occurrence of such a recovery process at room temperature has been suggested by reports of "aging" phenomena in commercial silver-tin alloys used in dentistry which have been stored for long periods of time [1, 2].[1] Since recovery may occur even at room temperature it is important that the line-broadening measurements be made on alloys which have not been stored for any appreciable time subsequent to their deformation by cold working. This was made possible through the cooperation of W. D. Kimmel of the L. D. Caulk Co. and W. S. Crowell of the S. S. White Manufacturing Co. who provided the silver-tin alloy particles which had been recently cold worked by machining the alloy ingots. Silver-tin alloy powders have also been prepared using an "atomization" process in which no cold working is involved [3]. These alloy particles are nearly spherical in shape and may be separated into portions consisting of various ranges of particle diameters. It is of interest to determine whether these spherical particles are relatively free of internal microstresses as one might expect from the nature of the "atomization" process. The spherical silver-tin alloy particles were, therefore, examined both by x-ray diffraction and by metallographic methods.

When silver-tin particles are reacted with limited amounts of mercury, a hardening of the mixture occurs which is accompanied by dimensional changes [1, 2]. It has been observed that amalgams prepared from freshly cut alloy particles harden faster and show a greater expansion during hardening than amalgams prepared from particles which have received an "aging" heat treatment in order to stabilize their behavior at room temperature over long periods of time [1, 2]. These observations suggest that the deformation introduced during the preparation of the alloy particles affects the subsequent behavior of these alloys during their reaction with mercury.

The observed correlation between the use of freshly cut alloy particles and the occurrence of a dimensional expansion when these alloys are reacted with mercury might be interpreted as being associated with a recovery process in which internal strains are relieved as mercury diffuses into the silver-tin alloy particles and thereby lowers the activation energy required to initiate such a recovery process. Since the recovery of these strains may also be thermally activated it is possible that a specimen containing no mercury would also exhibit a nonrecoverable change in dimensions during heating. This effect would be superimposed on the normal thermal expansion. Such an effect has been observed and must, therefore, be associated with the behavior of the silver-tin alloy alone rather than with the products of a reaction with mercury.

2. Experimental Procedures

The compositions of the alloys used in this investigation are given in table 1. The alloys were obtained in the form of fine shavings which passed a 180-mesh

[1] Figures in brackets indicate the literature references at the end of this paper.

TABLE 1. *Approximate chemical compositions of alloys*

Alloy	Composition—% by weight			
	Silver	Tin	Copper	Zinc
Spherical alloy*	70.6	26.1	2.5	0.4
50	Not determined			
51	68.5	26.0	4.8	.7
52	72.9	26.1	1.0	.0
53	72.2	25.8	1.0	1.0
54	69.6	26.4	3.8	0.2
55	69.7	26.5	3.8	.0
59	72.2	25.8	1.0	1.0
60	69.6	26.4	3.8	0.2
61	69.7	26.5	3.8	.0
112–9	70.9	25.7	2.4	1.0

*Composition was obtained by chemical analysis [3].

screen. These shavings were produced from cast ingots by machining them in a lathe.

It was considered desirable also to examine an ingot in the "as-cast" condition; one of the alloys was therefore cast in the shape of a rectangular plate 1 in. wide by 2 in. long by ⅛ in. thick. This casting was produced in an investment-type mold under conditions similar to those used in casting the other ingots. The rectangular shape was necessary due to the limitations imposed on sample geometry by the sample holder in the diffractometer and because a flat surface which has not been subjected to a machining operation is needed.

The spherical alloy powders were prepared by the Federal Mogul Division[2] and the details of their analysis and preparation have been reported previously [3]. The spherical silver-tin alloy had been stored at room temperature for over one year, however, and it was suspected that a considerable amount of recovery might have occurred during this prolonged period of time. It is desirable to know whether the "atomization" process can be used in preparing metal particles which are relatively strain free. This information was obtained by examining a sample consisting of spherical palladium particles which had been prepared by the same "atomization" process and which had been stored for only four months at room temperature. The x-ray pattern obtained from the spherical palladium particles is given in figure 1 together with x-ray patterns obtained from spherical silver-tin alloy particles in both the "as received" condition and after an annealing treatment consisting of heating for 8 hr at 100 °C in a vacuum.

Silver-tin alloy particles which had received different annealing treatments or varying amounts of deformation at room temperature were mixed with mercury to form amalgam alloys which hardened in several hours at a temperature of 37 °C. Dimensional changes which occurred during the hardening reaction were measured with an optical interferometer and some typical results are presented in figure 2. X-ray diffraction patterns were obtained from the same samples of silver-tin alloy particles which were used in preparing these amalgams and the equivalent patterns are shown in figure 3. Each

[2] Federal Mogul Division, Federal-Mogul-Bower Bearings, Inc., Ann Arbor, Mich.

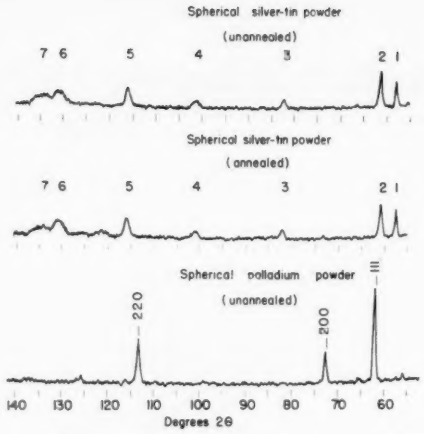

FIGURE 1. *X-ray diffraction patterns for annealed and unannealed spherical silver-tin alloy powders and for a spherical palladium powder.*

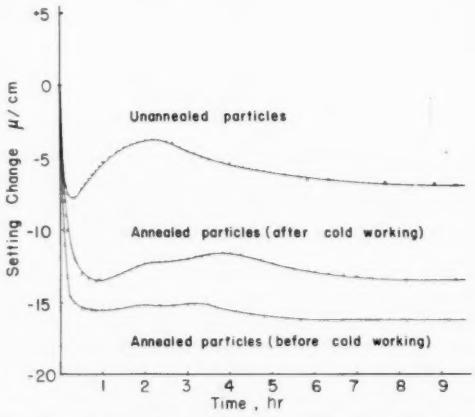

FIGURE 2. *Dimensional changes during hardening for amalgams prepared from a commercial silver-tin alloy (Alloy 112–9).*

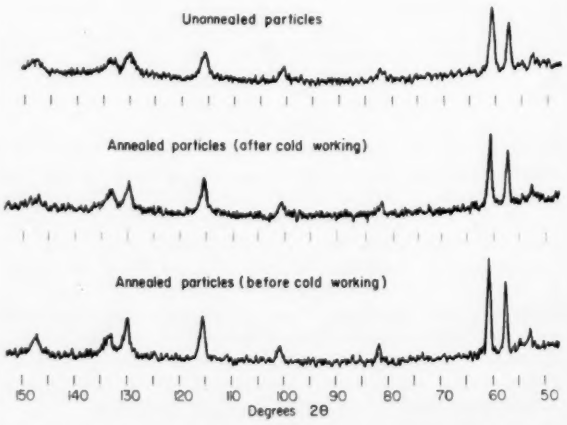
Unannealed particles
Annealed particles (after cold working)
Annealed particles (before cold working)
150 140 130 120 110 100 90 80 70 60 50
Degrees 2θ

FIGURE 3. *X-ray diffraction patterns of annealed and of cold-worked commercial silver-tin alloy (Alloy 112–9).*

amalgam specimen contained 0.6 g of silver-tin alloy particles and was mixed with 0.9 g of mercury in a commercial amalgamator which shakes the mixture vigorously for about 60 sec in order to wet the particles and initiate the hardening reaction. The mixture was then packed into cylindrical steel molds using a steel instrument to pack the mixture firmly. Some excess mercury was removed during this operation. After the amalgam specimens had been packed in the steel mold, they were of a standard size and shape suitable for the measurements of dimensional changes. They were then promptly removed from the steel mold and immediately placed in the interferometer in order that the dimensional changes might be observed as the hardening reaction progressed.

The x-ray diffraction patterns were obtained using a General Electric XRD–5 diffractometer. The specimens were prepared by sprinkling the alloy powder uniformly over the surface of a glass slide and then spraying the surface of the powder with a thin coat of Krylon acrylic resin to hold it in place. This procedure avoids the introduction of any deformation during the process of specimen preparation. All data were obtained using filtered chromium radiation and the line widths were measured directly from the recorder chart. Each peak was measured at a position corresponding to one half its total peak height. Instrumental broadening of lines was not considered since all patterns were obtained under identical conditions and since only the differences in line broadening rather than the absolute breadth of the lines were used in establishing conclusions.

In order to identify the epsilon phase, it is necessary to make measurements at high angles which are inaccessible to the diffractometer. These measurements were obtained using a Phillips 114.59 mm diam powder camera with filtered chromium radiation.

The metallographic specimens were polished using standard techniques except that diamond polishing followed by magnesium oxide polishing was used in the final stages. Two different etching methods were used. The first method is essentially the one used by Crowell [4]. This etch delineates the grain boundaries and reveals twinning but shows little color contrast between the epsilon phase and retained zeta phase. Therefore, in alloys containing retained zeta phase a duplex etch was used which has been described by Wing [5] and was developed primarily for use with dental amalgams. With this etch the zeta phase particles were seen to have a darker color while the epsilon phase remained unattacked.

TABLE 2. *Results of measurements of line widths in annealed and in unannealed silver-tin alloys*

Sample identification	High-temperature anneal	Low-temperature anneal	Observed relative half widths								
			2θ	57°	61°	82°	101°	115°	130°	133°	148°
			hkl	002	111 021	112 022	200 130	113 023	202 132	221 041	004
50A	None	None		6.0	7.0	9.0	17.0	11.5	14.0	18.0	
50B	None	100 °C—1 hr		3.5	4.0	6.0	10.0	6.0	10.0	14.0	
51A	None	None		5.0	6.0	9.0	12.0	14.0	17.0	18.0	
51B	None	100 °C—1 hr		4.5	5.5	7.0	9.5	7.5	10.0	15.0	
51C	None	100 °C—3 hr		4.0	5.0	6.0	9.0	6.0	13.0	12.0	
52A	432 °C—72 hr	None		4.0	4.0	4.0	12.0	10.0	14.5	16.0	
52B	432 °C—72 hr	100 °C—1 hr		3.5	4.5	5.0	5.0	7.0	9.0	12.0	
52C	432 °C—72 hr	100 °C—3 hr		3.0	4.0	5.0	7.0	6.0	10.0	14.0	
53A	432 °C—72 hr	None		5.0	4.0	7.0	7.5	13.0	19.0	19.0	
53B	432 °C—72 hr	100 °C—1 hr		4.0	4.0	5.0	7.0	7.0	11.0	15.0	
53C	432 °C—72 hr	100 °C—3 hr		4.0	4.0	5.0	8.0	5.0	12.0	13.0	
54A	None	None		4.0	5.0	6.0	13.0	10.0	17.0	21.0	
54B	None	100 °C—1 hr		3.5	4.5	6.0	10.0	7.0	8.0	17.5	
54C	None	100 °C—3 hr		4.0	4.0	5.0	7.0	9.0	9.0	15.0	
55A	None	None		5.0	6.0	5.0	8.0	10.0	15.0	21.0	
55B	None	100 °C—1 hr		3.0	4.0	5.0	7.0	5.0	9.5	12.0	
55C	None	100 °C—3 hr		3.0	4.0	5.0	8.0	6.0	8.0	13.0	
59A	None	None		5.0	5.0	10.0	10.0	13.0	15.0	22.0	
59B	None	100 °C—1 hr		3.0	3.5	4.0	9.0	5.0	7.5	14.0	
60A	432 °C—72 hr	None		6.0	6.0	11.0	11.5	10.0	15.0	25.0	
60B	432 °C—72 hr	100 °C—1 hr		3.5	4.5	3.0	8.0	6.0	11.0	17.0	
61A	432 °C—72 hr	None		5.0	5.5	9.0	18.0	11.5	13.0	31.0	
61B	432 °C—72 hr	100 °C—1 hr		4.0	5.0	10.0	10.0	6.0	12.0	11.0	
112–9A	None	100 °C—3 hr		4.0	4.5	11.0	12.0	10.0	15.0	21.0	16.0
112–9B	400 °C—16 hr	None (cold worked)		4.0	5.5	11.0	11.5	13.0	16.0	20.0	20.0
112–9C	400 °C—16 hr	100 °C—3 hr		3.0	4.0	5.0	8.5	7.0	9.0	13.5	11.0
112–9D	400 °C—16 hr	100 °C—3 hr and then cold worked		4.0	4.5	8.0	13.0	8.0	9.5	14.0	20.0
Average for unannealed particles				5.0	5.8	8.8	12.6	11.6	15.3	22.0	20.0
Average for all particles annealed at 100 °C				3.6	4.3	5.8	8.4	6.6	10.3	14.3	13.5
Flat casting 1A	None	None		6.5	8.5	11.0	15.0	17.0	22.0	24.0	
Flat casting 1B	None	100 °C—24 hr		5.0	7.0	8.5	8.5	10.5	23.0	17.0	
Flat casting 1C	400 °C—24 hr	None		2.5	5.5	5.0	4.0	6.0	12.0	8.0	

3. Experimental Results

A comparison of the results of line-width measurements for annealed and unannealed epsilon phase alloys is given in table 2. The annealing treatments produced a marked reduction in the line widths as shown in figures 3 and 4. The angular dependence of the line broadening is irregular but the higher angle lines are broadened to a greater extent than low angle lines as is usually the case in x-ray patterns obtained from cold-worked metals.

In the commercial silver-tin alloys annealed at 100 °C, the use of high-temperature annealing treatments at about 400 °C prior to cold working may sometimes result in x-ray patterns having slightly narrower lines than would be obtained in similar samples which had not received a prior high-temperature anneal. This result suggests the presence of composition gradients and chemical inhomogeneity which is removed by interatomic diffusion at 400 °C but is not appreciably affected at 100 °C over short periods of time.

The x-ray pattern obtained from the flat rectangular ingot of silver-tin alloy in the "as-cast" condition contains broad lines which become narrower after annealing at 100 °C. Annealing this ingot at 400 °C produces a much greater reduction in line width. This indicates the presence of chemical inhomogeneity in the cast ingot and probably also some internal strains resulting from nonuniform stress distribution imposed by thermal contractions during cooling.

X-ray patterns obtained from spherical alloy particles are unaffected by low temperature annealing treatments (fig. 1). The breadth of the lines may be reduced, however, by high-temperature annealing at 400 °C. Apparently considerable chemical inhomogeneity is retained in these particles but they do not contain the large amount of internal strains which are present in particles which have been cold-worked during their preparation. The spherical palladium particles are also quite free of internal strains as indicated by the sharp peaks in the x-ray pattern shown in figure 1. It is unlikely that appreciable recovery could occur in pure palladium at room temperature in four months and therefore the particles must have been quite free of internal strains even immediately following their initial preparation by the "atomization" process. Since compositional segregation cannot occur in a pure metal, the x-ray patterns for pure palladium spherical particles are sharp, whereas x-ray patterns from spherical silver-tin particles contain broader lines as a result of this type of segregation.

Metallographic observations support such an interpretation of line broadening effects in silver-tin spherical particles. Figure 5 shows the microstructure of the spherical silver-tin particles after annealing at only 100 °C. The matrix is epsilon phase with very small globules of a second phase distributed uniformly throughout the matrix. The second phase is removed by annealing at 400 °C as shown in figure 6 and the microstructure is then essentially single phase. The individual grains are now quite large relative to the dimensions of each particle and they contain numerous twins. An x-ray diffraction pattern was obtained for this specimen in the Phillips camera and this pattern was completely indexed on the basis of an orthorhombic unit cell similar to the one proposed by Nial, Almin, and Westgren [7] for the epsilon phase, Ag_3Sn. The unit cell dimensions obtained for the spherical alloy were $a_0=2.983$ Å, $b_0=5.132$ Å, and $c_0=4.760$ Å.

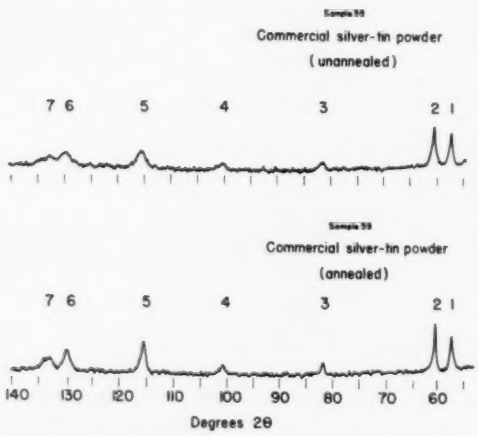

FIGURE 4. *X-ray diffraction patterns for annealed and unannealed commercial silver-tin alloy powders.*

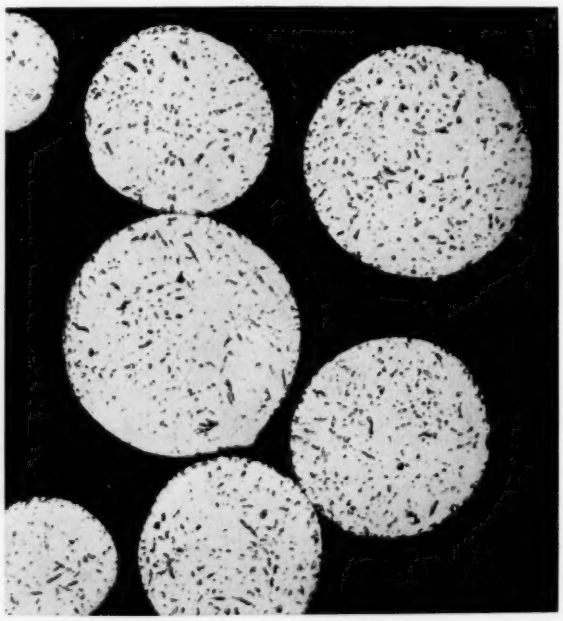

FIGURE 5. *Microstructure of spherical silver-tin alloy particles annealed for 1 hr at 100 °C.*

Epsilon phase matrix containing a dispersion of small globules of zeta phase 500 ×.

A correlation is established between dimensional expansion in silver-tin amalgams during the hardening reaction and the presence of cold work in the silver-tin alloy particles by consideration of figures 2 and 3. This correlation is in accord with previous observations [1, 2] and is particularly significant in the present study since particles which had been annealed in order to obtain strain-free and homogeneous structures have now been cold worked by grinding in a mortar and pestle and subsequently checked for x-ray line broadening as well as for dimensional expansion during hardening of their amalgams.

An increased dimensional expansion and a broadening of x-ray lines are produced by cold working the previously strain-free and homogeneous particles as can be seen in figures 2 and 3. The question now arises whether the expansion is due to products of the reaction with mercury or whether much of this expansion results from the presence of internal strains in the silver-tin alloy particles. An experiment was performed in order to help resolve this question. If the presence of deformation in the silver-tin alloy particles is responsible for a significant amount of the expansion obtained during amalgamation, then presumably the internal strains associated with this deformation are recoverable by the diffusion of mercury into the silver-tin alloy particles. These internal strains might, therefore, also be recoverable in silver-tin alloys which contain no mercury by heating them to a temperature at which recovery may occur by a thermally activated process. Accordingly a commercial silver-tin alloy powder was compressed in a cylindrical steel mold at room temperature under a pressure of approximately 140,000 psi. This pressure was sufficient to produce severe plastic deformation. The small specimen was then heated uniformly in a specially designed high-temperature interferometer in which dimensional changes are automatically recorded during both heating and cooling of the sample [6]. An expansion was observed during heating which was independent of the normal thermal expansion and superimposed upon it. The amount of expansion produced seemed to depend on both time and temperature. This expansion was permanent and could not be removed by cooling to room temperature; in other words the specimen had a permanent increase in length after returning to room temperature. Further expansion occurred in a subsequent reheating when the maximum temperature reached in the previous heating was exceeded. These results will be reported in detail in a subsequent publication [6]. The total expansion obtained in heating this specimen to 150 °C was about 10 μ/cm; a value which is certainly significant when compared to the expansions shown in figure 2 for the silver-tin amalgams.

4. Discussion

The broadening of x-ray diffraction lines may be caused by compositional inhomogeneity in an alloy as a result of segregation which occurs as the alloy cools from the liquid state. Examination of the binary silver-tin constitution diagram [8] in the composition range corresponding approximately to that of the alloys used in this study shows that a pronounced tendency toward segregation would be expected. The observed data confirm this expectation but also indicate that all of the observed line broadening cannot be due to this effect since significant reductions in line widths occur at a temperature of 100 °C which is too low to permit the long range interatomic diffusion necessary to remove chemical segregation. Figures 5 and 6 support such a conclusion since the anneal at 100 °C did not remove the second phase while a subsequent anneal at 400 °C was quite effective in dissolving it.

X-ray diffraction lines are broadened by the presence of small particles, and coherency strains could also have some effect on line broadening when more than one phase is present. In a homogeneous, single phase alloy, however, changes in the width of x-ray diffraction lines are due primarily to the introduction of internal defects which disturb or modify the perfect periodicity of the atomic arrangement [9]. These internal defects may be introduced either during the growth of the crystal or by subsequent mechanical working at a temperature which is too low to permit their removal by thermally activated processes. It has been shown in this study that line broadening is produced in homogeneous, strain-free epsilon phase alloy particles when they are subjected to the cold working effects of grinding in a mortar and pestle. Prior to receiving such treatment these particles produced x-ray patterns in which the lines were very

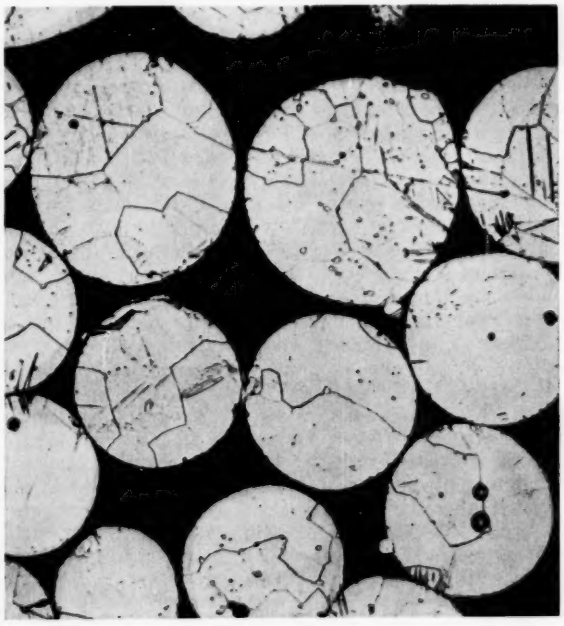

FIGURE 6. *Microstructure of spherical silver-tin alloy particles annealed for 24 hr at 400 °C.*

Large grains of epsilon phase containing twins. 500 ×.

narrow and sharp (fig. 3). This implies that any defects which may have been present in these alloys as a result of crystal growth processes are not responsible for the observed changes in line width and that the observed line broadening is the result of cold working.

The nature of the defects produced in cold-worked metals is a subject of considerable controversy. It has been suggested that the effects on line width are due to the presence of internal microstresses [9, 10]. The line broadening has also been attributed to the presence of small coherently diffracting [9, 10] domains produced by cold working. The angular dependence of line broadening would differ for each of these two mechanisms but complications which produce an irregular angular dependence in the present study also prevent any conclusion regarding the nature of the cold-worked metal.

These complications arise from the presence of a second phase in many of the alloys used. Lines from this second phase superimpose on the epsilon phase lines thus preventing measurements of the line broadening originating only in the epsilon phase. Even in the single phase alloys, however, a quantitative analysis of the line broadening depends to a great extent on a detailed knowledge of the atomic structure including such information as the nature and degree of ordering which is as yet unavailable for the epsilon phase alloys.

It has been shown in this study that the principal constitutent of these alloys has a crystal structure which is probably isomorphous with the structure of the binary silver-tin epsilon phase (Ag_3Sn) as reported by Nial, Almin, and Westgren [7]. Some of the silver atoms, however, are presumably replaced by copper atoms in such a way as to preserve the "ideal" stoichiometric formula $(Ag, Cu)_3$ Sn. When cooled from the liquid state these alloys contain varying amounts of a second phase which is probably the zeta phase. The zeta phase has a close-packed hexagonal crystal structure [7, 8]. The crystal structure of the epsilon phase is similar to that of the zeta phase except for a small distortion which might be associated with a different ordering of the silver and tin atoms. The orthorhombic distortion produces a slight "splitting" of the x-ray diffraction lines for the close-packed hexagonal structure and this "splitting" is detectable principally at higher angles. The presence of small quantities of zeta phase in an epsilon phase silver-tin alloy would, therefore, be difficult to detect in x-ray diffraction patterns of these alloys. Metallographic studies, however, have been successful in identifying the major constituent of these alloys as the epsilon phase.

The fine dispersion of zeta phase globules in the spherical silver-tin particles (fig. 5) is probably attributable to the rapid cooling rates involved in the "atomization" process which tend to suppress the peritectic reaction involved in the formation of the epsilon phase. Annealing these particles at a high temperature (400 °C) which lies below the temperature of the peritectic reaction produces an equilibrium structure (fig. 6) which is essentially that of a single-phase epsilon alloy. This is confirmed by the x-ray diffraction measurements as well as by the metallographic observations. In figures 2 and 3 an interesting correlation is established between the presence of cold work in silver-tin alloy particles and the observed dimensional changes as these particles react with mercury. This effect receives further clarification in the experiment which demonstrated that silver-tin alloys subjected to considerable plastic deformation in compression will subsequently exhibit a permanent nonrecoverable expansion when heated.

The evidence suggests that internal strains or other lattice defects produced by cold working these alloys may be relieved through a recovery process which occurs over long periods of time at room temperature and is accelerated at higher temperatures. This recovery process is probably thermally activated. When mercury is dissolved in the silver-tin alloys it apparently lowers the activation energy required for this recovery process perhaps by lowering the melting point and weakening the interatomic binding forces. When this occurs the thermal energy available at room temperature is sufficient to activate the recovery process.

5. Conclusions

The results of this study lead to the following conclusions:

1. X-ray diffraction techniques may be used to detect lattice deformation in epsilon phase silver-tin alloys which have been recently subjected to cold working. Alloys of this type are commonly used in preparing dental amalgams and such a technique would, therefore, be useful in evaluating their properties.

2. The internal deformation may be removed through a recovery process which occurs when the alloys are heated to higher temperatures. The recovery process may also occur at room temperature when considerable time is available or when mercury is allowed to dissolve in the alloy particles.

3. The "atomization" process used to prepare spherical alloy particles results in the production of particles which are relatively strain free in the size ranges tested. Compositional segregation is not prevented but occurs as a fine, uniform dispersion of a second phase. The alloy particles may subsequently be homogenized by a heat treatment at high temperatures.

4. The x-ray pattern of the epsilon phase in these silver-tin base alloys has been identified as that of an orthorhombic crystal structure similar to the one proposed by Nial, Almin, and Westgren for the phase Ag_3Sn.

5. It is likely that significant dimensional changes occur when silver-tin alloy particles react with mercury as a result of the release of internal strains in the cold-worked alloy particles.

6. References

[1] E. W. Skinner and R. W. Phillips, The Science of Dental Materials, 5th ed. p. 359 (W. B. Saunders Co., 1960).

[2] F. A. Peyton et al., Restorative Dental Materials, p. 347 (1960).
[3] N. C. Demaree and D. F. Taylor, Properties of dental amalgams made from spherical alloy particles, J. Dental Res. **41,** 890 (1962).
[4] Crowell, W. S., The metallography of dental amalgam alloys, J. Dental Res. **33,** 592 (1954).
[5] G. W. Wing, The metallography of dental amalgam Thesis—University of Sydney, Sydney, Australia (1961).
[6] G. Dickson, to be published (1964).
[7] O. Nial, A. Almin, and A. Westgren, Z. Physik. Chem. **B14,** 83 (1931).
[8] M. Hansen and K. Anderko, Constitution of Binary Alloys, 2d ed. p. 52 (McGraw-Hill Book Co., Inc. New York, N.Y., 1958).
[9] Barrett, C. S., Structure of Metals, 2d ed., pp. 414–439 (McGraw-Hill Book Co., New York, N.Y.).
[10] O. P. Agnihotri and G. B. Mitra, On the investigation of pure x-ray diffraction line breadths in deformed copper, Phil. Mag. **8,** 1161 (1963).

(Paper 68A3–279)

JOURNAL OF RESEARCH of the National Bureau of Standards—A. Physics and Chemistry
Vol. 68A, No. 3, May–June 1964

Vapor Pressures of Ruthenium and Osmium

N. J. Carrera,* R. F. Walker,** and E. R. Plante

(January 1, 1964)

The vapor pressures and heats of sublimation of ruthenium and osmium have been measured using a microbalance technique based on the Langmuir method. Heats of sublimation at 298 °K were calculated with the aid of free energy functions. Least squares lines for the vapor pressure data, heats of sublimation, and normal boiling points were obtained as follows:

(1) Ruthenium:

$$\text{Log } P_{\text{atm}} = 7.500 - \frac{32{,}769}{T} \quad (1940\text{–}2377\,°\text{K})$$

$$\Delta H^{\circ}_{s}(298) = 156.1 \pm 1.5 \text{ kcal/mole}$$

$$\text{bp} = 4150 \pm 100\,°\text{K}$$

(2) Osmium:

$$\text{Log } P_{\text{atm}} = 7.484 - \frac{39{,}880}{T} \quad (2157\text{–}2592\,°\text{K})$$

$$\Delta H^{\circ}_{s}(298) = 189.0 \pm 1.4 \text{ kcal/mole}$$

$$\text{bp} = 5300 \pm 100\,°\text{K}$$

The indicated uncertainties are estimates of the overall limits of error.

1. Introduction

This paper is the third in a series covering the vapor pressures of the platinum metals. Two previous papers [1, 2] [1] gave the vapor pressures and heats of sublimation of Pd, Pt, Ir, and Rh. Simultaneously with the current measurements on Ru and Os, similar measurements were carried out by Paule and Margrave [3] and by Panish and Reif [4]. In two instances (ref. 3 and sample 2 of the present paper) samples cut from the same stock were utilized in the course of the measurements on ruthenium.

Until this recent work no measurements of the vapor pressures of Ru and Os had been reported. Estimates of their heats of sublimation at 298 °K, ΔH°_{s} (298), were given by Brewer [5] and by Stull and Sinke [6]. The estimated and experimental values are listed in table 1.

The present results were obtained primarily by the Langmuir method, using variations of a microbalance technique previously described [1, 7, 8] and a sample heated directly by induction. In applying the Langmuir method it was assumed that the vaporization coefficients of Ru and Os are unity and that they vaporize predominantly to monatomic gaseous species over the temperature range of the measurements. Paule and Margrave [3] also used the Langmuir method, making similar assumptions, but their sample of Ru was suspended from a microbalance into a tube furnace of graphite lined with tantalum. Panish and Reif [4] made measurements by both the Langmuir and Knudsen methods which tended to confirm the assumptions and used a time-of-flight mass spectrometer in an unsuccessful search for polyatomic species. A direction-focusing mass spectrometer with a Knudsen cell was also used for measurements on Ru in the present work. Monatomic species alone were observed, and the data did not suggest that the vaporization coefficient was significantly different from unity. However, owing to the larger temperature uncertainties and the imprecision of converting observed ion currents to vapor pressures, the data are considered less accurate than the Langmuir measurements and are not reported in detail.

TABLE 1. *Heats of sublimation of ruthenium and osmium*

Substance	2d Law	ΔH°_{s} (298)	3d Law	Reference
		kcal/mole		
Ruthenium		160		Brewer [5].
		144		Stull, Sinke [6].
	155.5±5		151.5±4	Paule, Margrave [3].
	151±10		154.9±1.3	Panish, Reif [4].
	151.6±2.1		156.1±1.5	This work.
Osmium		174		Brewer [5].
		160		Stull, Sinke [6].
	192±10		187.4±0.9	Panish, Reif [4].
	184.1±3.0		189.0±1.4	This work.

*Present address: Dept. of Physics, University of Illinois, Urbana, Ill.
**Present address: Laboratory for the Physics and Chemistry of Solids, University of Cambridge, England.
[1] Figures in brackets indicate the literature references at the end of this paper

2. Experimental Technique

In principle, the equilibrium vapor pressure (P) of each metal at temperature T can be determined from its rate of sublimation in a vacuum, in accordance with the equation:

$$P=\frac{m}{\alpha}\sqrt{\frac{2\pi RT}{M}}.$$

In the present work the rate of sublimation (m, g cm^{-2} sec^{-1}) was measured by suspending a sample of known surface area from the microbalance. The vaporization coefficient (α) was taken to be unity, and the molecular weight of the vapor species (M) is that of the monomer. The value of the gas constant R used in the calculation of ΔH_s^0 is 1.98726 cal/deg mole. Actual vapor pressures would be somewhat lower than calculated if polymeric species were involved.

2.1. Apparatus

Two pieces of apparatus were used for the measurements. The first of these, which was used only for the first series of measurements on ruthenium, was the oil-pumped vacuum microbalance apparatus described previously [1, 5]. A significant change was, however, made in the method of temperature measurement, as discussed in section 2.4 below.

In general principle the second apparatus, which was used for the remaining four series of measurements on ruthenium and for the series on osmium, was similar to the first apparatus, with the exception that it was ion pumped. This second apparatus has also been described in some detail recently [8], and only the essential features will be repeated here.

The sample was suspended from an equi-arm, quartz beam microbalance by a chain of 0.025 cm diam sapphire rods. An 0.025 cm diam hole through one end of the sample allowed a short loop of fine wire (0.005 cm diam iridium for the Ru sample and 0.0125 cm diam tungsten for the Os sample) to pass through the sample and hang over the hook of the lowest sapphire suspension rod. The presence of the hole and the loop (which was not heated significantly by the induction field) was ignored when calculating the effective surface area of the sample.

The sample hung inside a glass tube, about 13 mm in diam; a water-cooled radiofrequency coil fitted closely around the tube and coupled directly with the sample. A fused quartz sleeve was fitted inside the glass tube to collect the sublimed metal.

The apparatus was pumped continuously throughout each run with an ion pump rated by the manufacturer at 90 liter/sec. Pressures were measured at the pump by the current drawn by the pump.

For the first three series of runs on ruthenium a 450 kc/s, 50 kw radio frequency generator was used to heat the samples. The long term stability of the output of the generator was not adequate for runs lasting several hours. Hence, a more stable 2 to 3 Mc/s, 2 kw generator was employed for the last two series on ruthenium and the series on osmium, during which more extended runs were made.

2.2. Samples

Two ruthenium samples having different impurity contents were used in the measurements. The first and purest sample, referred to as sample 1, was used for one series of measurements on each of the two microbalance systems mentioned above. It consisted of a short rod about 1.9 cm long by 0.32 cm diam. The sample was prepared by swaging and heating in vacuo to 1450 °C. At the conclusion of the series 1 experiments on sample 1, remeasurement of the sample dimensions showed that some volume expansion of the sample had occurred. This was presumably due to recrystallization of the sample. As a result, the porosity increased during the experiments from an initial value close to zero to a final value of about 10 percent while the area increased by about 13 percent. The average of the initial and final areas was used as the room temperature area of the sample.

The purity of sample 1 was determined by spectrochemical analysis before each series of runs. A summary of the results of the analysis is shown in table 2. The International Nickel Co., which donated the sample, furnished the analysis of the sample as used at the start of the first series of measurements. After this series the sample was analyzed again at NBS. It will be noted in table 2 that some purification of the sample occurred during the series, but the absence of Os in the second analysis is unexplained. Other small discrepancies in the impurity contents are probably attributable to the limited precision of the spectrochemical technique.

TABLE 2. *Spectrochemical analyses of samples*

Impurity element detected	Ruthenium			Osmium
	Sample 1		Sample 2	
	INCO %	NBS %	NBS %	NBS %
Ag		?	?	0.0001–0.001
Al		?	0.0001–0.001	.0001– .001
Au		0	0	.0001– .001
Ba		—	—	.001– .01
Be		0	0	<0.0001
Ca		?	.01– .1	.01 – .1
Co		0	0	.001 – .01
Cr		0	0	.001 – .01
Cu		0.0001–0.001	.0001– .001	.001 – .01
Fe	0.0025	.0001– .001	.001 – .01	.01 – .1
Mg		<0.0001	.0001– .001	.01 – .1
Mn			0	.001 – .01
Ni	.0002		0	.001 – .01
Os	.02	0	0	
Pb	.0005	?	<0.0001	.0001– .001
Pd	<.001	?	.0001–0.001	.0001– .001
Pt		?	.01 –0.1	.001 – .01
Rh	.007	?	?	
Ru				.001 – .01
Sb	<.001		0	
Si		0.0001–0.001	.0001–0.001	.01 – .1
Sn	.003	0	0	.0001– .001
Estimated purity maximum	99.97%	99.997–99.9997%	99.8–99.98%	99.5–99.95%

0=Not detected. ?=Detection uncertain.

The second ruthenium sample (referred to as sample 2) was initially used as a rectangular bar, cut from the same stock as was used by Paule and Margrave [3]. The stock appeared to have been prepared by cold pressing and sintering and retained some porosity. As used for the third and fourth series of measurements on Ru, the bar was about 1.14 cm long with about a 0.39 cm square cross section. For the fifth series of measurements the bar was remachined to a rod of the same length with a diameter of about 0.37 cm. Table 2 gives an analysis of the stock material as received.

The osmium sample was 0.23 cm diam and 1.47 cm long; it was machined from a larger, cold-pressed and sintered bar. As received, the material was not particularly pure, but was purified by heating to a high temperature (~2000 °C) in a vacuum for an extended period to vaporize off the more volatile impurities. The analysis shown in table 2 was made on the sample after purification and before the series of measurements of its rate of vaporization. It may be presumed that further puricfiation occurred during the series, but no effects attributable to this cause were detected.

Samples were hung in the coil with their principal axes vertical. The surface areas at the run temperatures were calculated from their overall geometry, using literature values for the thermal expansion coefficients. No corrections were applied for the slight change in surface area due to sublimation. Assuming each sample sublimed uniformly over its surface area, the error introduced by neglecting this change in the surface area was less than 0.3 percent.

2.3. Procedure

The experimental procedure was generally similar to that used previously. The microbalance was used as a deflection instrument, deflections of its beam being directly proportional to changes in mass of the sample. Beam deflections were measured with a cathetometer readable to 1 μ displacements. The microbalance was calibrated, with each sample *in situ*, using Class M microbalance weights previously calibrated by the Mass Section of NBS.

Interaction between the rf field and the sample caused the balance to be displaced full scale. Therefore, the balance was first read with the sample at room temperature. The sample was then heated rapidly, held at constant temperature for a given length of time, then cooled rapidly. When the sample had returned to room temperature, the balance was then read again to obtain the total mass change during the course of each run. As explained previously [1], no significant weight loss occurred during the short heating and cooling periods.

The duration of the runs ranged from ½ min at the highest temperature to over 7 hr at the lowest for ruthenium, and 3 min to 52 hr for osmium. The uncertainty in the measurement of the weight losses was about ±4 percent for a weight loss as small as 25 μg, but was proportionately smaller for larger weight losses.

For the oil-pumped apparatus pressures were in the range 2×10^{-6} to 8×10^{-5} torr throughout each run, as discussed previously [1]. The ion-pumped apparatus permitted pressures of 1×10^{-9} torr to be obtained initially in the cold system. During the first heating of a series, the pressure generally rose to a maximum of about 5×10^{-8} torr. Subsequent runs yielded successively lower maximum pressures, so that during the later runs of a series the pressure was maintained continuously within the range 1 to 5×10^{-9} torr. No trends in the data with changes in pressure were detected.

2.4. Temperature Measurement

A common source of error in measurements by the Langmuir method arises from uncertainties in the emittance of the surface of the sample, and hence, in the conversion of observed brightness temperatures to thermodynamic temperatures. A method of introducing a blackbody hole into the sample was described previously [2] for the measurements on palladium. For a substance having a vaporization coefficient of unity the presence of the hole does not increase the effective surface area of the sample and eliminates the emittance problem. In the present measurements an easier-to-use method of introducing the hole was employed.

A hole having a length : diameter ratio of 10 or greater was drilled into the bottom of each sample along its principal axis. The diameters of the holes were in the range 0.076–0.102 cm, depending on the lengths permitted by the overall size of the samples. An NBS calibrated pyrometer with a magnifying objective was used to measure temperatures by sighting up the holes through a calibrated window (with magnetic shutter) and with the aid of a calibrated mirror. The window and mirror calibrations were checked periodically.

Using this technique, the principal source of error in the temperature measurements arose from the instability of the rf generators, causing temperature fluctuations. The fluctuations were normally within the range ±5 °C of the temperatures given in the tables of results.

One additional small, but undetermined source of temperature error was inadvertently introduced for the second series of measurements on sample 1 of Ru. After the first series, a piece was broken from the bottom of the sample for analysis. In lengthening the blackbody hole, the drill broke through the 0.025 cm hole, close to the top of the sample, which was used for suspension purposes. Observations confirmed that the hole did not meet blackbody conditions, but the extent of the departure could not be determined with precision.

3. Results and Discussion

3.1. Ruthenium

The results of the five series of measurements on the two samples of ruthenium are given in table 3. Calculated values of the vapor pressures and the third law heats of sublimation are also given in the

TABLE 3. *Vapor pressures and heats of sublimation of ruthenium***

Temperature	Duration of run	Weight loss	Vapor pressure	$\Delta H^\circ_s(298)$
		Sample 1, series 1 $So=2.108$ cm²		
°K	min	μg	atm	kcal/mole
1974	30	30.3	$7.72\cdot10^{-10}$	155.8
2007	30	45.1	$1.16\cdot10^{-9}$	156.8
2081	15	111.3	$5.81\cdot10^{-9}$	155.9
2141	10	153.8	$1.22\cdot10^{-8}$	157.1
2131	7.5	77.4	$8.17\cdot10^{-9}$	158.1
2135	10	150.8	$1.20\cdot10^{-8}$	156.8
2164	8	163.1	$1.63\cdot10^{-8}$	157.6
2228	5	341.0	$5.51\cdot10^{-8}$	156.8
2317	1	333.3	$2.74\cdot10^{-7}$	155.6
2208	1	52.3	$4.21\cdot10^{-8}$	156.6
2246	1	66.2	$5.37\cdot10^{-8}$	158.2
2324	(40 sec)	219.5	$2.71\cdot10^{-7}$	156.1
2323	(25 sec)	148.2	$2.93\cdot10^{-7}$	155.7
2279	1	146.1	$1.19\cdot10^{-7}$	156.9
2198	4	156.4	$3.14\cdot10^{-8}$	157.2
1940	90	42.0	$3.54\cdot10^{-10}$	156.2
2043	15	50.8	$2.63\cdot10^{-9}$	156.2
2280	1	122.6	$1.00\cdot10^{-7}$	157.7
2275	1	126.7	$1.04\cdot10^{-7}$	157.2
2316	1	220.0	$1.81\cdot10^{-7}$	157.4
2292	2	292.3	$1.20\cdot10^{-7}$	157.7
2262	1.5	153.3	$8.32\cdot10^{-8}$	157.3
		Sample 1, series 2 $So=1.810$ cm²		
1954	45	38.0	$7.48\cdot10^{-10}$	154.4
2023	17	50.5	$2.68\cdot10^{-9}$	154.7
2228	2	157.4	$7.41\cdot10^{-8}$	155.5
2058	6	32.2	$4.87\cdot10^{-9}$	154.9
2214	1.5	93.0	$5.82\cdot10^{-8}$	155.6
2076	5	34.4	$6.27\cdot10^{-9}$	155.2
2308	1.5	387.2	$2.47\cdot10^{-7}$	155.5
2199	1.5	92.1	$5.75\cdot10^{-8}$	154.6
2168	2	75.1	$3.49\cdot10^{-8}$	154.6
2107	2.5	26.4	$9.69\cdot10^{-9}$	155.6
2152	2	60.4	$2.80\cdot10^{-8}$	154.4
2274	1.5	289.3	$1.83\cdot10^{-7}$	154.6
2102	3	31.7	$9.69\cdot10^{-9}$	155.3
2142	3	62.6	$1.93\cdot10^{-8}$	155.3
2171	2	70.6	$3.28\cdot10^{-8}$	155.1
2198	2	104.2	$4.88\cdot10^{-8}$	155.3
2257	1	144.0	$1.36\cdot10^{-7}$	154.8
2314	0.5	173.5	$3.33\cdot10^{-7}$	154.5
2377	0.5	592.4	$1.15\cdot10^{-6}$	152.8
1952	60	39.8	$5.88\cdot10^{-10}$	155.2
		Sample 2, series 1 $So=2.142$ cm²		
2069	15	105.8	$5.43\cdot10^{-9}$	155.2
2060	5	31.7	$4.87\cdot10^{-9}$	155.0
2130	3	41.4	$1.08\cdot10^{-8}$	156.9
2155	2	50.6	$1.98\cdot10^{-8}$	156.1
2163	4	118.6	$2.33\cdot10^{-8}$	156.0
2242	1.5	129.3	$6.88\cdot10^{-8}$	156.8
2140	2	24.0	$9.38\cdot10^{-9}$	158.2
2098	5	34.2	$5.30\cdot10^{-9}$	157.5
2160	2	43.4	$1.70\cdot10^{-8}$	157.1
1996	30	55.2	$1.39\cdot10^{-9}$	155.2
2047	8	27.6	$2.64\cdot10^{-9}$	156.5
2098	2.5	16.9	$5.23\cdot10^{-9}$	157.6
2099	7	64.9	$7.18\cdot10^{-9}$	156.3
2048	10	33.2	$2.54\cdot10^{-9}$	156.8
2107	6	54.7	$7.07\cdot10^{-9}$	157.0
2129	2.5	29.6	$9.23\cdot10^{-9}$	157.5
2159	1.5	35.8	$1.87\cdot10^{-8}$	156.6
2222	1	60.3	$4.80\cdot10^{-8}$	157.0
2302	0.5	81.8	$1.32\cdot10^{-7}$	157.9
2178	1.5	46.5	$2.44\cdot10^{-8}$	156.9

TABLE 3. *Vapor pressures and heats of sublimation of ruthenium***—Continued

Temperature	Duration of run	Weight loss	Vapor pressure	$\Delta H^\circ_s(298)$
		Sample 2, series 2 $S_o=2.142$ cm²		
°K	min	μg	atm	kcal/mole
1942	50	27.4	$4.09\cdot10^{-10}$	155.8
1976	30	33.0	$8.28\cdot10^{-10}$	155.7
2017	15	31.4	$1.59\cdot10^{-9}$	156.3
2048	10	37.0	$2.83\cdot10^{-9}$	156.3
2080	5	37.0	$5.71\cdot10^{-9}$	155.9
2089	5	40.0	$6.18\cdot10^{-9}$	156.2
2139	2	26.9	$1.05\cdot10^{-8}$	157.6
2163	2	48.2	$1.89\cdot10^{-8}$	156.9
2159	2	49.2	$1.93\cdot10^{-8}$	156.5
2079	5	33.5	$5.17\cdot10^{-9}$	156.2
1885	1446	20.3	$1.03\cdot10^{-11}$	*165.1
1912	1000	131.8	$9.78\cdot10^{-11}$	*158.8
1932	135	52.7	$2.91\cdot10^{-10}$	156.3
1918	150	46.1	$2.28\cdot10^{-10}$	156.1
2328	3.25	825.4	$2.06\cdot10^{-7}$	157.7
1900	240	21.3	$6.56\cdot10^{-11}$	*159.4
1862	7295	30.4	$3.05\cdot10^{-12}$	*167.6
		Sample 2, series 3 $S_o=1.568$ cm²		
1995	20	28.2	$1.46\cdot10^{-9}$	155.0
2037	12	44.5	$3.87\cdot10^{-9}$	154.2
2075	5	33.2	$6.99\cdot10^{-9}$	154.7
1978	30	9.5	$3.26\cdot10^{-10}$	*159.5
2010	18	29.1	$1.68\cdot10^{-9}$	155.6
1986	60	53.6	$9.21\cdot10^{-10}$	156.1
1945	75	5.9	$8.03\cdot10^{-11}$	*162.3
1948	130	21.8	$1.71\cdot10^{-10}$	*159.6
2022	12	25.4	$2.20\cdot10^{-9}$	155.4
2054	6	28.6	$4.99\cdot10^{-9}$	154.5
2083	5	36.4	$7.67\cdot10^{-9}$	154.9
2075	6	31.4	$5.51\cdot10^{-9}$	155.6
2040	9	29.5	$3.42\cdot10^{-9}$	155.0
2008	18	24.5	$1.41\cdot10^{-9}$	156.1
1996	30	40.9	$1.41\cdot10^{-9}$	155.2
1981	30	15.0	$5.15\cdot10^{-10}$	*158.0
1965	90	33.6	$3.83\cdot10^{-10}$	*157.9
1949	180	9.5	$5.40\cdot10^{-11}$	*164.2
1952	120	32.7	$2.79\cdot10^{-10}$	*158.1
1959	110	49.5	$4.61\cdot10^{-10}$	*156.7
1942	314	39.5	$1.28\cdot10^{-10}$	*160.3
1910	430	4.5	$1.06\cdot10^{-11}$	*167.1
2138	3	42.7	$1.52\cdot10^{-8}$	156.0
2168	2.5	53.6	$2.30\cdot10^{-8}$	156.4
2178	2.25	56.4	$2.70\cdot10^{-8}$	156.4
2205	2.17	77.7	$3.88\cdot10^{-8}$	156.8
2208	2	83.6	$4.53\cdot10^{-8}$	156.3
2230	2.08	130.4	$6.82\cdot10^{-8}$	156.0
2255	1	102.7	$1.12\cdot10^{-7}$	155.5

**Experimental sequence. *Data rejected.

table. Adjusted values of the free energy functions given by Stull and Sinke [6] were used to obtain the heats. Clusius and Piesbergen [9] give for the normal entropy of solid ruthenium at 298 °K: $S^\circ_{298}=6.82\pm0.05$ cal deg^{-1} mole^{-1}. This value was used to adjust the values of S°_T and $-(F^\circ_T-H^\circ_{298})/T$ listed by Stull and Sinke by -0.08 cal deg^{-1} mole^{-1}. Table 4 summarizes the data of table 3 in the form of the mean third law heats and the standard deviations for each series of runs. A second law heat of sublimation and standard deviation was computed from the least squares line through a plot of ln P versus $1/T$ for each series of runs. The second law values were referred to 298 °K using the $H^\circ_T-H^\circ_{298}$

TABLE 4. *Heat of sublimation of ruthenium*

Determination	ΔH_s° (298) and standard deviation	
	3d Law*	2d Law
Sample 1: 99.9997-99.997% Ru		*Kcal/mole*
1. Oil pumped. 5×10^{-6} torr ○ 450 kc/s generator.	156.9±0.8	153.0±2.9
2. Ion pumped. 5×10^{-9} torr ○ 450 kc/s generator. Small departure from blackbody hole in sample	154.9±0.6	157.6±2.6
Sample 2: 99.98-99.8% Ru		
1. Ion pumped. □ 450 kc/s generator	156.7±0.9	143.4±5.3
2. Ion pumped. □ 2 Mc/s generator	156.4±0.5	148.3±2.2
3. Ion pumped. ○ 2 Mc/s generator	155.6±0.7	147.1±3.7
All 94 measurements	156.1±1.1	151.6±2.1

*Means of accepted measurements.
○indicates circular cross-section sample.
□indicates square cross-section sample.
The 2 Mc/s generator had a better long term stability than the 450 kc/s generator and could be used for measurements at lower temperatures.

values of Stull and Sinke and are given in table 4. Also shown in this table are the second and third law heats of sublimation obtained by treating all the data of the five series as a unit.

Figure 1 shows a plot of $-\ln P$ versus $1/T$ for the five series of runs. The least squares line representing all the data for the temperature range 1940 to 2377 °K is given by:

$$\text{Log}\, P_{\text{atm}} = 7.500 - \frac{32{,}769}{T}.$$

A normal boiling point of 4150 ± 100 °K is obtained by using the third law heat of sublimation and extrapolating the free energy function data of Stull and Sinke [6].

As indicated in table 3, a total of 14 runs during the last two series on sample 2 were rejected in calculating the results given in table 4. The reasons for the rejection may be briefly summarized as follows.

With a view to obtaining second law heats of vaporization that were closer to the third law values, an attempt was made to extend the temperature range over which the measurements were made. In particular, attempts were made during both series to extend the temperature range downward. As is apparent from figure 1, however, it was found that below a vaguely defined temperature the rates of vaporization were unexpectedly low, and the calculated vapor pressures departed markedly from the straight line $\ln P$ versus $1/T$ plot of the data obtained at higher temperatures. There was some indication that the temperature at which this departure was detected increased with more extended heating of the sample. Thus, no cause was found to reject the data of the first run of sample 2, series 2 which were obtained at 1942 °K. Only data of this series which were obtained at 1912 °K or below were rejected. During series 3, however, it appeared necessary to reject all data obtained at 1981 °K and below. (In order to be consistent, one later value obtained at 1959 °K was rejected, even though the data yielded a heat of sublimation that was within the range of the accepted values.)

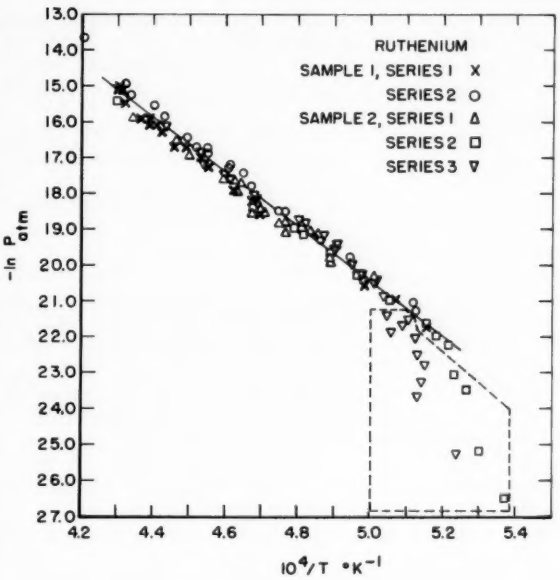

FIGURE 1. *Logarithm of calculated vapor pressures of ruthenium versus reciprocal of absolute temperature.*
All data enclosed by the broken line were rejected.

The cause of the departure is at present unexplained, but the effect is very similar to an effect which was observed during measurements on platinum [1]. One possible explanation which was suggested at that time was that contamination of the surface of the sample occurred, either from its surroundings or by migration of impurities from within. In the present case, however, the surface of the sample was remachined between series 2 and 3. While impurities such as carbon or oxygen (which are not detected by the spectrochemical analyses) may contribute to the problem, further work will be necessary before its nature can be more clearly elucidated.

The relatively large uncertainty in the room temperature area, So, for the sample 1, series 1 measurements can introduce a maximum uncertainty of ±0.3 kcal in individual third law heats for this series. Since this error is well within the precision of the measurements and will tend to cancel in obtaining the average third law heat, the data from this series were accepted.

The question also arises as to whether all the data of the second series of runs on sample 1 should be rejected, in view of the larger temperature error of the series which was discussed in section 2.4. As shown in table 4 this series yielded the lowest mean third law heat of sublimation, but the mean is not in disagreement with the means of the other four series, within the limits of precision. All the data

of the series were, therefore, retained, and were used along with the other accepted data, to arrive at a final estimate of the heat of sublimation based on the combined data of the five series and the third law method.

The overall limits of error of the absolute value of $\Delta H_s°$ (298) were estimated by taking into account the scatter of the data, the uncertainty in the temperature (± 10 °K), and the uncertainty of the weight loss measurements. No allowance was made for the uncertainty in the free energy functions or in the vaporization coefficient. The overall limits of error of the absolute value were estimated to be ± 1.5 kcal/mole, and the corresponding overall limits of error of the vapor pressures are about ± 35 percent. Within the limits of the uncertainty of the temperature measurement the second law value of $\Delta H_s°$ (298) for all 94 measurements (shown in table 4) is in agreement with the third law value.

The final estimate of the absolute value of $\Delta H_s°$ (298) for ruthenium is, therefore, 156.1 ± 1.5 kcal/mole. The value is in agreement with the values of Paule and Margrave [3] and Panish and Reif [4] within the limits of experimental error.

3.2. Osmium

The vapor pressures of osmium calculated from the measured rates of vaporization are given in table 5, together with the corresponding values of $\Delta H_s°$ (298). The free energy functions of Stull and Sinke [6] were used to obtain the heats of sublimation.

Figure 2 shows a Clausius-Clapeyron plot of the data shown in table 5. The least squares line through the data may be represented by:

$$\text{Log } P_{\text{atm}} = 7.484 - \frac{39{,}880}{T}$$

for the temperature range 2157 to 2592 °K. This equation leads to a second law value of $\Delta H_s°$ (298) of 184.1 kcal/mole with a standard deviation of ± 3.0 kcal/mole. A normal boiling point of 5300 ± 100 °K is obtained by using the third law heat and extrapolating the free energy function data of Stull and Sinke [6].

Neglecting uncertainties in the free energy functions and assuming a vaporization coefficient of unity, the overall limits of error in the absolute value of $\Delta H_s°$ (298) were estimated to be ± 1.4 kcal/mole. These limits were applied to the mean third law value to obtain a corresponding error of ± 30 percent in the vapor pressures. The overall error in the temperature measurement is sufficient to account for the discrepancy between the second and third law values.

Based on the mean third law value, the best estimate of the absolute value of $\Delta H_s°$ (298) is, therefore, 189.0 ± 1.4 kcal/mole. This value agrees well with the value of Panish and Reif [4] within the limits of experimental error.

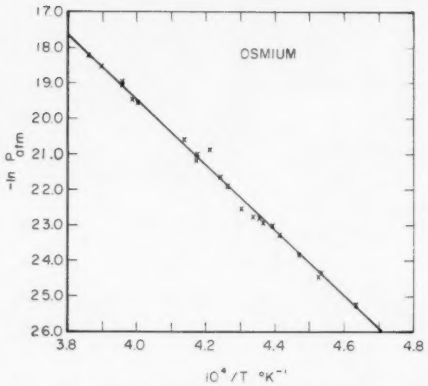

FIGURE 2. *Logarithm of vapor pressure of osmium versus reciprocal of absolute temperature.*

TABLE 5. *Vapor pressures and heats of sublimation of osmium**

Temperature	Duration of run	Weight loss	Vapor pressure	$\Delta H_s°$ (298)
°K	min	μg	atm	kcal/mole
2374	60	45.4	$8.58 \cdot 10^{-10}$	186.3
2419	20	18.7	$1.07 \cdot 10^{-9}$	188.8
2528	5	23.2	$5.41 \cdot 10^{-9}$	189.0
2569	5	37.4	$8.80 \cdot 10^{-9}$	189.6
2592	3	31.6	$1.24 \cdot 10^{-8}$	189.5
2397	30	16.5	$6.25 \cdot 10^{-10}$	189.6
2396	100	63.2	$7.20 \cdot 10^{-10}$	188.9
2358	205	71.3	$3.93 \cdot 10^{-10}$	188.7
2346	105	28.1	$3.01 \cdot 10^{-10}$	189.0
2323	172	25.4	$1.66 \cdot 10^{-10}$	190.0
2305	302	36.5	$1.35 \cdot 10^{-10}$	189.4
2290	465	45.9	$1.10 \cdot 10^{-10}$	189.1
2530	5	24.0	$5.62 \cdot 10^{-9}$	189.0
2510	6	18.3	$3.54 \cdot 10^{-9}$	189.8
2500	7	19.2	$3.18 \cdot 10^{-9}$	189.6
2210	1010	22.1	$2.24 \cdot 10^{-11}$	189.3
2296	310	34.5	$1.25 \cdot 10^{-10}$	189.0
2278	303	28.3	$1.05 \cdot 10^{-10}$	188.4
2267	543	38.5	$7.91 \cdot 10^{-11}$	188.7
2237	732	30.1	$4.56 \cdot 10^{-11}$	188.7
2205	1390	32.7	$2.60 \cdot 10^{-11}$	188.5
2157	3136	32.3	$1.12 \cdot 10^{-11}$	188.0
Mean and standard deviation				189.0±0.8

*Experimental sequence.
So=1.141 cm².

4. References

[1] R. F. Hampson, Jr., and R. F. Walker, J. Res. NBS **65A** (Phys. and Chem.), No. 4, 289 (1961).

[2] R. F. Hampson, Jr., and R. F. Walker, J. Res. NBS **66A** (Phys. and Chem.), No. 2, 177 (1962).

[3] R. C. Paule and J. L. Margrave, J. Phys. Chem. **67,** 1896 (1963).

[4] M. B. Panish and L. Reif, J. Chem. Phys. **37,** No. 1, 128 (1962).

[5] L. Brewer, The chemistry and metallurgy of miscellaneous materials: thermodynamics, L. L. Quill, ed., pp. 13 et seq. (McGraw-Hill Book Company, Inc., New York, N.Y., 1950).

[6] D. R. Stull and G. C. Sinke, Thermodynamic properties of the elements (Am. Chem. Soc., Washington, D.C., 1956).

[7] R. F. Walker, Vacuum microbalance techniques, Vol. 1, pp. 87–110, M. J. Katz, ed. (Plenum Press, New York, N.Y., 1961).

[8] N. J. Carrera, R. F. Walker, W. Nalley, and C. Steggerda, Vacuum microbalance techniques, Vol. 3, pp. 153–177, K. Behrndt, ed. (Plenum Press, New York, N.Y., 1963).

[9] K. Clusius and U. Piesbergen, Z. Naturforsch. **14a,** 23 (1959).

(Paper 68A3–280)

JOURNAL OF RESEARCH of the National Bureau of Standards—A. Physics and Chemistry
Vol. 68A, No. 3, May–June 1964

The 0–2 Transition of CO in Condensed Oxygen, Nitrogen, and Argon

Stanley Abramowitz[1] and H. P. Broida[2]

(January 31, 1964)

Infrared absorption spectra of CO in the region of the first overtone have been observed in dilute (approximately 1 to 10 parts in 1000) liquid solutions of oxygen, nitrogen, and argon, and clear crystalline nitrogen and argon matrices. The overtone band was found at 4249.0, 4252.4, and 4252.0 cm^{-1} with half widths of 18.4, 17.8, and 13.7 cm^{-1} in liquid oxygen, nitrogen, and argon solutions at 82, 78, and 82 °K, respectively. The half width in liquid oxygen varied from 18.4 to 10.0 cm^{-1} in the temperature range 82 to 57 °K. The band position was the same but its width was smaller in the crystalline nitrogen matrix. Two bands were observed in the clear crystalline argon solid at 4245 and 4256 cm^{-1}. The solution results cannot be interpreted with the recent theory of Buckingham.

Infrared absorption spectra of carbon monoxide in the region of the first overtone have been observed in the liquid solvents oxygen, nitrogen, and argon. In addition, the spectra have been obtained in clear crystalline solutions of argon and of nitrogen near the triple points of these solvents. The purpose of these experiments was to determine the influence of temperature, phase changes, and solvents on half width, position, and shape of the CO absorption band.

A Perkin-Elmer model 99 monochromator with a 2000 lines/cm grating blazed at 10° (1.7μ in first order) was used in the first order with a spectral slit width of about 1 cm^{-1}. An antireflection coated germanium filter eliminated the higher orders from the 1000 w tungsten filament lamp used as the light source. The quartz absorption cell used, recently described by Bass and Broida [1], was modified slightly by recessing the windows further into the coolant tube. The resultant increased thermal contact between the refrigerant and the solution greatly simplified the growing of the clear crystalline matrices. The temperature of the refrigerant, liquid oxygen, was regulated by pumping on it with a small vacuum pump (capacity 14 liters/min). The vapor pressure of the liquid oxygen refrigerant, measured with an aneroid type gauge, provided an indication of the temperature. The direct measurement of the vapor pressure above the solution with a mercury manometer also provided an indication of the temperature. Solutions were prepared from the gases which had been mixed in the ratios of 1 to 10 parts carbon monoxide to 1000 parts of the various solvents. The position, the half width, and the shape of the spectral band did not depend on the concentration in this range. The clear solid solutions were grown slowly from the liquids at or near the triple points of the solvents.

[1] National Academy of Sciences-National Research Council Postdoctoral Research Associate at the National Bureau of Standards.
[2] Present address: Department of Physics, University of California, Santa Barbara, Calif.

The measured frequencies and half widths of the 0–2 transition of CO in condensed oxygen, nitrogen, and argon are summarized in table 1. In liquid oxygen and liquid nitrogen, the band was symmetrical both at the half width and twice the half width and had a Lorentzian shape (using the width at twice the half-band width as the criterion [2]). There were no changes in the position or the shape of the band in liquid oxygen at temperatures from 57 to 82 °K. However the half-band width varied from 10.0 to 18.4 cm^{-1} in this temperature range. In liquid argon the band is slightly asymmetric with more absorption on the high-frequency side.

Although the position of the band in clear crystalline solid nitrogen is not greatly different from that of the corresponding liquid solution, the half width is reduced by one-third and the shape is asymmetric and broader on the high-frequency side in the solid matrix. The absorption in the wings of the band is less than one would expect for a Lorentzian band shape. This observation is in apparent agreement with Wieder and Dows [3] who recently have observed vibrational bands of solid C_2H_4 and C_2D_4 which had shapes between the Gaussian and Lorentzian forms. In clear crystalline argon, the band is split into two overlapping peaks with the high-frequency peak about 50 percent more intense than the other peak.

Results for the band positions obtained in this study are in good agreement with the recently published results of Vu, Atwood, and Vodar [4]. The band contours which are shown by them appear quite similar to the ones observed in this study but half widths were not listed, so that a further comparison of our results with theirs is not possible. These workers did not study the influence of temperature on the spectrum.

In an effort to find an explanation for the observations of the 0–2 band of CO in condensed phases, several theoretical models have been tried.

TABLE 1. *The 0–2 transition of CO in condensed oxygen, nitrogen and argon*

Solvent	Phase	T	ν	$\Delta\nu_{1/2}$
		°K	cm^{-1}	cm^{-1}
	gas	300	4260.0	
O_2	liq	57	4249.0 ±0.5	10.0 ±0.5
O_2	liq	82	4249.0 ±0.5	18.4 ±0.5
N_2	liq	78	4252.4 ±0.5	17.8 ±0.5
Ar	liq	82	4252.0 ±0.5	13.7 ±0.5
N_2	solid	62	4252.0 ±0.5	12.3 ±0.5
Ar	solid	67	[4245.0 ±1.0] [4256.0 ±1.0]	25.0 ±2.0

Unfortunately none of these theories easily account for the band shapes and shifts.

Ewing [5] has observed the CO fundamental vibration in the liquid phase, in nitrogen and argon solutions. The bands he observed were not only asymmetric but also broader than the 0–2 bands observed in this study. The carbon monoxide fundamental had half widths of 26 cm^{-1} and 18 cm^{-1} in liquid nitrogen and argon, respectively, at temperatures comparable to those in this study. Ewing ascribed the asymmetry and increased absorption to the high-frequency side of the bands to a low barrier to rotation. From the asymmetry he estimated the barrier to be 42 cm^{-1} in pure liquid carbon monoxide, while slightly lower and slightly higher barriers were estimated for carbon monoxide solutions in liquid nitrogen and argon, respectively. A comparison with the present results (table 1) shows that the harmonic band is about two-thirds as broad as that of the fundamental. Moreover, the lack of asymmetry of the band in liquid nitrogen coupled with its narrowness in comparison to Ewing's observations of the fundamental seems to indicate that either hindered rotation is not the disordering mechanism contributing to the band width observed, or the barrier is several times higher than kT.

The observation of a variation of the half width of the CO harmonic in liquid oxygen from 10.0 to 18.4 cm^{-1} in the temperature range of 57 to 82 °K is surprising in the light of existing theories. If the band contour is determined principally by a strong collision process, in which the duration of the collision is small compared to the time between collisions, a Lorentzian band contour should be observed. The half width of such a band should be proportional to $T^{1/2}$ [6, 7]. The observed dependence is clearly a function of a higher power of the temperature.

If hindered rotation is responsible for the band width, then an increase in half-band width and asymmetry to the high-frequency side of the band is to be expected with a rise in temperature if the barrier is comparable to kT. If the barrier is much higher than kT the band width is independent of temperature. Since the population of the J levels of a rotator is proportional to $T^{1/2}$, one would expect the width of the band to vary roughly as $T^{1/2}$ if free or hindered rotation is causing the observed breadth. The observed dependence of approximately $T^{3/2}$ coupled with the lack of asymmetry seems to rule out this explanation for CO in oxygen.

It has recently been suggested by Rakov in application to organic materials that the width of bands could be represented by an exponential of the form

$$\Delta\nu_{1/2}=A \exp\ (-E/RT) \tag{1}$$

where E is the potential barrier for reorientation of the molecules [8, 9]. Rakov has further indicated that if Brownian motion is responsible for the observed band widths this E should be equivalent to the energy of viscous flow, E_{vis}, which is defined by Glasstone, Laidler, and Eyring [10] through the relationship

$$\eta=B \exp\ (E_{vis}/RT) \tag{2}$$

where η is the viscosity of the liquid medium. Using the data in table 1 for the band width of the CO harmonic in liquid oxygen at 57 °K and 82 °K, one may calculate the E appearing in eq (1). This value of E is about a factor of two smaller than the E_{vis} calculated for liquid oxygen in this temperature range from the available data on the viscosity of liquid oxygen [11]. It appears therefore that this theory does not fit the phenomena observed in this study.

Recently Buckingham [12, 13, 14] presented a theory to account for solvent effects on vibrational transitions of diatomic molecules. One of the unique predictions of this theory is that the $(s-1)$ overtone of a diatomic molecule should be s times as broad as the fundamental. The half widths observed in this study of the first overtone of carbon monoxide are decidedly *smaller* than the widths of the fundamental in these same solvent systems observed by Ewing [5]. This indicates the failure of Buckingham's theory in predicting band widths for the simple system carbon monoxide in nitrogen and argon solutions. The solvent shifts $(\nu_{vap}-\nu_{sol'n})$ observed for the carbon monoxide harmonic in nitrogen is 7.6 cm^{-1}, which is about 2.5 times the solvent shift of 3 cm^{-1} for the fundamental observed by Ewing. Buckingham's theory as well as the earlier theory of Kirkwood, Bauer, and Magat [15, 16] predicts that the solvent shift of the harmonic should be twice that of the fundamental.

In conclusion, the first overtone of carbon monoxide has been observed in condensed phases of oxygen, nitrogen, and argon. Both the shape and half width are significantly changed in the transition of liquid solution to solid solution, while the band position is not appreciably altered in the phase change. (Changes were not observed for the methane-argon system [17].) The recent theory of Buckingham as well as the earlier theory ascribed to Kirkwood, Bauer, and Magat have been found not to apply to these systems. No explanation is apparent for the two overlapping bands observed for carbon monoxide in the clear crystalline argon solid. The explanation of Vu et al. [4] implies that a combination band involving the fundamental band and a lattice mode is more intense than the respective fundamental. This explanation is not consistent with the observation of one band for the ν_3 vibration

of methane in a clear crystalline argon solid [17]. The variation of the half width of the 0–2 band of CO in liquid oxygen in the temperature range of 57 to 82 °K cannot be readily explained with existing theories.

References

[1] A. M. Bass and H. P. Broida, J. Mol. Spect. **12,** 221 (1964).
[2] S. Abramowitz and R. P. Bauman, J. Chem. Phys. **39,** 2757 (1963).
[3] G. M. Wieder and D. A. Dows, J. Chem. Phys. **37,** 2990 (1962).
[4] H. Vu, M. R. Atwood, and B. Vodar, J. Chem. Phys. **38,** 2671 (1963).
[5] G. E. Ewing, J. Chem. Phys. **37,** 2250 (1962).
[6] D. A. Ramsay, J. Am. Chem. Soc. **74,** 72 (1952).
[7] K. S. Seshadri and R. N. Jones, Spectrochim. Acta **19,** 1013 (1963).
[8] A. V. Rakov, Opt. Spectr. **13,** 203 (1962).
[9] A. V. Rakov, Opt. Spectr. **7,** 128 (1959).
[10] S. Glasstone, K. J. Laidler, and H. Eyring, The theory of rate processes, McGraw-Hill Book Co. (1941), p. 477.
[11] V. J. Johnson, A compendium of the properties of materials at low temperatures, phase 1 part I properties of fluids WADD Tech. Rpt. 60–56 (1960).
[12] A. D. Buckingham, Proc. Roy. Soc. Lond. **A248,** 169 (1958).
[13] A. D. Buckingham, Trans. Far. Soc. **56,** 753 (1960).
[14] A. D. Buckingham, Proc. Roy. Soc. Lond. **A255,** 32 (1960).
[15] W. West and R. T. Edwards, J. Chem. Phys. **5,** 14 (1937).
[16] E. Bauer and M. Magat, J. Phys. Rad. **9,** 319 (1938).
[17] S. Abramowitz and H. P. Broida, J. Chem. Phys. **39,** 2383 (1963).

(Paper 68A3–281)

JOURNAL OF RESEARCH of the National Bureau of Standards—A. Physics and Chemistry
Vol. 68A, No. 3, May–June 1964

Publications of the National Bureau of Standards*

Selected Abstracts

Fringe pattern of an oscillating Fabry-Perot interferometer, K. D. Mielenz, *J. Res. NBS* **68C** (Eng. and Instr.), No. 2, 73–82 (Apr.–June 1964).
The dependence of the fringe pattern of an oscillating Fabry-Perot interferometer upon the vibration amplitude is discussed experimentally and theoretically. If the fringes of the stationary interferometer are wide, the fringe pattern tends to disappear at certain values of the amplitude. If the stationary fringes are narrow, a splitting of fringes occurs at certain amplitudes. In both cases, the stationary pattern reappears, with reduced contrast, at intermediate amplitudes. The practicability of using these effects for the measurement of vibration amplitudes is discussed.

Mean electron density variations of the quiet ionosphere No. 12, February 1960, J. W. Wright, L. R. Wescott, and D. J. Brown, *NBS Tech. Note 40–12 (Dec. 6, 1963), 35 cents.*
The CRPL has initiated a program for large-scale computation of electron density profiles from ionospheric vertical soundings. Scaling is performed at field stations, permitting computation of hourly profiles at the Central Laboratory. These profiles are combined to form hourly mean quiet profiles for each station and month. The results of this program for the month of February are illustrated graphically. This report is the twelfth of a series illustrating the electron density variations in the mean quiet ionosphere between latitudes 15° N and 50° N along the 75° W meridian.

A technique for extrapolating the 1 kc values of secondary capacitance standards to higher frequencies, R. N. Jones, *NBS Tech. Note 201 (Nov. 5, 1963), 15 cents.*
A simple technique is described for extrapolating the 1 kc values of certain two-terminal capacitors to higher frequencies without incurring serious losses in accuracy. The method is intended for use with air capacitors having binding post or banana plug type connectors. Because of inherent errors, such connectors are not appropriate for measurement where the highest accuracy is required. For this reason, it is recommended that calibration of this type be performed by secondary laboratories and not be submitted to the National Bureau of Standards.

Thermodynamic property values for gaseous and liquid carbon monoxide from 70° to 300 °K with pressures to 300 atmospheres, J. G. Hust and R. B. Stewart, *NBS Tech. Note 202 (Now. 30, 1963), 60 cents.*
The internal energy, entropy, enthalpy, and density of carbon monoxide are tabulated as functions of pressure and temperature from 70 to 300 °K and 0.1 to 300 atmospheres. A compressibility factor-pressure chart and a temperature-entropy chart are also included. The P-ρ-T values have been calculated using the Su principle of corresponding states with nitrogen as a model. Extensive comparisons are included, illustrating the deviations of the calculated values from the experimental data and from other correlated data. Equations representing the P-ρ-T surface and the vapor pressure are given.

A low-pressure arc source for the emission spectrum of the FeO molecule, R. K. Dhumwad and A. M. Bass, *Appl. Opt.* **2,** *No. 12, 1335 (Dec. 1963).*
The emission spectrum of FeO has been produced without interference from atomic iron lines. The source for this spectrum is described.

Dissociative ionization of H_2; A study of angular distributions and energy distributions of resultant fast protons, G. H. Dunn and L. J. Kieffer, *Phys. Rev.* **132,** *No. 5, 2109–2117 (Dec. 1, 1963).*
Protons with energies between 2 ev and 14 ev have been observed from dissociative ionization of H_2 using a rotatable collision chamber in conjunction with a small 60 sector magnetic spectrometer, and using electrons with energies ranging from threshold to 1500 ev. The degree of anisotropy and its electron energy dependence on measurements of cross sections and the energy distribution of protons is investigated. The energy distribution of protons is measured as a function of electron energy, and quite good agreement is found with predictions of the Franck-Condon principle. This is in rather sharp contrast with results of previous investigators.

First-order phase transition in a gas of long thin rods, R. Zwanzig, *J. Chem. Phys.* **39,** *No. 7, 1714–1721 (Oct. 1, 1963).*
Onsager's prediction of a first order phase transition in a gas of long thin rods is verified by extensive calculations on a simple model. The molecules are rectangular parallelopipeds, of length l and square cross section $d \times d$. The long molecular axes can point in only three mutually perpendicular directions. Virial coefficients, up to the seventh, are calculated exactly as functions of orientation, in the limit $l \to \infty$, $d \to 0$, and $l^2 d$ = constant. The transition predicted by Onsager's theory, based on a second virial approximation to the potential of mean force in the space of relative orientations, is observed also when all virial coefficients up to the seventh are included. The virial expansion appears to converge usefully in the vicinity of the transition.

Gamma irradiation of polytetrafluoroethylene in chlorine, R. E. Florin and L. A. Wall, *SPE Trans.* **3,** *No. 4, 290–299 (Oct. 1963).*
In chlorine polytetrafluoroethylene, irradiated in halogen atmospheres, decrease in ultimate tensile strength and elongation at break almost as rapidly as in oxygen. The rate of degradation is approximately independent of chlorine pressure down to about 1 mm Hg. The phenomena can be explained semiquantitatively in terms of first order, cage reactions of scission, recombination, and reaction with chlorine, complicated by diffusion at low pressures. However, all reaction and diffusion parameters must shift with gradual increase of crystallinity.
For a given decrease of elongation at break, polytetrafluoroethylene irradiated in a vacuum retains a relatively higher ultimate tensile strength. In the copolymer of tetrafluoroethylene and hexafluoropropylene, the changes in ultimate tensile strength and elongation at break are much slower under all conditions. Both polytetrafluoroethylene and the copolymer retain appreciable tensile strength but little elongation up to a dose of 2×10^8r.

The validity of crystal field theory as applied to rare earth ions: An analysis of the spectrum of praseodymium trichloride, J. C. Eisenstein, *Low Symposium on Paramagnetic Resonance I, 253–260 (Academic Press, Inc., New York, N.Y., 1963).*
The spectrum of $PrCl_3$ below 25,000 cm^{-1} is analyzed from the point of view of crystal field theory. Coulomb, spin-orbit and crystal field interactions are taken into account. The Coulomb integrals, the spin-orbit coupling constant and the quantities $A_l^m\langle r^l \rangle$ which characterize the crystal field are treated as parameters. The eigenvalue problem for the f^2 configuration is solved by diagonalization of the complete interaction matrices.
The calculated positions of the energy levels are compared with the experimental results. This comparison indicates the existence of appreciable interaction between the f^2 and higher configurations. Also it appears that no single set of crystal field parameters will give good agreement between calculated and observed levels for all multiplets. This difficulty may also be ascribable to neglect of configuration interaction.

Kinetics of desorption. III. Rb^+, K^+, and Na^+ on rhenium, M. D. Scheer and J. Fine, *J. Chem. Phys.* **39,** *No. 7, 1752–1755 (Oct. 1, 1963).*

JOURNAL OF RESEARCH of the National Bureau of Standards—A. Physics and Chemistry
Vol. 68A, No. 3, May–June 1964

Publications of the National Bureau of Standards*

Selected Abstracts

Fringe pattern of an oscillating Fabry-Perot interferometer, K. D. Mielenz, *J. Res. NBS* **68C** (Eng. and Instr.), No. 2, 73–82 (Apr.–June 1964).
The dependence of the fringe pattern of an oscillating Fabry-Perot interferometer upon the vibration amplitude is discussed experimentally and theoretically. If the fringes of the stationary interferometer are wide, the fringe pattern tends to disappear at certain values of the amplitude. If the stationary fringes are narrow, a splitting of fringes occurs at certain amplitudes. In both cases, the stationary pattern reappears, with reduced contrast, at intermediate amplitudes. The practicability of using these effects for the measurement of vibration amplitudes is discussed.

Mean electron density variations of the quiet ionosphere No. 12, February 1960, J. W. Wright, L. R. Wescott, and D. J. Brown, *NBS Tech. Note 40–12 (Dec. 6, 1963), 35 cents.*
The CRPL has initiated a program for large-scale computation of electron density profiles from ionospheric vertical soundings. Scaling is performed at field stations, permitting computation of hourly profiles at the Central Laboratory. These profiles are combined to form hourly mean quiet profiles for each station and month. The results of this program for the month of February are illustrated graphically. This report is the twelfth of a series illustrating the electron density variations in the mean quiet ionosphere between latitudes 15° N and 50° N along the 75° W meridian.

A technique for extrapolating the 1 kc values of secondary capacitance standards to higher frequencies, R. N. Jones, *NBS Tech. Note 201 (Nov. 5, 1963), 15 cents.*
A simple technique is described for extrapolating the 1 kc values of certain two-terminal capacitors to higher frequencies without incurring serious losses in accuracy. The method is intended for use with air capacitors having binding post or banana plug type connectors. Because of inherent errors, such connectors are not appropriate for measurement where the highest accuracy is required. For this reason, it is recommended that calibration of this type be performed by secondary laboratories and not be submitted to the National Bureau of Standards.

Thermodynamic property values for gaseous and liquid carbon monoxide from 70° to 300 °K with pressures to 300 atmospheres, J. G. Hust and R. B. Stewart, *NBS Tech. Note 202 (Nov. 30, 1963), 60 cents.*
The internal energy, entropy, enthalpy, and density of carbon monoxide are tabulated as functions of pressure and temperature from 70 to 300 °K and 0.1 to 300 atmospheres. A compressibility factor-pressure chart and a temperature-entropy chart are also included. The P-ρ-T values have been calculated using the Su principle of corresponding states with nitrogen as a model. Extensive comparisons are included, illustrating the deviations of the calculated values from the experimental data and from other correlated data. Equations representing the P-ρ-T surface and the vapor pressure are given.

A low-pressure arc source for the emission spectrum of the FeO molecule, R. K. Dhumwad and A. M. Bass, *Appl. Opt.* **2,** *No. 12, 1335 (Dec. 1963).*
The emission spectrum of FeO has been produced without interference from atomic iron lines. The source for this spectrum is described.

Dissociative ionization of H_2; A study of angular distributions and energy distributions of resultant fast protons, G. H. Dunn and L. J. Kieffer, *Phys. Rev.* **132,** *No. 5, 2109–2117 (Dec. 1, 1963).*
Protons with energies between 2 ev and 14 ev have been observed from dissociative ionization of H_2 using a rotatable collision chamber in conjunction with a small 60 sector magnetic spectrometer, and using electrons with energies ranging from threshold to 1500 ev. The degree of anisotropy and its electron energy dependence on measurements of cross sections and the energy distribution of protons is investigated. The energy distribution of protons is measured as a function of electron energy, and quite good agreement is found with predictions of the Franck-Condon principle. This is in rather sharp contrast with results of previous investigators.

First-order phase transition in a gas of long thin rods, R. Zwanzig, *J. Chem. Phys.* **39,** *No. 7, 1714–1721 (Oct. 1, 1963).*
Onsager's prediction of a first order phase transition in a gas of long thin rods is verified by extensive calculations on a simple model. The molecules are rectangular parallelopipeds, of length l and square cross section $d \times d$. The long molecular axes can point in only three mutually perpendicular directions. Virial coefficients, up to the seventh, are calculated exactly as functions of orientation, in the limit $l \to \infty$, $d \to 0$, and $l^2 d$ = constant. The transition predicted by Onsager's theory, based on a second virial approximation to the potential of mean force in the space of relative orientations, is observed also when all virial coefficients up to the seventh are included. The virial expansion appears to converge usefully in the vicinity of the transition.

Gamma irradiation of polytetrafluoroethylene in chlorine, R. E. Florin and L. A. Wall, *SPE Trans.* **3,** *No. 4, 290–299 (Oct. 1963).*
In chlorine polytetrafluoroethylene, irradiated in halogen atmospheres, decrease in ultimate tensile strength and elongation at break almost as rapidly as in oxygen. The rate of degradation is approximately independent of chlorine pressure down to about 1 mm Hg. The phenomena can be explained semiquantitatively in terms of first order, cage reactions of scission, recombination, and reaction with chlorine, complicated by diffusion at low pressures. However, all reaction and diffusion parameters must shift with gradual increase of crystallinity.
For a given decrease of elongation at break, polytetrafluoroethylene irradiated in a vacuum retains a relatively higher ultimate tensile strength. In the copolymer of tetrafluoroethylene and hexafluoropropylene, the changes in ultimate tensile strength and elongation at break are much slower under all conditions. Both polytetrafluoroethylene and the copolymer retain appreciable tensile strength but little elongation up to a dose of 2×10^8r.

The validity of crystal field theory as applied to rare earth ions: An analysis of the spectrum of praseodymium trichloride, J. C. Eisenstein, *Low Symposium on Paramagnetic Resonance I, 253–260 (Academic Press, Inc., New York, N.Y., 1963).*
The spectrum of $PrCl_3$ below 25,000 cm^{-1} is analyzed from the point of view of crystal field theory. Coulomb, spin-orbit and crystal field interactions are taken into account. The Coulomb integrals, the spin-orbit coupling constant and the quantities $A_t^q \langle r^l \rangle$ which characterize the crystal field are treated as parameters. The eigenvalue problem for the f^2 configuration is solved by diagonalization of the complete interaction matrices.
The calculated positions of the energy levels are compared with the experimental results. This comparison indicates the existence of appreciable interaction between the f^2 and higher configurations. Also it appears that no single set of crystal field parameters will give good agreement between calculated and observed levels for all multiplets. This difficulty may also be ascribable to neglect of configuration interaction.

Kinetics of desorption. III. Rb^+, K^+, and Na^+ on rhenium, M. D. Scheer and J. Fine, *J. Chem. Phys.* **39,** *No. 7, 1752–1755 (Oct. 1, 1963).*

The mean adsorption lifetimes (τ_3) of Rb^+, K^+, and Na^+ ions on a clean polycrystalline rhenium surface have been measured in the millisecond region as a function of temperature under conditions of very low surface coverage. The results of these measurements are given by

$$Rb^+: \tau_3 = (0.8 \pm 0.3) \times 10^{-13} \exp\left[\frac{26{,}400 \pm 350}{T}\right] \text{ sec}, \quad 1000 < T < 1250\ ^\circ\text{K};$$

$$K^+: \tau_3 = (1.0 \pm 0.3) \times 10^{-13} \exp\left[\frac{27{,}000 \pm 350}{T}\right] \text{ sec}, \quad 1050 < T < 1260\ ^\circ\text{K};$$

$$Na^+: \tau_3 = (0.2 \pm 0.1) \times 10^{-13} \exp\left[\frac{31{,}900 \pm 300}{T}\right] \text{ sec}, \quad 1160 < T < 1400\ ^\circ\text{K}.$$

The interaction of the alkali ion with the metal surface was described by a one dimensional potential function of the form $V(x) = l_+ \left[1 + \frac{1}{m-1}\left(\frac{r_e}{x}\right)^m - \frac{m}{m-1}\left(\frac{r_e}{x}\right)\right]$ where x is the perpendicular distance of the adsorbed ion from the surface and l_+ is the observed desorption energy. By choosing the Pauling ionic radii r_i as the distance of closest approach to the surface for an ion with energy l_+ the parameters m and r_e were calculated for each alkali ion. It was found that the values of m increase and $(r_e - r_i)$ decrease as the atomic number of the alkali ion increases.

The reactions of methyl radicals in the solid-, liquid-, and gas-phase photolysis of dimethylmercury, R. E. Rebbert and P. Ausloos, *J. Am. Chem. Soc.* **85,** *No. 20, 3086–3089 (Oct. 20, 1963).*
The gas-phase photolysis of CD_3COCD_3 has been investigated in the presence of CH_3HgCH_3 from 376° to 453 °K. From the isotopic distributions of the methane and ethane fractions, evidence was obtained for the occurrence of the reaction:

$$CD_3 + CH_3HgCH_3 - CD_3HgCH_3 - CH_3$$

($E_{act} = 12.6$ kcal/mole). This reaction is also postulated to occur in the liquid-phase photolysis of dimethyl mercury. From the isotopic distribution of the ethane produced in the liquid—and solid-phase photolysis of $CH_3HgCH_3 - CD_3HgCD_3$ mixtures, it was concluded that cage recombination of methyl radicals does take place. Contrary to the conclusions reached in an earlier work by Derbyshire and Steacie, no evidence could be obtained for hot methyl radical effects in the liquid-phase photolysis of dimethyl Mercury.

Radiation-induced polymerization at high pressure of *n*-tetradecafluoroheptene-1; 1,1,2-trifluorovinyl phenyl ether; and 1,2,3,4,5-pentafluorophenyl 1,1,2-trifluorovinyl ether, D. W. Brown and L. A. Wall, *SPE Trans.* **3,** *No. 4, 300–308 (Oct. 1963).*
The radiation-induced polymerization of n-tetradecafluoroheptene-1 was investigated at pressures of 8,100, 11,900, and 17,100 atmospheres and temperatures between 90 °C and 267 °C. Both the rate of polymerization and the molecular weight of the polymer first increase and then decreases as temperature is increased at constant pressure. The maximum number-average molecular weight was 28,000. The data are interpreted in terms of a free radical mechanism. The polymer has a low ceiling temperature. As temperature is increased the depropagation step becomes important and reduces the rate of polymerization. Under some conditions transfer seems to be a significant part of the mechanism.
Several radiation-induced polymerizations at high pressure were carried out with 1,1,2-trifluorovinylphenyl ether as well as one with 1,2,3,4,5-pentafluorophenyl 1,1,2-trifluorovinyl ether. The results suggest transfer limits the molecular weight of the polymers.

On the growth of helical dislocations, R. deWit, *Trans. Met. Soc. AIME* **227,** *1443–1452 (Dec. 1963).*
Conclusions reached in a paper by Weertman are amplified in a mathematical and graphical way. It is shown that in a stressed crystal a straight dislocation may be in a position of unstable equilibrium with respect to helix development; how a small perturbation may start the dislocation off on its helical path. Helix development occurs by diffusion; bulk diffusion is necessary for development from a screw, but core diffusion is sufficient for development from an edge dislocation. For a mixed dislocation helix development can take place by core diffusion if the helix also climbs; a diffusion reversal takes place when the slope of the helix equals the slope of the Burgers vector. The work done on a crystal by the external forces is graphically shown to be consistent with the direction of motion of the dislocation in helix development. Finally a detailed mechanism for tangle formation from helices is presented. In the course of helix development a glide situation may be reached where a segment of each helix loop lies in a slip plane in which it can expand by glide. Thus it is visualized how a helix can deteriorate into a tangle.

A study of anthracene fluorescence excited by the ruby giant pulse laser, J. L. Hall, D. A. Jennings, and R. M. McClintock, *Phys. Rev. Letters* **11,** *No. 8, 364–366 (Oct. 15, 1963).*
The unfocused red output light of a ruby Q switched laser has been used to excite blue fluorescence in single crystals of anthracene. The intense normal singlet fluorescence coincident in time with the laser pulse is attributed to two-photon processes. Second harmonic generation and reabsorption is ruled out on the basis of the measured low SHG efficiency of anthracene for the 1.06 micron output of neodymium glass Q switched laser. In addition, a much weaker blue fluorescence is still observable milliseconds after the giant laser pulse. This delayed fluorescence is consistent with bimolecular recombination of triplet excitons. Numerical values are obtained for the four parameters of the model which describes the observed fluorescence.

Knight shifts and line widths of the nuclear magnetic resonance of Pb^{207} in lead-indium alloys, R. J. Snodgrass and L. H. Bennett, *Phys. Rev.* **132,** *1465–1474 (Nov. 15, 1963).*
The nuclear magnetic resonance of Pb^{207} was observed and accurately measured at room temperature and 77° K, in pure lead metal powder and in a series of lead-indium alloy powders containing up to 75% indium. Upon the addition of indium, the central frequency of the Pb^{207} absorption line increases by a small fraction of the line width. At 5 Mc/sec, this frequency shift between pure lead and 20 at. % In is 800 cps, compared to a linewidth of 18 kc/sec in the 20 at. % In sample. The increase in frequency is also a small fraction of the Knight shift, $\Delta k/k = 1.3\%$ up to 20 at. % In. In the cubic lead phase, the frequency shift is linear with composition. From the temperature dependence of the linewidth, the spin-lattice relaxation time is found to be $T_1 = 3.6 \times 10^{-4}$ sec at 77° K. The absorption linewidth increases rapidly upon alloying, due to a combination of indirect spin exchange and pseudo-dipolar coupling. The line shape changes from Lorentzian to Gaussian. A second moment analysis yields a value for the near-neighbor exchange constant $h^{-1}|A| = 2.5$ kc/sec. The pseudo-dipolar exchange constant is found to be $h^{-1}|B| = 1.1$ kc/sec. The relatively large value of 0.4 for the ratio BA^{-1} indicates that the amount of p-character probably exceeds the amount of s-character in the electron wave functions at the Fermi surface in this alloy. Volume effects which are comparable to the observed change in Knight shift preclude the possibility of confirming or denying the existence of charge oscillations of the type discussed by Friedel and others.

Calculations of the potential and effective diffusion constant in a polyelectrolyte solution, S. R. Coriell and J. L. Jackson, *J. Chem. Phys.* **39,** *2418 (1963).*
Numerical computations of the electrostatic potential and the effective diffusion constant of counterions in a periodic polyelectrolyte solution are reported. Some results for the potentials for various polyion charge densities and polyion sizes are presented graphically. The calculated diffusion constants are compared with experimental data on the diffusion of labeled sodium ions in polyacrylic acid-sodium hydroxide solutions as well as with the earlier approximate calculations

Recalibration of NBS standards of spectral transmittance, H. J. Keegan, J. C. Schleter, and M. A. Belknap, *J. Opt. Soc. Am.* **54,** *No. 1, 69–74 (Jan. 1964).*
In 1934, Gibson, Walker, and Brown developed sets of four colored glass filters to serve as working standards of spectral transmittance for checking the reliability of spectrophotometers. Several sets of these glasses were measured carefully and reserved and designated as future reference standards. Duplicate standards evaluated by comparison with the reference standards are available by purchase to the public. The current set of reference standards was established in the years 1945 to 1947, and one of these reference standards (selenium-red) was recalibrated in 1952. This paper reports a recalibration, made in 1961 and 1962, of all four glasses (selenium-red, carbon-yellow, copper-green, cobalt-blue) on three spectrophotometers (Cary 14, Beckman DU, König-Martens). Except for the cobalt-blue standard, the values of spectral transmittance found differ from those previously assigned by amounts differing at some wavelengths by as much as or slightly more than the uncertainties estimated for the present values, though not by amounts exceeding the combined uncertainties of the present and previous determinations. The indicated changes for these three standards are fairly regular, however, and support the view that the selenium-red and carbon-yellow standards are changing chiefly by formation of a reflectance-reducing film on the surfaces. The indicated rate of upward drift is slow, and suggests that it takes about 10 years for the drift to exceed the assigned uncertainty.

Surface flammability measurements by the radiant-panel method, A. F. Robertson, Am. Soc. Testing Mat. Spec. Tech. Publ. **344,** 33–46 (1962).
It is suggested that the flammability of solids may be considered as a function of the ratio of heat release rate to critical ignition energy of the material being studied. Based on this concept, the radiant-panel flammability test method has shown its usefulness as a research tool. A review is included of previous studies made by use of this method.
Recently obtained experimental data are presented which illustrate the large changes in flammability which can occur with changes of the relative humidity of the ambient conditioning atmosphere. Data are presented which suggest that the subsurface heat-dissipation behavior of the material under test may have an important influence on flammability.
The paper concludes with the suggestion that, although the radiant panel flammability test method has achieved some recognition, it would be a mistake to assume that it, or any other test method, would be ideal for prediction of the surface flammability hazard of all materials in all situations.

Stress-strain relationships in yarns subjected to rapid impact loading. Part X: Stress-strain curves obtained by impacts with rifle bullets, J. C. Smith, C. A. Fenstermaker, and P. J. Shouse, Textile Res. J. **33,** *919–934 (Nov. 1963).*
When a yarn is struck transversely, a V-shaped wave of transverse motion is caused to spread outwards at a velocity U depending upon the impact velocity V. In this research data on U vs V for impact velocities between 10 m/sec and 700 m/sec are analyzed to determine stress-strain behavior in high-tenacity nylon and polyester yarns. The data are obtained by shooting rifle bullets at a yarn and recording the resulting configurations by microflash photography. A strain-rate-independent theory for transverse impact behavior is used to calculate stress-strain data.
It was found that the time required to break a yarn depended upon the impact velocity. Nylon yarns broke 10 μsec after impact at 650 m/sec with a calculated breaking strain of 10.0% and tenacity of 77 g/tex. At 495 m/sec velocity the yarn broke within 100 μsec at 7.4% strain and 52 g/tex tenacity. The corresponding values in polyester yarn were, for a 10-μsec break, 620 m/sec, 10.5%, and 67 g/tex; for a 100-μsec break, 420 m/sec, 6.5%, and 40 g/tex.

Wavelength of Hg^{198} Zeeman filter relative to that of the 2537-A absorption line of an atomic beam, W. G. Schweitzer, Jr., and K. G. Kessler, *J. Opt. Soc. Am.* **53,** *No. 12, 1382–1388 (Dec. 1963).*
We have made a precise comparison of the wavelength passed by a Hg^{198} Zeeman filter with that of the 2537-Å absorption line of an atomic beam. This was done by passing the light from the filter through the atomic beam and then comparing the amplitudes of the two peaks in the resulting reversed lines. A calibration was obtained by measuring the ratio of peak amplitudes with the beam tilted at various angles to the optic axis so as to introduce known Doppler shifts. The wavelengths of the Zeeman filter and atomic beam are shown to be equal to about one part in 10^9.

Numerical solutions of the convolution-hypernetted chain integral equation for the pair correlation function of a fluid. I. The Lennard-Jones (12, 6) potential, M. Klein and M. S. Green, *J. Chem. Phys.* **39,** *No. 6, 1367–1387 (Sept. 15, 1963).*
The integral equation of the convolution-hypernetted chain approximation is solved numerically at five temperatures for the Lennard-Jones (12, 6) potential. Due to an inconsistency in the approximation there are two equations of state associated with it. These are compared with each other, with other theories, and with the experimental argon equation of state. At high temperatures, the two equations of state agree both with experiment and with more *a priori* theory at low densities and bracket them at higher densities, their mean giving a good representation of both. The integral equation is found to be singular at certain temperature-density points, their locus forming a dome shaped curve in the T-ρ plane. These points are shown to correspond to the limits of metastability in the van der Waals gas, the highest temperature point being the critical point. The nonsingular points below the critical point correspond either to a homogeneous gas (low densities) or liquid (high densities) phase. The former are in good agreement with the three-term virial series, as expected, and the latter are a considerable improvement over it. The equation of state is a considerable improvement over that obtained from the Born-Green equation by Kirkwood, Lewinson, and Alder, the latter predicting negative pressures over most of the liquid range while these results show only positive pressures. The comparisons with experiment are obscured by the inadequacy of the (12, 6) potential function. The use of temperature "compensated" potential parameters (as determined by the second virial coefficient) indicates that the use of a more reasonable potential function in the theory will give a relatively good representation of the equation of state of a a fluid over a wide range of temperatures and densities.

The three-body scattering operator in nonequilibrium statistical mechanics, J. Weinstock, *Phys. Rev.* **132,** *No. 1, 470–482 (Oct. 1, 1963).*
A method is presented for calculating the time dependent irreducible clusters—$\beta_s(t)$—which appear in the kernel of the equation of evolution derived in the preceding article. The clusters $\beta_1(t)$ and $\beta_2(t)$—which correspond to binary and ternary collisions, respectively—are calculated in detail. They are each found to divide into the two following parts: (1) a "completed" collision part which corresponds to those collisions completed before time t, and (2) an "incompleted" part which corresponds to those collisions not completed by time t. The incompleted collision parts contribute to the "memory" of the equation of evolution and are shown to be relatively small when t is large. The completed collision parts, which play a central role in the theory of transport coefficients, are time independent scattering operators in momentum space and do not contribute to the memory. By means of the "binary collision expansion" a systematic method is presented for the calculation of the three-body scattering operator $[\lim_{t\to\infty} t^{-1}\beta_2(t)]$ which is directly applicable to interaction forces with infinite repulsions. An approximate formula is then derived for this scattering operator in a form which can be readily used to calculate the density correction to transport coefficients which arises from ternary collisions.

Macro-pores in leather as determined with a mercury porosimeter, J. R. Kanagy, *J. Am. Leather Chemists Assoc.* **LVIII,** *No. 9, 524–550 (Sept. 1963).*
A study was made of the pore structure in leather and in other

porous materials with a mercury porosimeter at absolute pressures ranging from 5 to 3000 psi. Pore radii corresponding to these pressures vary from 50 to 0.04 microns. This range is referred to as the macro-pore range. Leather and other natural collagenous materials were compared to microporous plastics and fritted-glass discs. The results indicate that a characteristic pore structure giving rise to many different-sized pores related to the fibrous structure exists in leather, whereas the pores in manufactured materials which are designed for a specific use are more uniform in size. A differential analysis of the integral volume-pressure curves indicates that a large part of the pore volume of collagenous materials in the form of hides occurs at radii of 5 to 0.5 microns. For rat tail tendons, a large fraction of the pore volume exists for pores in close proximity to this, 2.5 to 0.5 microns. The pores which constitute these volumes are believed to exist between the primitive fibers. The volume from pores smaller than 0.25 micron in radius very probably are within the fibril region.

Cluster formulation of the exact equation for the evolution of a classical many-body system, J. Weinstock, *Phys. Rev.* **132,** *No. 1, 454–469 (Oct. 1, 1963).*
An exact non-Markoffian equation is derived for the evolution of an infinite homogeneous system. This equation—which may be viewed as a time dependent analogue of the equilibrium virial expansion—may be readily applied when the forces between particles include infinite repulsions. The derivation of this equation from Liouville's equation is analogous to Mayer's derivation of the virial expansion from the partition function. Fourier expansions and expansions in powers of the interaction potential are avoided by dealing with s-body Green functions (propagators) which are always convergent functions of the interaction potential. These functions correspond to multiplet collisions in ordinary configuration space and are time dependent analogues of the irreducible clusters well-known in equilibrium statistical mechanics.
The kernel (memory) of the equation of evolution consists of a linear sum of the time dependent irreducible clusters. The non-Markoffian behavior of the equation of evolution is, thus, directly given by the time dependence of these clusters, and is explicitly related to incompleted collisions. The equation of evolution is solved in the asymptotic limit of long times. In this limit it is found (because the kernel rapidly vanishes) that the equation reduces to a Markoffian master equation involving a scattering operator for both completed and incompleted collisions in configuration space.

An analysis of pressure and stress distribution under rigid Bridgman-type anvils, J. W. Jackson and M. Waxman, *Book, High-Pressure Measurement, pp. 39–58, ed. Giardini and Lloyd (Butterworth, London, England, 1963).*
Analytical expressions are derived for the pressure and stress distribution in a short cylinder compressed by Bridgman type anvils, assuming the anvils to be rigid plates. The short cylinder is considered to be composed of an inner cylinder bound by an outer shell. The deformation for each may be elastic or plastic.

Interaction energies and transport coefficients of Li+H and O+H gas mixtures at high temperatures, P. H. Krupenie, E. A. Mason, and J. T. Vanderslice, *J. Chem. Phys.* **39,** *No. 10, 2399–2408 (Nov. 15, 1963).*
Accurate potential energy curves for the $X^1\Sigma_g^+$, $A^1\Sigma_u^+$, $B^1\Pi_u$, and $C^1\Pi_u$ states of the Li_2 molecule are calculated from observed spectroscopic data by the method of Rydberg-Klein-Rees (RKR), and compared with previous quantum-mechanical calculations. Long-range attractive potentials are estimated by extrapolation of functions fitted to the RKR ground-state curves of Li_2, LiH, and OH. From these, the repulsive potentials derivable from interacting ground-state atoms are estimated semiempirically. Collision integrals computed from the potentials, and transport coefficients of the gaseous systems Li+Li, Li+H, and O+H are calculated for temperatures of 1000 to 10,000 °K.
A surprising result is the extraordinarily large values of the collision integrals for Li+Li (and Li+H) interactions, which result in unexpectedly small values of diffusion coefficient, viscosity and thermal conductivity. For traces of Li in Li+H mixtures at low temperature, the thermal diffusion factor is very large. Various approximate formulas for viscosity and thermal conductivity of mixtures are seen to give poor agreement with exact calculations for the systems considered.

Inertial effects in the phenomenological theory of thermal diffusion in liquids, R. E. Nettleton, *Il Nuovo Cimento* **28,** *Serie X, 952–969 (Dec. 7, 1962).*
The energy flux carried by diffusing molecules in a binary liquid solution is shown to obey a rate equation linking its time rate of change to energy-exchange and particle-scattering terms and to driving terms proportional to the temperature and concentration gradients. This equation together with a similar equation for the energy flow carried by high-frequency sound waves, is written in terms of thermodynamic forces which are assumed linear in the two heat flux components, and it is found that these forces may be calculated by interpreting the rate equations as thermodynamic phenomenological relations and then applying Onsager's theorem and Maxwell's relations. From the forces, one can determine explicitly the dependence of the free energy per molecule A on the energy flux vectors and, in the limit of low acoustic frequencies, the dependence of A on the square of the concentration gradient. The low-frequency limits of the rate equations also give an expression for the thermal diffusion coefficient.

Mass spectra and metastable transitions of H_2S, HDS, and D_2S, V. H. Dibeler and H. M. Rosenstock, *J. Chem. Phys.* **39,** *No. 11, 3106–3111 (Dec. 1, 1963).*
Mass spectra are reported for isotopic hydrogen sulfides. The occurrence of metastable transitions and the effect of isotopic substitution on the relative abundance are discussed. Appearance potential are given for the molecule and fragment ions in H_2S, the molecule ions of HDS and D_2S, and the principal metastable transition in each species. The latter process is interpreted as resulting from electronic transitions rather than from vibrational relaxation processes.

Spectrum of Nd^{3+} in $LaCl_3$, J. C. Eisenstein, *J. Chem. Phys.* **39,** *No. 9, 2134–2140 (Nov. 1, 1963).*
The energy levels of the Nd^{3+} ion in $LaCl_3$ are calculated by finding the eigenvalues of the matrices for the combined Coulomb, spin-orbit and crystal field interactions within the f^3 configuration. By judicious choice of the three Slater integrals and the spin-orbit coupling constant the standard deviation between the calculated and the experimental positions of 21 terms can be reduced to 93 cm^{-1}. Crystal field parameters can be chosen which yield a standard deviation of 0.90 cm^{-1} between the calculated and the measured splittings of 31 levels in 7 terms. The calculated Zeeman splitting factors in the direction parallel to the crystal axis are in good agreement with the measured values.

Two assumptions in the theory of attractive forces between long saturated chains, R. Zwanzig, *J. Chem. Phys.* **39,** *No. 9, 2251–2258 (Nov. 1, 1963).*
A recent calculation by Salem of the attractive forces between two long parallel hydrocarbon chains was based on two assumptions: (1) local pairwise additivity of dispersion forces between individual groups on each chain, and (2) local isotropy of the polarizability of a group on the chain. The validity of these assumptions is assessed here by means of a Drude model calculation of the interaction between two parallel linear lattices of dispersion oscillators. We conclude that the assumptions are not valid, because of strong induced dipole interactions between neighbors along the chain. Salem's numerical results are essentially correct, however, due to use of an experimentally determined bond polarizability at a crucial stage of the calculation. This allowed for the effects of interactions between neighbors.

Binary mixtures of dilute bose gases with repulsive interactions at low temperatures, D. M. Larsen, *Ann. Phys.* **24,** *89–101 (Oct. 1963).*
This work is a theoretical investigation of the behavior of mixtures of two species of bosons with repulsive interactions at temperatures in the neighborhood of absolute zero. Using

the Bogoliuboy approximation and a novel canonical transformation we investigate the excitation spectra, ground state energy, excitation wave functions, and ground state pair correlation function of the mixture, valid for interactions of short range, in the low density limit.
A criterion for phase separation is given and varified thermodynamically for the case in which the interactions among the particles can be replaced by the two body S-wave pseudopotential. It is shown that two dilute hard sphere bose gases of different mass do not mix in any proportions at absolute zero.

Statistics of irreversible termination in homogeneous anionic polymerization, B. D. Coleman, F. Gornick, and G. Weiss, *J. Chem. Phys.* **39,** *No. 12, 3233–3239 (Dec. 15, 1963).*
The effect of irreversible termination on the molecular weight distribution of a polymer prepared by homogeneous anionic polymerization is examined for cases in which the initiator is monofunctional and initiation is instantaneous. A general procedure for the calculation of the chain length distribution, as well as its moments, is presented. The procedure is then illustrated by an exact treatment of an isothermal batch polymerization for which we obtain the ratio $r_\sigma(t)$ of the weight to number average molecular weights as a function of the fraction of monomer consumed, the ratio σ of the initial terminator concentration to that of the initiator, the ratio ρ of the rate constant for termination to the rate constant for propagation, and the average degree of polymerization at time t, $\overline{n}^1(t)$.
When σ is much less than unity, and the limiting number average D.P. $\overline{n}^1(\infty)$ is very large, $r_\sigma(t)$ approaches the following value as the reaction nears completion: $r_\sigma(\infty)=1+\sigma\rho(2+\rho)^{-1}$.

The structure of gaseous copper (II) nitrate as determined by electron diffraction, R. E. LaVilla and S. H. Brauer, *J. Am. Chem. Soc.* **85,** *3597–3600 (Nov. 1963).*
Anhydrous copper nitrate has a sufficient vapor pressure at 180–200 °C to permit the recording of electron diffraction photographs. That this gas is monomeric has been demonstrated by Addison, *et al.*, by means of vapor density measurements and confirmed with mass spectrometry; its range of stability has also been ascertained.
Visually estimated intensities were used for the inversion to a radial distribution, and were compared with computed intensity curves for many models. The analysis indicates the molecular structure of gaseous copper nitrate to be of the bidentate form with the copper atom occupying the center of inversion. The central copper atom has four nearest oxygen atoms at 2.00 ±0.02Å, and two Cu-N distances of 2.30 ±0.03Å, <O-N-O=120° ±2° and <O-Cu-O≈70°. The errors shown are mean deviations.

Spectrum of Er^{3+} in $LaCl_3$, J. C. Eisenstein, *J. Chem. Phys.* **39,** *No. 9, 2128–2133 (Nov. 1, 1963).*
The energy levels of the Er^{3+} ion in $LaCl_3$ are calculated by finding the eigenvalues of the matrices for the combined Coulomb, spin-orbit and crystal field interactions within the f^{11} configuration. For suitably chosen values of the three Slater integrals and the spin-orbit coupling constant the root-mean-square (rms) deviation between the calculated and the experimental positions of 20 terms is 140 cm^{-1}. Crystal field parameters can be chosen which reduce the rms deviation between the calculated and the measured splittings of 72 levels to 3.84 cm^{-1}. Zeeman splitting factors in the direction parallel to the crystal axis are also calculated. The results for Er^{3+} in $LaCl_3$ are compared with those for Nd^{3+} in $LaCl_3$.

Large-angle inelastic scattering of 500-kev electrons. J. W. Motz and R. C. Placious, *Phys. Rev.* **132,** *No. 3, 1120–1122 (Nov. 1, 1963).*
Experimental results are given for the energy spectra of electrons inelastically scattered at 100 degrees, with 500 kev electrons incident on thin targets of gold and of aluminum. This large angle inelastic scattering arises primarily from the two processes of bremsstrahlung and of atomic K-shell ionization with a small contribution from double or plural scattering effects. In the 300 kev energy region for the scattered electron, the sum of the theoretical cross sections evaluated with the Born calculations of Racah and of Weber, Deck, and Mullin for the respective two processes is approximately an order of magnitude smaller than the experimental values. This disagreement can be attributed to the breakdown in this energy region of both the high energy approximation in the latter calculation and the Born approximation in both calculations.

Investigation of shallow reference cavities for high-temperature emittance measurements, D. G. Moore (*Symp. Measurement of Thermal Radiation Properties of Solids, Dayton, Ohio, Sept. 5–7, 1962*), *Natl. Aeron. and Space Admin. SP–31, Session V, Paper 52, p. 515 (1963).*
Total normal emittance measurements were made on small specimens with shallow reference holes of circular cross section. The ratio of the radiant flux density from the surface to the flux density from the hole was measured and this value then converted to emittance by a theoretical expression based on hole dimensions. The expression applies only to diffusely reflecting materials.
Measurements were made on four different diffusely reflecting materials. Specimens of oxidized nickel that had reference holes with depth-to-radius ratios of 1.7 to 3.7 gave corrected total normal emittance values at 1350° K in the range 0.85 to 0.87. The emittance of oxidized Inconel, when determined for a specimen with a reference hole having a depth-to-radius ratio of 1.7, was found to be in good agreement with values obtained by a heated strip method. The emittance measurements on four sintered alumina specimens varied from 0.43 to 0.47 when measured in air at 1375° K.
The determined emittance for a polished specimen of high-purity graphite with a shallow reference hole increased with temperature linearly from 0.59 at 1100° K to 0.74 at 2150° K. These values were in good agreement with those reported for polished graphite when measured by the rotating specimen method.

An approach to thermal emittance standards, J. C. Richmond, W. N. Harrison, and F. J. Shorten (*Symp. Measurement of Thermal Radiation Properties of Solids, Dayton, Ohio, Sept. 5–7, 1962*), *Natl. Aeron. and Space Admin. SP–31, Session IV, Paper 41, p. 403 (1963).*
A double-beam ratio-recording infrared spectrometer was modified to record directly the normal spectral emittance of strip specimens that are heated by passing a current through them. A laboratory blackbody furnace and a hot specimen at the same temperature serve as sources for the respective beams. Temperature equalization is achieved by means of a differential thermocouple. Automatic data-processing equipment corrects for "zero-line" and "100%-line" errors on the basis of previously-recorded calibrations, and also computes from the spectral data, as the measurement progresses, total emittance or absorptance for radiant energy having any known spectral distribution of flux.

Broadening of the ν_3 lines of HCN due to argon, carbon dioxide, and hydrogen chloride. R. J. Thibault, A. G. Maki, and E. K. Plyler, *J. Opt. Soc. Am.* **53,** *No. 11, 1255–1258 (Nov. 1963).*
The pressure broadening effect of argon, carbon dioxide, and hydrogen chloride on the ν_3 band of HCN has been measured. The broadening effects of the different gases are found to be in qualitative agreement with the theory. Of particular importance is the observation of an oscillatory behavior in the J dependence of the line half width for HCl+HCN. This oscillatory behavior is explained as due to a dipole-dipole interaction for which the large difference between the rotational levels of perturber and absorber molecules causes some levels to be in resonance while others are not.

Other NBS Publications

J. Res. NBS 68C (Eng. and Instr.), No. 2 (Apr.–June 1964), 75 cents.

Fringe pattern of an oscillating Fabry-Perot interferometer. K. D. Mielenz. (See above abstracts.)

Interferometer for testing extended surfaces such as surface plates and precision ways. J. B. Saunders and J. V. McDermott.

Ferrimagnetic resonance in polycrystalline ferrite and garnet disks at L-band frequencies. W. E. Case, R. D. Harrington, and L. B. Schmidt.

Changes in the influence of atmospheric humidity during fatigue of an aluminum alloy. J. A. Bennett.

The theory of a stable high-speed externally pressurized gas-lubricated bearing. H. Sixsmith and W. A. Wilson.

Infrared spectra of asphalts: some aspects of the changes caused by photooxidation. P. G. Campbell and J. R. Wright.

Radio Sci. J. Res. NBS/USNC–URSI, Vol. 68D, No. 2 (Feb. 1964), $1.00.

Generation of an electromagnetic pulse by an expanding plasma in a conducting half-space. A. P. Stogryn and R. N. Ghose.

Impedance of a monopole antenna with a radial-wire ground system on an imperfectly conducting half-space, part II. S. W. Maley and R. J. King.

Capacitor type biconical antennas. J. Galejs.

Simulated angular response patterns for transhorizon propagation. J. W. Strohbehn and A. T. Waterman, Jr.

Radio-star scintillations from ionospheric waves. J. W. Warwick.

Ionosonde studies of some chemical releases in the ionosphere. J. W. Wright.

Diurnal changes and transmission time in the artic propagation of VLF waves. W. T. Blackband.

Geometrical optics convergence coefficient for the whistler case. J. H. Crary.

Comments on a paper "Collisional Detachment and the Formation of an Ionospheric" by E. T. Pierce. H. R. Arnold.

The quasi-longitudinal approximation in the generalized theory of radio wave absorption. R. F. Benson.

Diurnal phase variation of VLF waves at medium distances. H. Volland.

Application of diffractions by convex surfaces to irregular terrain situations. H. T. Dougherty and L. J. Maloney.

Effect of lossy earth on antenna gain. R. J. Coe and W. L. Curtis.

Propagation of radio waves with frequency 99.9 Mhz as a function of the vertical structure of the atmosphere derived from daily radiosonde observations. G. P. A. Braam.

Radio Sci. J. Res. NBS/USNC–URSI, Vol. 68D, No. 2 (Mar. 1964), $1.00.

An interpretation of rapid changes in the phase of horizontally polarized VLF waves recorded at night over a short path in the southwestern United States. E. E. Gossard and M. R. Paulson.

Precise phase and amplitude measurements on VLF signals propagated through the Arctic zone. F. H. Reder, C. J. Abom, and G. M. R. Winkler.

On the long term phase stability of the 19.8 kc/s signal transmitted from Hawaii, and received at Boulder, Colorado. A. H. Brady.

Oblique propagation of groundwaves across a coastline. Part III. J. R. Wait.

Impedance of a monopole antenna with a radial-wire ground system on an imperfectly conducting half space, Part III. S. W. Maley and R. J. King.

A simplified theory of diffraction at an interface separating two dielectrics. J. Kane and S. N. Karp.

Variational solution for the admittance of long cylindrical antenna. R. A. Hurd.

Admittance of annular slot antennas radiating into a plasma layer. J. Galejs.

Propagation of plasma waves in a "spoke-wheel" magnetic field. R. L. Liboff.

An experimental investigation of signal strength in the area around a transmitter's antipode. R. M. Pipp and J. B. Webster.

Relationship between simultaneous geomagnetic and ionospheric oscillations. H. Rishbeth and O. K. Garriott.

Radio Sci. J. Res. NBS/USNC–URSI, Vol. 68D, No. 4 (Apr. 1964), $1.00.

Some basic microwave phase shift equations. R. W. Beatty.

A light-modulated scattering technique for diffraction field measurements. A. M. Vural and D. K. Cheng.

Radiation from an aperture in a coated plane. C. M. Knop and G. I. Cohn.

Impedance of a cylindrical dipole having a sinusoidal current distribution in a homogeneous anisotropic ionosphere. W. S. Ament, J. C. Katzin, M. Katzin, and B. Y.-C Koo.

Propagation of electromagnetic waves through a continuously varying stratified anisotropic medium. G. H. Price.

Lunar semi-diurnal tides in $h'F$ and their influence on trans-equatorial radio progapation. J. A. Thomas.

Some statistical parameters related to the Nakagami-Rice probability distribution. W. R. Burns.

The U.S. National Committee Report for Commission 6 of URSI. Subcommission 6.3, Electromagnetics.

Radio Sci. J. Res. NBS/USNC–URSI, Vol. 68D, No. 5 (May 1964), $1.00.

URSI National Committee Report, XIV General Assembly, Tokyo, September 1963:

Commission 1. Radio measurement methods and standards.
Commission 2. Tropospheric radio propagation.
Commission 3. Ionospheric radio.
Commission 4. Magnetospheric radio.
Commission 5. Radio and radar astronomy.
Commission 7. Radio electronics.

Radio Sci. J. Res. NBS/USNC–URSI, Vol. 68D, No. 6 (June 1964), $1.00.

Electrical properties of sea ice at 0.1 to 30 Mc/s. F. L. Wentworth and M. Cohn.

ELF and VLF waves below an inhomogeneous anisotropic ionosphere. J. Galejs.

The effects of a small local change in phase velocity on the propagation of a VLF radio signal. D. D. Crombie.

Auroral-zone absorption effects on an HF arctic propagation path. R. D. Hunsucker.

Amplitude-probability distribution of atmospheric radio noise. P. Beckmann.

An approximate method for computing diffraction patterns caused by ionospheric irregularities. R. Gagnon.

Wave propagation in stratified random media. Y. M. Chen.

Radar scattering from coated perfect conductors: application to the semi-infinite cone and use of exact eikonal. H. Überall.

Methods for the dynamic calibration of pressure transducers, J. L. Schweppe, L. C. Eichberger, D. F. Muster, E. L. Michaels, and G. F. Paskusz, NBS Mono. 67 (Dec. 12, 1963), 60 cents.

Curves of input impedance change due to ground for dipole antennas, L. E. Vogler and J. L. Noble, NBS Mono. 72 (Jan. 31, 1964), 35 cents.

Radioactivity, Recommendations of the International Commission on Radiological Units and Measurements, NBS Handb. 86 (Nov. 29, 1963), 40 cents. (This publication supersedes parts of H78. Handbooks 84 through 89 extend and largely replace H78.)

Safety standard for non-medical x-ray and sealed gamma-ray sources, Part I. General, NBS Handb. 93 (Jan. 3, 1964), 30 cents.

Weights and measures standards of the United States, a brief history, L. V. Judson, NBS Misc. Publ. 247 (Oct. 1963), 35 cents. (Supersedes Sci. Paper No. 17 and Misc. Publ. 64).

Survey of the literature on safety of residential chimneys and fireplaces, H. Shoub, NBS Misc. Publ. 252 (Dec. 17, 1963), 15 cents.

Report of the 48th National Conference on Weights and Measures 1963, NBS Misc. Publ. 254 (Dec. 30, 1963), 75 cents.

Vitreous china plumbing fixtures, CS20–63, 20 cents. (Supersedes CS20–56).

Grading of a diamond powder in sub-sieve sizes, C.S. 261–63, 10 cents. (Supersedes in part CS123–49).

Vises (machinists' and other bench-mounted vises), SPR 229–63, 10 cents. (Supersedes R229–48).

Forms for two-way concrete joist floor and roof construction, SPR 265–63, 5 cents.

Gypsum board products, SPR 266–63, 10 cents.

Photometry of projectors at the National Bureau of Standards, L. Chernoff, NBS Tech. Note 198 (Dec. 17, 1963), 25 cents.

BOUMAC, A macro-programming system for scientific computation, J. H. Devenney and J. J. Sopka, NBS Tech. Note 203 (Dec. 18, 1963), 30 cents.

Calculations of the field near the apex of a wedge surface, J. R. Wait and C. M. Jackson, NBS Tech. Note 204 (Nov. 21, 1963), 45 cents.

The normal phase variations of the 18 kc/s signals from NBA observed at Frankfurt, Germany, A. H. Brady, A. C. Murphy, and D. D. Crombie, NBS Tech. Note 206–1 (Dec. 8, 1963), 25 cents.

Solar heating, radiative cooling, and thermal movement—their effects on built-up roofing, W. C. Cullen, NBS Tech. Note 231 (Dec. 16, 1963), 25 cents.

A redetermination of some optical properties of calcium fluoride, I. H. Maltison, Appl. Opt. **2,** No. 11, 1103–1107 (Nov. 1963).

Colorimetric method for measuring polyester degradation due to weathering, V. E. Gray and J. R. Wright, J. Appl. Polymer Sci. **7,** 2161–2174 (1963).

Optical T-bench method for measurement of optical path difference, F. E. Washer and W. R. Darling, SPIE J. **1,** 211–217 (Sept. 1963).

Auroral-zone observations of infrasonic pressure waves related to ionospheric disturbances and geomagnetic activity, W. H. Campbell and J. M. Young, J. Geophys. Res. **68,** No. 21, 5909–5916 (Nov. 1, 1963).

Programmed maneuver-spectrum fatigue tests of aircraft beam specimens, L. Mordfin and N. Halsey, ASTM STP Symp. Fatigue Tests of Aircraft Structures, No. 338, 251–272 (Sept. 1963).

Differential dielectric apparatus for determining water added to solvents, W. C. Wolfe, Anal. Chem. **35,** 1884–1887 (Nov. 1963).

Radio star scintillations and spread-*F* echoes, H. J. A. Chivers, J. Atmospheric and Terrest. Phys. **25,** 468–473 (Aug. 1963).

Some derivatives of 2,2′-(phenylimino)diethanol, A. Cohen and R. S. Tipson, J. Med. Chem. **6,** 822–824 (1963).

Effect of hydrogen-hydrogen exchange collisions, P. L. Bender, Phys. Rev. **132,** No. 5, 2154–2158 (Dec. 1, 1963).

The Pythagorean theorem in certain symmetry classes of tensors, M. Marcus and H. Minc, Trans. Am. Math. Soc. **104,** No. 3, 510–515 (Sept. 1962).

Error bounds for first approximations in turning-point problems, F. W. J. Olver, J. Soc. Indust. Appl. Math. **11,** No. 3, 748–772 (Sept. 1963).

Numerical solutions of the convolution-hypernetted chain integral equation for the pair correlation function of a fluid. II. The hard-sphere potential, M. Klein, J. Chem. Phys. **39,** No. 6, 1388–1397 (Sept. 15, 1963).

Comparison of the 3-out-of-7 ARQ with Bose-Chaudhuri-Hocquenghem coding systems, M. Nesenbergs, IEEE Trans. Commun. Systems **CS–11,** No. 2, 202–212 (June 1963).

Form and angular distribution of proton groups at about $Q=0$ Mev in the proton spectra of (d,p) reactions of heavy nuclei, J. Pfleger, U. Schmidt-Rohr, V. Spiegel, P. Turek, and W. Zuckschwerdt, Nuclear Physics **48,** No. 1, 22–32 (Sept. 1963).

Galvanic currents observed during outdoor exposure of an iron-nickel cell. A progress report (AES Research Project No. 19), F. Ogburn and R. L. Myklebust, 50th Annual Tech. Proc. American Electroplaters Society, pp. 24–28 (1963).

Determination of propylene in ethylene-propylene copolymers by infrared spectroscopy, J. E. Brown, M. Tryon, and J. Mandel, Anal. Chem. **35,** 2172–2176 (Dec. 1963).

Syntactic integration carried out mechanically, I. Rhodes, Inform. Storage and Retrieval **1,** 215–219 (1963).

A method for localized variation of the paths of two paraxial rays, L. E. Sutton, Appl. Opt. **2,** No. 12, 1275–1280 (Dec. 1963).

Scheme for obtaining integral and fractional multiples of a given radiance, D. E. Erminy, J. Opt. Soc. Am. **53,** 1448–1449 (Dec. 1963).

Pitfalls in thermal emission studies, W. N. Harrison (Symp. Measurement of Thermal Radiation Properties of Solids, Dayton, Ohio, Sept. 5–7, 1962), Natl. Aeron. and Space Admin. Sp-31, Session 1, Paper 1, p. 3 (1963).

Foundations of the Callaway theory of thermal conductivity, R. E. Nettleton, Phys. Rev. **132,** No. 5, 2032–2038 (Dec. 1, 1963).

Wavelength passed by Hg^{198} Zeeman-split absorption filter, W. G. Schweitzer, Jr., J. Opt. Soc. Am. **53,** No. 11, 1250–1252 (Nov. 1963).

Status of frequency and time control, W. D. George, Frequency **1,** 27–29 (Nov.–Dec. 1963).

Effect of rate loading, time of trituration and test temperature on compressive strength value of dental amalgam, H. J. Caul, R. Longton, W. T. Sweeney, and G. C. Paffenbarger, J. Am. Dental Assoc. **67,** 670–678 (Nov. 1963).

The method for mechanical translation used by the National Bureau of Standards group and the structure of its machine glossary, I. Rhodes, Am. Documentation Inst. 26th Annual Meeting, pp. 23–24 (Chicago, Ill., Oct. 1963).

Temperature measurements below 1000°K (Abstract), J. L. Riddle (Symp. Measurement of Thermal Radiation Properties of Solids, Dayton, Ohio, Sept. 5–7, 1962), Natl. Aeron. and Space Admin. SP–31, Session 1, Paper 2, p. 11 (1963).

ν_3 vibration of methane in condensed oxygen, nitrogen, and argon, S. Abramowitz and H. P. Broida, J. Chem. Phys. **39,** No. 9, 2383–2384 (Nov. 1, 1963).

On the redefinition of the second and the velocity of light. G. E. Hudson and W. Atkinson, IEEE Trans. Instr. Measurement **IM–12,** No. 1, 44–46 (June 1963).

Computed transmission spectra for 2.7-micron H_2O band, D. M. Gates, R. F. Calfee, and D. W. Hansen, Appl. Opt. **2,** No. 11, 1117–1122 (Nov. 1963).

Thermal radiation properties of solids at low temperatures, R. J. Corruccini (Symp. Measurement of Thermal Radiation Properties of Solids, Dayton, Ohio, Sept. 5–7, 1962), Natl. Aeron. and Space Admin. SP–31, Session II, Paper 4, p. 33 (1963).

Periodic heat flow in a hollow cylinder rotating in a furnace with a viewing port, B. A. Peavy and A. G. Eubanks (Symp. Measurement of Thermal Radiation Properties of Solids, Dayton, Ohio, Sept. 5–7, 1962), Natl. Aeron. and Space Admin. SP–31, Session V, Paper 56, p. 553 (1963).

A mechanism for the production of certain types of very-low-frequency emissions, S. F. Hansen, J. Geophys. Res. **68,** No. 21, 5925–5935 (Nov. 1, 1963).

Recent advances in cryogenic engineering, Cryogenic Engineering Laboratory, NBS, Boulder, Chemistry **38,** 8–15 (Oct. 1963).

Method for comparing two nearly equal potentials directly in parts per million, C. J. Saunders, Rev. Sci. Instr. **34,** No. 12, 1452–1453 (Dec. 1963).

Highly ionized atoms: The configurations $s^2p^n(n=1, 2, 4, 5)$, F. Rohrlich and C. Pecker, Astrophys. J. **138,** No. 4, 1246–1261 (Nov. 15, 1963).

A plasma instability resulting in field-aligned irregularities in the ionosphere, D. T. Farley, Jr., J. Geophys. Res. **68,** 6083–6097 (Nov. 15, 1963).

Faraday effect in semiconductors, I. M. Boswarva, R. E. Howard, and A. B. Lidiard, Proc. Royal Soc. **A269,** 125–141 (1962).

Plasma resonances in the upper ionosphere, W. Calvert and G. B. Goe, J. Geophys. Res. **68,** No. 22, 6113–6120 (Nov. 15, 1963).

Annual "Observatory Report" on research at NBS, C. E. Moore and L. M. Branscomb, Astron. J. **68,** No. 9, 658–659 (Nov. 1963).

An operational information retrieval system in the field of cryogenics, N. A. Olien, Proc. Am. Documentation Inst. pp. 157–158 (Chicago, Illinois, Oct. 1963).

Thermocouple and radiation thermometry above 900°K, H. J. Kostkowski and G. W. Burns (Symp. Measurement of

Thermal Radiation Properties of Solids, Dayton, Ohio, Sept. 5–7, 1963), Natl. Aeron. and Space Admin. SP–31, Session I, Paper 3, p. 13 (1963).

Coefficient of thermal expansion and Young's modulus for a one-dimensional model of a solid, J. Mazur and R. J. Rubin, Am. J. Phys. **34,** No. 11, 835–836 (Nov. 1963).

Zeros of polynominals and fractional order differences of their coefficients, G. T. Cargo and O. Shisha, J. Math. Anal. Appl. 7, No. 2, 176–182 (Oct. 1963).

The nightglow, F. E. Roach, Book; Advances in Electronics and Electron Physics **18,** 1–44 (Academic Press Inc., New York, N.Y., 1963).

Electron monochromator utilizing the scattering resonance in helium, J. A. Simpson, C. E. Kuyatt, and S. R. Mielczarek, Rev. Sci. Instr. **34,** 1454–1455 (Dec. 1963).

Synchronization of two remote atomic time scales, J. A. Barnes and R. L. Fey, Proc. IEEE **51,** 1665 (Nov. 1963).

Room temperature oxidation of iron at low pressure, J. Kruger and H. T. Yolken, Corrosion **20,** No. 1, 29t–33t (Jan. 1964).

Vacuum ultraviolet photochemistry. VIII. Photolysis of *n*-butane, H. Okabe, and D. A. Becker, J. Chem. Phys. **39,** No. 10, 2549–2555 (Nov. 15, 1963).

NBS activities for the American Rubber Industry, G. M. Kline, L'industria della gomma **VII,** No. 6, 29–33 (June 1963).

Annual "Observatory Report" on research at JILA, L. M. Branscomb, Astron. J. **68,** No. 9, 660–662 (Nov. 1963).

**Publications for which a price is indicated are available by purchase from the Superintendent of Documents, Government Printing Office, Washington, D.C., 20402 (foreign postage, one-fourth additional). Reprints from outside journals and the NBS Journal of Research may often be obtained directly from the authors.*

U.S. GOVERNMENT PRINTING OFFICE: 1964

UNIVERSITY MICROFILMS
313 NORTH FIRST STREET
ANN ARBOR, MICHIGAN
SJR-A-OCT

UNITED
GOVERNMENT PRI
DIVISION OF PUBLIC DOCUMENTS
WASHINGTON, D.C. 20402

OFFICIAL BUSINESS

PENALTY FOR PRIVATE USE TO AVOID
PAYMENT OF POSTAGE, $300

JOURNAL OF RESEARCH of the National Bureau of Standards
A. Physics and Chemistry

Vol. 68A, No. 3 May–June 1964

Contents

	Page
Compressibility of natural rubber at pressures below 500 kg/cm². Lawrence A. Wood and Gordon M. Martin.	259
A copolymer with lamellar morphology. R. K. Eby.	269
Variation of glass temperature with pressure in polypropylene. Elio Passaglia and Gordon M. Martin.	273
Perfluorophenyl ether and related polymers. Walter J. Pummer and Leo A. Wall.	277
Cyclic polyhydroxy ketones II. *xylo*-Trihydroxycyclohexenediolic acid and keto-inositols. Alexander J. Fatiadi and Horace S. Isbell.	287
Tritium-labeled compounds. XI. Mechanism for the oxidation of aldehydes and aldoses-*1-t* with sodium chlorite. Horace S. Isbell and Lorna T. Sniegoski.	301
Medium effects on the dissociation of weak acids in methanol-water solvents. E. E. Sager, R. A. Robinson, and R. G. Bates.	305
Crystallization of anhydrous copper sulfate from sulfuric acid—ammonium sulfate mixtures. Paul M. Gruzensky.	313
Detection of lattice deformation and recovery in epsilon phase silver-tin alloys. R. M. Waterstrat and G. E. Hicho.	317
Vapor pressures of ruthenium and osmium. N. J. Carrera, R. F. Walker, and E. R. Plante.	325
The 0–2 transition of CO in condensed oxygen, nitrogen, and argon. Stanley Abramowitz and H. P. Broida.	331
Publications of the National Bureau of Standards.	335

Library of Congress Catalog Card Number: 62-37059

For sale by the Superintendent of Documents, U.S Government Printing Office, Washington, D.C., 20402. Price 70 cents (single copy)
Subscription price: $4 a year; 75 cents additional for foreign mailing.
UNITED STATES GOVERNMENT PRINTING OFFICE, WASHINGTON : 1964